Supplementary Information

Planar-chiral arene ruthenium complexes: synthesis, separation of enantiomers, and application for catalytic C-H activation

Mikhail A. Boym,[a,b] Roman A. Pototskiy,[a] Evgeniya S. Podyacheva[a,b] Denis A. Chusov,[a,b]
Yulia V. Nelyubina,[a,c] Dmitry S. Perekalin[a,b,*]

a. N. Nesmeyanov Institute of Organoelement Compounds of Russian Academy of Sciences, Moscow, 119334, Russia.
b. National Research University Higher School of Economics, 7 Vavilova str., Moscow, 117312, Russia.
c. Moscow Institute of Physics and Technology, 9 Institutskiy per., Dolgoprudny, 141700, Russia.

* Corresponding author, e-mail: dsp@ineos.ac.ru.

Table of Contents

Author contributions

M.A. Boym, R.A. Pototskiy, E.S. Podyacheva, Y.V. Nelyubina – investigation; D.A. Chusov – conceptualization, resources; D.S. Perekalin – investigation, conceptualization, supervision, writing original draft.

General Information

Unless otherwise stated all reactions were carried out under argon atmosphere in anhydrous solvents, which were purified and dried using standard procedures, while the isolation of products was carried out in air. Commercial 1,1,1,3,3,3-Hexafluoroisopropanol (HFIP) was used without any prior purification. N-methoxybenzamide substrates,[1] (*R*)-1-phenylethanol,[2] N-allylphthalimide,[3] N-vinyl substituted alkenes,[4] and $[(cymene)RuCl_2]_2$ complex[5] were synthesized according to the literature procedures. All other reagents were obtained from commercial sources and used without further purification.

NMR spectra were measured on Bruker Avance 400, Bruker Avance 300, and Varian Inova 400 spectrometers. Chemical shifts (δ) are given in ppm relative to solvent residual signals for $CDCl_3$ (^1H: δ = 7.27 ppm; ^{13}C: δ = 77.2 ppm), DMSO-d_6 (^1H: δ = 2.50 ppm; ^{13}C: δ = 39.52 ppm). Splitting patterns are designated as s, singlet; d, doublet; t, triplet; q, quartet; sept, septet; m, multiplet, br, broad, coupling constants (J) in Hz. High-resolution mass spectra were recorded on Bruker microTOF II instrument using electrospray ionization (ESI). The measurements were done in the positive ion mode (interface capillary voltage – 4500 V) with mass range from m/z 50 to 3000 Da; external or internal calibration was done with the Electrospray Calibrant Solution (Fluka). Enantiomeric excess values were measured using Shimadzu HPLC equipped with Daicel Chiralpak IA-3 (4.6 × 150 mm) column and diode array detector; flow rate 1 mL/min was adjusted in all experiments unless specified otherwise.

Synthesis of ligands, complexes, and separation of diastereomers

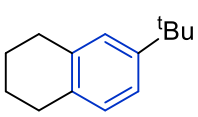

1

Synthesis of 6-(tert-butyl)-1,2,3,4-tetrahydronaphthalene (1). In an argon flushed 250 mL two-neck round bottom flask equipped with a reflux condenser, and a drying tube on top of it tetralin (61 g, 0.46 mol, 1.0 eq.) and tert-butyl chloride (46 g, 0.5 mol, 1.1 eq) were placed. Then solid anhydrous $FeCl_3$ (1.1 g, 6.9 mmol, 0.01 eq.) was added in small portions over the course of 1 h. (CAUTION! Vigorous HCl evolution!) Once the addition was completed, the reaction mixture was left to stir until gas evolution ceased (~20 min). Then 10 g of tert-butyl chloride was added to the mixture, and it was allowed to stir for 30 min. After the indicated time, saturated $NaHCO_3$ solution (100 mL) was slowly added to the mixture. The organic phase was separated, washed with brine (50 mL), dried over anhydrous Na_2SO_4, and excess t-BuCl was removed in vacuo. The resulting oil was distilled to obtain the desired product (45.0 g, 59% yield, 88−98 °C at 2 mbar) as colorless oil.

^1H NMR (400 MHz, $CDCl_3$) δ = 7.31 (d, J = 8.1 Hz, 1H), 7.26 (s, 1H), 7.18 (d, J = 8.0 Hz, 1H), 2.93 (m, 4H), 1.96 (m, 4H), 1.48 (s, 9H). ^{13}C NMR (101 MHz, $CDCl_3$) δ = 148.34, 136.61, 134.26, 128.98, 125.99, 122.71, 34.36, 31.58, 29.83, 29.05, 23.51, 23.50. NMR data was in agreement with those reported previously.[6]

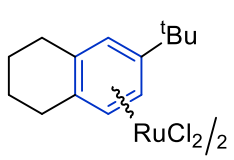

(±)-**3**

Synthesis of racemic ruthenium complex (3). In a 10 ml Schlenk flask $[(cymene)RuCl_2]_2$ (200 mg, 0.33 mmol, 1.0 equiv.) and 6-(tert-butyl)-1,2,3,4-tetrahydronaphthalene (2.46 g, 13 mmol, 40 equiv.) were placed. The flask was subjected to vacuum and refilled with argon three times. Then the flask was connected to a two-neck round-bottom flask, and the whole apparatus was flushed with argon for 5 min. Then the stirred mixture was heated with a heat gun (~200 °C) until bubbling of the free cymene was observed and then for 3 minutes more. Then the reaction mixture was allowed to cool to room temperature. After cooling the red precipitate was formed, and it was washed with hexane (4x6 mL). The obtained red powder was dissolved in chloroform (1 mL), and the solution was passed through a small pad of celite. Then chloroform was evaporated, and the solid residue was triturated with hexane, filtered, and dried in vacuo to obtain the desired product as red powder (202 mg, 86%).

HRMS (ESI): Exact mass calculated for $[(C_{14}H_{20})Ru(HCOO)]^+$= 335.0585, found 335.0587 (0.1% HCOOH in MeOH was used as eluent for ESI). ^{1}H NMR (400 MHz, $CDCl_3$) δ = 5.78 (t, J = 5.7 Hz, 1H), 5.42 (t, J = 7.1 Hz, 1H), 5.30 (s, 1H), 3.12 – 2.97 (m, 1H), 2.85 – 2.71 (m, 1H), 2.29 (dd, J = 14.5, 8.1 Hz, 1H), 2.09 (dd, J = 16.5, 6.8 Hz, 1H), 2.02 – 1.88 (m, 2H), 1.71 – 1.52 (m, 2H), 1.35 (s, 9H). ^{13}C NMR (101 MHz, $CDCl_3$) δ = 80.43, 80.34, 80.04, 79.87, 79.75, 79.53, 34.06, 30.73, 26.36, 26.30, 21.54, 21.35.

Optimization of separation of diastereomeric adducts of the complex 3. In the air, a solution of complex **3** (2 mg, 0.006 mmol, 1.0 equiv.) in MeOH (1 mL) was mixed with an equivalent amount of ligand (**L1**–**L9**) and K_2CO_3 (in case of **L5**, **L7**, and **L9**), and the reaction mixture was stirred for 10 min. Then the reaction mixture was analyzed with TLC in different eluents. Only in case of **L4** notable separation of complexes was achieved in hexane/Et_2O=2/1 mixture without decomposition on TLC plate.

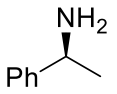

L1

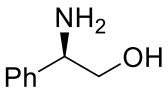

L2

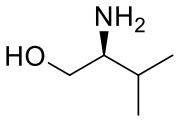

L3

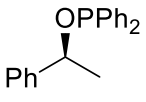

L4

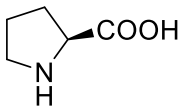

L5

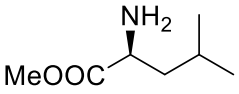

L6

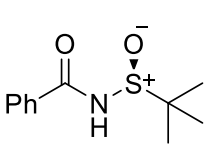

L7

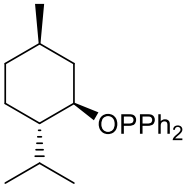

L8

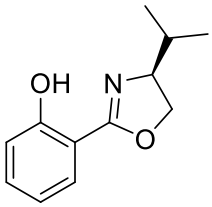

L9

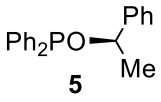

5

Synthesis of (*R*)-diphenyl(1-phenylethoxy)phosphine (5). The procedure was adapted from the literature.[7] A solution of Ph_2PCl (1.31 g, 5.95 mmol, 1.0 equiv.) in diethyl ether (5 mL) was added dropwise to a precooled solution of (R)-1-phenylethanol (800 mg, 6.55 mmol, 1.1 equiv., 96:4 er purity) and pyridine (518 mg, 6.55 mmol, 1.1 equiv.) in a mixture of diethyl ether and hexane (20 mL, 1:1) at –30 °C with vigorous stirring under argon atmosphere. After addition, the reaction mixture was allowed to warm to rt and stirred overnight. Then the pyridinium salt was filtered off, washed with hexane (10 mL), and then the combined filtrates were concentrated in vacuo to give the target crude phosphinite. Then it was dissolved in a minimum amount of hexane/dichloromethane mixture (5:1) and passed through a dry column containing neutral Al_2O_3 (2.0 g) and celite (0.5 g) using hexane as eluent under argon. Then the resulting solution was evaporated in vacuo to obtain the desired product as almost colorless oil that crystallized upon cooling in the freezer (1.6 g, 88%). The product was stored under argon to avoid oxidation.

^{1}H NMR (300 MHz, $CDCl_3$) δ 7.45 – 7.21 (m, 15H), 5.01 (dq, J = 8.9, 6.4 Hz, 1H), 1.59 (d, J = 6.5 Hz, 3H). ^{1}H NMR data was in agreement with those reported previously.[8]

Synthesis and separation of diastereomeric phosphine adducts (6a and 6b). In the air, a solution of complex **3** (200 mg, 0.28 mmol, 1.0 equiv.) in CH_2Cl_2 (2 mL) was mixed with a solution of phosphine **5** (187 mg, 0.61 mmol, 2.4 equiv.) in CH_2Cl_2 (2 mL), and the reaction mixture was stirred for 10 min, at which point it turned deep red. Then the solvent was evaporated in vacuo, and the resulting oil was triturated with hexane to obtain the equimolar mixture of two diastereomeric adducts in quantitative yield.

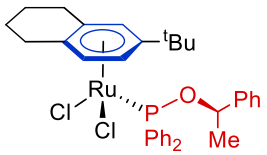

6a

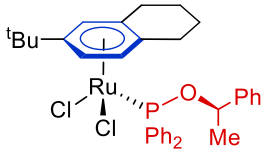

6b

To separate the complexes, 150 mg of the mixture was dissolved in a minimum amount of CH_2Cl_2. The resulting solution was transferred to a silica-packed column and chromatographed with hexane/Et_2O mixtures (10:1 to 2:1) as eluent (Figure S1). The fractions containing diastereomeric complexes were combined separately and evaporated to obtain pure complexes **6a** (52 mg, 35%, eluted first) and **6b** (41 mg, 26%, eluted second) as red powders. In case the diastereomeric purity of the complexes was low according to NMR, they were additionally purified by chromatography. No decomposition was observed during this process; the yields are lower that theoretically possible 50% due to incomplete separation of the fractions. X-ray quality crystals of **6a** were grown by slow diffusion of pentane vapors into its saturated solution in CH_2Cl_2.

6a. Rf(hexane/Et2O=2/1) = 0.47 after two elutions on silicagel TLC plate. HRMS (ESI): Exact mass calculated for $C_{34}H_{39}ClOPRu$ $[M\text{-}Cl]^+$ = 631.1470, found 631.1455. ^{1}H NMR (400 MHz, $CDCl_3$) δ = 8.06 – 7.91 (m, 4H), 7.45 – 7.34 (m, 2H), 7.33 – 7.22 (m, 11H), 5.78 (s, 1H), 5.68 (dq, J = 12.6, 6.4 Hz, 1H), 4.86 (t, J = 5.4 Hz, 1H), 4.08 (d, J = 5.5 Hz, 1H), 3.35 – 2.95 (m, 1H), 2.24 (dt, J = 17.4, 5.5 Hz, 1H), 1.89 – 1.62 (m, 2H), 1.34 (s, 9H), 1.58 – 1.12 (m, 4H). ^{13}C NMR (101 MHz, $CDCl_3$) δ = 134.9 (d, J = 10.7 Hz), 131.8 (d, J = 10.5 Hz), 130.5 (d, J = 19.8 Hz), 128.6, 127.8 (d, J = 10.1 Hz), 127.5, 127.1 (d, J = 9.8 Hz), 125.5, 110.3, 92.4, 87.8 (d, J = 14.9 Hz), 85.8, 76.6 (d, J = 4.3 Hz), 70.6, 35.8, 30.2, 26.1, 25.9, 24.3, 21.2, 21.1. ^{31}P NMR (162 MHz, $CDCl_3$) δ = 110.21.

6b. Rf(hexane/Et2O=2/1) = 0.54 after two elutions on silicagel TLC plate. HRMS (ESI): Exact mass calculated for $C_{34}H_{39}ClOPRu$ $[M\text{-}Cl]^+$ = 631.1470, found 631.1455. ^{1}H NMR (400 MHz, $CDCl_3$) δ = 7.83 (dt, J = 17.2, 9.0 Hz, 4H), 7.54 – 6.75 (m, 11H), 5.80 (s, 1H), 5.46 (dt, J = 12.8, 6.3 Hz, 1H), 4.74 (t, J = 5.0 Hz, 1H), 4.40 (d, J = 5.4 Hz, 1H), 3.18 (dt, J = 16.4, 7.6 Hz, 1H), 2.44 – 2.32 (m, 1H), 1.90 (dt, J = 13.5, 7.6 Hz, 2H), 1.83 – 1.47 (m, 4H), 1.34 – 1.25 (m, 12H). ^{13}C NMR (101 MHz, $CDCl_3$) δ = 133.3 (d, J = 10.7 Hz), 133.1 (d, J = 10.7 Hz), 130.5, 128.1, 127.5 (d, J = 9.8 Hz), 127.3, 127.3 (d, J = 9.1 Hz), 126.2, 110.3 (d, J = 6.3 Hz), 95.4, 88.1 (d, J = 13.2 Hz), 84.4, 77.1, 74.4, 35.4, 30.2, 26.1, 25.4, 25.2 (d, J = 3.7 Hz), 21.4, 21.1. ^{31}P NMR (162 MHz, $CDCl_3$) δ = 111.60.

Figure S1. Photo of a typical column used for separation of diastereomers **6a** and **6b**.

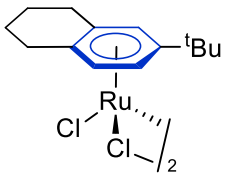

(pR)-**3**

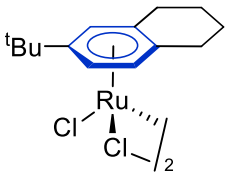

(pS)-**3**

Synthesis of enantiomerically pure dichloride complexes ((*pR*)-**3** and (*pS*)-**3**). The procedure was adapted from the literature.[9] In a 25 ml Schlenk flask complex **6a** (or **6b**) (130 mg, 0.20 mmol, 1.0 equiv.), cyclooctadiene (850 mg, 7.80 mmol, 40 equiv.), and Na_2CO_3 (124 mg, 1.17 mmol, 6.0 equiv.) were placed. Then ^{i}PrOH (12 mL) was added to the flask and the resulting mixture was refluxed for 3 h (during reflux the deep red mixture turned brownish-yellow). Then the mixture was allowed to cool to room temperature and evaporated to dryness. Hexane (5 mL) was added to it, and the obtained suspension was vigorously stirred to ensure complete dissolution of the diene complex (more hexane can be added if needed). The resulting yellow solution was loaded on an alumina-packed column and eluted with hexane under argon. The yellow band was collected in another Schlenk flask, and then HCl in dioxane (1 mL, 4M, 3.9 mmol, 20 equiv.) was added to it dropwise with stirring and orange precipitate of the crude product started to form.

The solution was stirred for 30 minutes and then cooled to -30 °C for complete precipitation. Afterwards, the solid was collected by filtration and was dissolved in chloroform (1 mL). The resulting solution was passed through a small pad of celite, and then chloroform was evaporated. The resulting solid residue was triturated with hexane, filtered, and dried in vacuo to obtain the enantiomerically pure dichloride complex (*pR*)-**3** (or (*pS*)-**3** in case of **6b**) as an orange powder (25 mg, 36%, > 95% *ee*). NMR spectra of both enantiomers coincided with those measured for the racemate.

To assess the optical purity of the obtained complexes, stock solution of (*S*)-1-phenylethylamine (1.68 mg, 0.014 mmol, 1.0 equiv.) was added to the solution of (*pR*)-**3** (or (*pS*)-**3** (5.0 mg, 0.007 mmol, 0.5 equiv.) in $CDCl_3$, at which point the color of the solution changed from red to yellow due to the formation of diastereomeric adducts. Then the ^1H NMR spectrum was recorded, and the enantiomeric purity was assessed via the integration of signals of the arene ligand (Figure **S2**). After recording ^1H NMR spectra, the enantiomer was regenerated. The sample was dissolved in CH_2Cl_2 (2 mL) and washed three times with 10 % aqueous HCl. The organic phase was separated, dried over anhydrous Na_2SO_4, and evaporated to dryness. The resulting residue was triturated with hexane to obtain (*pR*)-**3** (or (*pS*)-**3**) in quantitative yield. For the method of assignment of planar chiral configuration please see the review.[10]

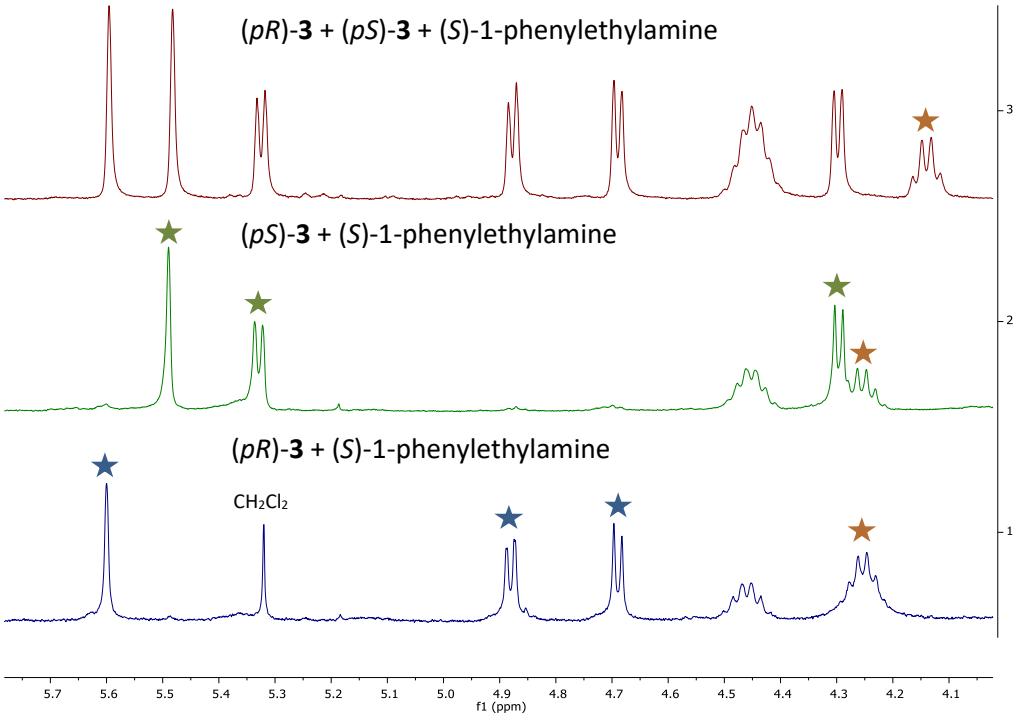

Figure S2. Fragments of ^1H NMR spectra of diastereomeric adducts of (*pR*)-**3** and (*pS*)-**3** with (*S*)-1 phenylethylamine. Signals of the arene ligand are marked with asterisks. Signals of the arene ligand are marked with blue and green asterisks. Signals of the excess (*S*)-1 phenylethylamine are marked with orange asterisks.

Catalytic reactions of N-methoxybenzamides with various alkenes

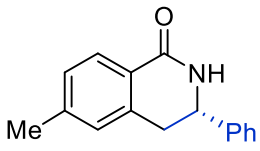

8a

(S)-6-methyl-3-phenyl-3,4-dihydroisoquinolin-1(2H)-one (*S*)**-8a.** N-methoxy-p-methylbenzamide **7a** (10.0 mg, 0.06 mmol, 1 equiv.), complex (*pR*)-**3** (2.2 mg, 0.003 mmol, 5 mol-%), NaOAc (5.0 mg, 0.06 mmol, 1 equiv.) and styrene (19.4 mg, 0.18 mmol, 3 equiv.) were placed in a 20 x 45 mm vial equipped with a stir bar. HFIP (0.150 mL) was added, and the reaction was stirred at 60°C for 24 h. Afterwards, the mixture was transferred to a round bottom flask. Silica was added to the flask and volatiles were evaporated under reduced pressure. The purification was performed by flash column chromatography on silica gel (eluent: Hexane:EtOAc = 3:1). After evaporation of the solvent the product was obtained as colorless crystals.

Yield 8.5 mg, 58%, 60:40 er. HPLC: Chiralpak IA-3 column (4.6 × 150 mm), heptane/i-PrOH 80:20, 1.0 ml/min; tr(major) = 8.1 min, tr (minor) = 12.5 min. ^{1}H NMR (400 MHz, $CDCl_3$) δ = 8.01 (d, J = 7.9 Hz, 1H), 7.46 – 7.30 (m, 5H), 7.16 (d, J = 7.8 Hz, 1H), 6.98 (s, 1H), 6.13 (s, 1H), 4.83 (dd, J = 10.5, 4.8 Hz, 1H), 3.11 (qd, J = 15.6, 7.8 Hz, 2H), 2.37 (s, 3H). ^{1}H NMR data was in agreement with those reported previously.[11]

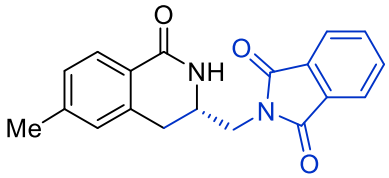

8b

(S)-2-((6-methyl-1-oxo-1,2,3,4-tetrahydroisoquinolin-3-yl)methyl)-isoindoline-1,3-dione (*S*)**-8b.** N-methoxy-p-methylbenzamide **7a** (10.0 mg, 0.06 mmol, 1 equiv.), complex (*pR*)-**3**[a] (2.2 mg, 0.003 mmol, 5 mol-%), NaOAc (5.0 mg, 0.06 mmol, 1 equiv.) and N-allylphthalimide (17.0 mg, 0.09 mmol, 1.5 equiv.) were placed in a 20 x 45 mm vial equipped with a stir bar. HFIP (0.150 mL) was added, and the reaction was stirred at 60 °C for 24 h. Afterwards, the mixture was transferred to a round bottom flask. Silica was added to the flask and volatiles were evaporated under reduced pressure. The purification was performed by flash column chromatography on silica gel (eluent: Hexane:EtOAc = 1:2). After evaporation of the solvent the product was obtained as grey powder.

Yield 15.5 mg, 80%, 62:38 er. HPLC: Chiralpak IA-3 column (4.6 × 150 mm), heptane/i-PrOH 60:40, 1.0 ml/min; tr(major) = 10.6 min, tr (minor) = 8.3 min. ^{1}H NMR (400 MHz, $CDCl_3$) δ = 7.82 – 7.79 (m, 3H), 7.70 – 7.65 (m, 2H), 7.06 (d, J = 8.1 Hz, 1H), 6.98 (s, 1H), 6.82 – 6.77 (m, 1H), 4.06 – 4.03 (m, 1H), 3.91-3.83 (m, 2H), 3.07 – 3.00 (m, 1H), 2.80 – 2.84 (m, 1H), 2.33 (s, 3H). ^{1}H NMR data were in agreement with those reported previously.[12]

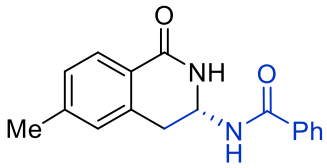

8c

(S)-N-(6-methyl-1-oxo-1,2,3,4-tetrahydroisoquinolin-3-yl)benzamide (*S*)**-8c.** N-methoxy-p-methylbenzamide **7a** (10.0 mg, 0.06 mmol, 1 equiv.), complex (*pR*)-**3** (2.2 mg, 0.003 mmol, 5 mol-%), NaOAc (5.1 mg, 0.06 mmol, 1 equiv.) and N-vinylbenzamide (27.4 mg, 0.18 mmol, 3 equiv.) were placed in a 20 x 45 mm vial equipped with a stir bar. HFIP (0.100 mL) and methanol (0.100 mL) were added, and the reaction was stirred at 60 °C for 24 h. Afterwards, the mixture was transferred to a round bottom flask. Silica was added to the flask and volatiles were evaporated under reduced pressure. The purification was performed by flash

[a] Chiral complex with *ee* = 90% was used

column chromatography on silica gel (eluent EtOAc:MeOH = 95:5). After evaporation of the solvent the product was obtained as grey powder.

Yield 14.3 mg, 82%, 74:26 er. HPLC: Chiralpak IA-3 column (4.6 × 150 mm), heptane/i-PrOH 80:20, 1.0 ml/min; tr(major) = 9.3 min, tr (minor) = 10.8 min. HRMS (ESI): Exact mass calculated for $C_{17}H_{16}N_2O_2Na$ $[M+Na]^+$ = 303.1109, found 303.1113. ^1H NMR (400 MHz, DMSO-d_6) δ = 9.07 (d, J = 6.9 Hz, 1H), 8.27 (s, 1H), 7.85 (d, J = 7.5 Hz, 2H), 7.78 (d, J = 7.8 Hz, 1H), 7.58 – 7.46 (m, 1H), 7.42 (t, J = 7.5 Hz, 2H), 7.17 (d, J = 8.0 Hz, 1H), 7.12 (s, 1H), 5.62 (dt, J = 6.9, 4.4 Hz, 1H), 3.22 (dd, J = 16.3, 5.2 Hz, 1H), 3.10 (dd, J = 16.3, 5.2 Hz, 1H), 2.32 (s, 3H). ^{13}C NMR (101 MHz, DMSO-d_6) δ = 166.10, 164.19, 141.93, 136.37, 133.85, 131.44, 128.73, 128.13, 127.64, 127.54, 127.18, 126.12, 57.28, 32.96, 21.10.

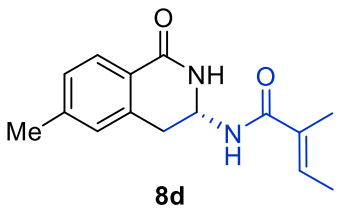

8d

(S,E)-2-methyl-N-(6-methyl-1-oxo-1,2,3,4-tetrahydroisoquinolin-3-yl)but-2-enamide (*S*)-**8d.** N-methoxy-p-methylbenzamide **7a** (10.0 mg, 0.06 mmol, 1 equiv.), complex (*pR*)-**3** (2.2 mg, 0.003 mmol, 5 mol-%), NaOAc (5.1 mg, 0.06 mmol, 1 equiv.) and (E)-2-methyl-N-vinylbut-2-enamide (23.3 mg, 0.18 mmol, 3 equiv.) were placed in a 20 x 45 mm vial equipped with a stir bar. HFIP (0.100 mL) and methanol (0.100 mL) were added, and the reaction was stirred at 60 °C for 24 h. Afterwards, the mixture was transferred to a round bottom flask. Silica was added to the flask and volatiles were evaporated under reduced pressure. The purification was performed by flash column chromatography on silica gel (eluent Hexane:EtOAc = 1:3). After evaporation of the solvent the product was obtained as white powder.

Yield 10.1 mg, 63%, 82:12 er. HPLC: Chiralpak IA-3 column (4.6 × 150 mm), heptane/i-PrOH 90:10, 1.0 ml/min; tr(major) = 18.5 min, tr (minor) = 20.9 min. HRMS (ESI): Exact mass calculated for $C_{15}H_{19}N_2O_2$ $[M+H]^+$ = 259.1447, found 259.1444. ^1H NMR (400 MHz, DMSO-d_6) δ = 8.31 (s, 1H), 8.08 (s, 1H), 7.75 (s, 1H), 7.15 (s, 1H), 7.09 (s, 1H), 6.27 (q, J = 6.8 Hz, 1H), 5.43 (s, 1H), 3.16 – 3.07 (m, 1H), 3.03 – 2.87 (m, 1H), 2.32 (s, 1H), 1.69 (s, 3H), 1.64 (d, J = 6.4 Hz, 3H). ^{13}C NMR (101 MHz, DMSO-d_6) δ = 141.70, 136.29, 131.26, 130.04, 128.51, 127.32, 127.00, 56.77, 32.83, 20.92, 13.44, 12.14.

Optimization studies

Substrate 1	Substrate 2	T, °C	Time, h	Solvent	Yield, %	ee, %
p-MeC$_6$H$_4$CONHOMe	N-vinylpivalamide (1.5 equiv.)	60	24	HFIP	29	72
p-MeC$_6$H$_4$CONHOMe	N-vinylpivalamide (1.5 equiv.)	60	24	HFIP:EtOAc=1:1	33	78
p-MeC$_6$H$_4$CONHOMe	N-vinylpivalamide (1.5 equiv.)	60	24	HFIP:DCE=1:1	traces	NA
p-MeC$_6$H$_4$CONHOMe	N-vinylpivalamide (1.5 equiv.)	60	24	HFIP:MeOH=1:1	24	82
p-MeC$_6$H$_4$CONHOMe	N-vinylpivalamide (1.5 equiv.)	60	24	HFIP:MeOH=1:5	traces[b]	NA
p-MeC$_6$H$_4$CONHO^{i}Pr	N-vinylpivalamide (1.5 equiv.)	60	24	HFIP	traces	NA
p-MeC$_6$H$_4$CONHOMe	N-vinylpivalamide (1.5 eq.)	75	72	HFIP:MeOH=1:1	38	NA[c]
p-MeC$_6$H$_4$CONHOMe	N-vinylpivalamide (3 equiv.)	60	24	HFIP:MeOH=1:1	62	82
p-MeC$_6$H$_4$CONHOMe	N-vinylpivalamide (3 equiv.)	60	24	HFIP:MeOH=1:2	25	NA[b]

Table S1. Optimization of the catalytic reaction conditions.

In air, corresponding benzamide (0.06 mmol, 1 equiv.), complex (*pR*)-**3** (0.005 mmol, 5 mol-%), NaOAc (0.005 mmol, 0.5 equiv.), and N-vinylpivalamide were placed in a 20 x 45 mm vial equipped with a stir bar. The indicated solvent was added using a microsyringe, and the reaction was stirred at the indicated temperature. Afterwards, the mixture was transferred to a round bottom flask. Silica was added to the flask and volatiles were evaporated under reduced pressure. The purification was performed by flash column chromatography on silica gel (eluent Hexane:EtOAc = 1:2). The product was dried in vacuo, and then the yield was determined.

General procedure for the synthesis of dihydroisoquinolinones from N-vinylpivalamide

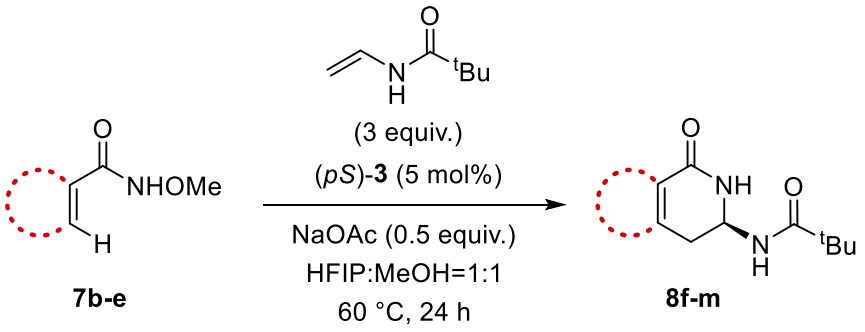

[b] p-Methylbenzamide was observed as a major product
[c] Achiral catalyst was used

In air, corresponding N-methoxybenzamide **7b-e** (0.1 mmol, 1 equiv.), complex (*pS*)-**3** (3.6 mg, 0.005 mmol, 5 mol-%, stock solution in HFIP), NaOAc (0.05 mmol, 0.5 equiv.) and N-vinylpivalamide (38.2 mg, 0.3 mmol, 3 equiv.) were placed in a 20 x 45 mm vial equipped with a stir bar. A mixture of HFIP (0.100 mL) and methanol (0.100 mL) or pure HFIP (0.200 mL, for **8g**[d] and **8h**[d]) were added, and the reaction was stirred at 60°C for 24 h. Afterwards, the mixture was transferred to a round bottom flask. Silica was added to the flask and volatiles were evaporated under reduced pressure. The purification was performed by flash column chromatography on silica gel with a gradient eluent of Hexane/EtOAc or EtOAc/MeOH mixtures.

Methylation of (*R*)-**8h**

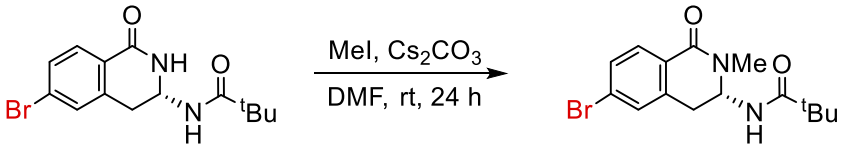

8h, 87:13 er **8h-Me**, 87%

Under argon atmosphere, to a mixture of (*R*)-**8h** (15.0 mg, 0.05 mmol, 1.0 equiv., 87:13 er) and Cs_2CO_3 (45.1 mg, 0.15 mmol, 3 equiv.) in anhydrous DMF (1.0 mL) was added MeI (20 mg, 0.15 mmol, 3 equiv.). The reaction was stirred at room temperature for 24 h. Afterwards, the reaction was quenched with H_2O (5 mL). The phases were separated and the organic phase was washed with H_2O (3×5 mL). Then the aqueous phase was extracted with ethyl acetate (3×5 mL). The combined organic layers were dried over Na_2SO_4, filtered, and evaporated under reduced pressure. The residue was purified by flash column chromatography on silica gel (Hexane:EtOAc = 1:1) to afford (*R*)-**8h-Me** (14.1 mg, 87% yield) as white powder. X-ray quality crystals of **8h-Me** were grown by slow diffusion of pentane vapors into its saturated solution in CH_2Cl_2.

^{1}H NMR (400 MHz, $CDCl_3$) δ = 7.94 (d, J = 8.3 Hz, 1H), 7.57 – 7.48 (m, 1H), 7.39 (s, 1H), 5.98 (d, J = 8.8 Hz, 1H), 5.74 (ddd, J = 8.9, 5.4, 2.0 Hz, 1H), 3.48 (dd, J = 16.5, 5.4 Hz, 1H), 3.15 (s, 3H), 2.91 (dd, J = 16.6, 2.1 Hz, 1H), 1.11 (s, 9H). ^{13}C NMR (101 MHz, $CDCl_3$) δ = 178.66, 163.26, 136.37, 131.23, 131.12, 130.29, 127.32, 62.99, 39.02, 33.80, 33.53, 27.50.

Attempted racemization of 8l

Under argon atmosphere, (*S*)-**8l** (5.0 mg, 0.017 mmol, 87:13 er) was dissolved in HFIP (0.100 mL), and the mixture was heated at 60°C for 72 h. Then the volatiles were evaporated and the solid residue was analyzed by chiral HPLC. No significant loss of optical purity was observed (86:14 er). HPLC: Chiralpak IA-3 column (4.6 × 150 mm), heptane/i-PrOH 90:10, 1.0 ml/min; tr(major) = 21.0 min, tr(minor) = 18.6 min.

[d] For these substrates using a mixture of solvents led to significantly lower yields.

Addition of HFIP to N-vinylpyrrolidone

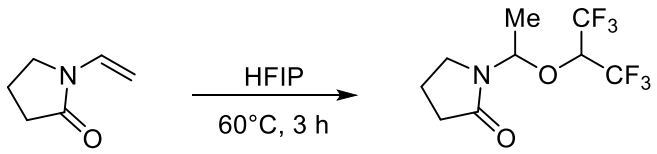

NVP **HFIP-NVP**, ~95%

In air, N-vinylpyrrolidone (100 mg, 0.9 mmol, 1 equiv.) and HFIP (1.00 mL, 9.5 mmol, 10 equiv.) were placed in a 20 x 45 mm vial equipped with a stir bar. The mixture was heated at 60°C for 3 h. Afterwards, the mixture was transferred to a round-bottom flask, and the volatiles were evaporated to provide crude **HFIP-NVP** as a yellowish transparent liquid in near quantitative yield[e].

1-(1-((1,1,1,3,3,3-hexafluoropropan-2-yl)oxy)ethyl)pyrrolidin-2-one (**HFIP-NVP**). HRMS (ESI): Exact mass calculated for $C_9H_{12}F_6NO_2$ $[M+H]^+$ = 280.0772, found 280.0769. ^{1}H NMR (300 MHz, $CDCl_3$) δ = 6.68 (s, 1H), 5.71 (q, J = 6.2 Hz, 1H), 4.45 (dq, J = 12.4, 6.2 Hz, 1H), 3.59 – 3.29 (m, 1H), 2.55 – 2.30 (m, 2H), 2.11 – 1.95 (m, 2H), 1.43 (d, J = 6.2 Hz, 3H). ^{13}C NMR (101 MHz, $CDCl_3$) δ = 178.39, 126.22 – 117.56 (m), 80.93, 74.01 (dt, J = 65.7, 32.5 Hz), 41.74, 31.31, 18.22, 17.94. ^{19}F NMR (282 MHz, $CDCl_3$) δ = -74.79 – -74.97 (m).

NMR spectroscopic data of synthesized compounds

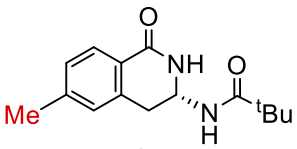

8e

(R)-N-(6-methyl-1-oxo-1,2,3,4-tetrahydroisoquinolin-3-yl)pivalamide (*R*)-**8e**[f]**.** White powder. Eluent: Hexane:EtOAc = 1:2. Yield 17.7 mg, 68%, 91:9 er. HPLC: Chiralpak IA-3 column (4.6 × 150 mm), heptane/i-PrOH 90:10, 1.0 ml/min; tr(major) = 14.5 min, tr (minor) = 13.9 min. HRMS (ESI): Exact mass calculated for $C_{15}H_{20}N_2O_2Na$ $[M+Na]^+$ = 283.1422, found 283.1425. ^{1}H NMR (400 MHz, DMSO-d_6) δ = 8.11 – 7.80 (m, 2H), 7.75 (d, J = 7.9 Hz, 1H), 7.25 – 7.03 (m, 2H), 5.48 – 5.36 (m, 1H), 3.18 – 2.89 (m, 2H), 2.32 (s, 3H), 1.06 (s, 9H). ^{13}C NMR (101 MHz, DMSO-d_6) δ = 177.32, 164.17, 141.86, 136.50, 128.51, 127.48, 127.12, 126.00, 56.80, 32.96, 27.18, 21.09.

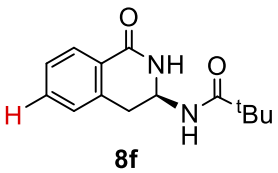

8f

(S)-N-(1-oxo-1,2,3,4-tetrahydroisoquinolin-3-yl)pivalamide (*S*)-**8f.** White powder. Eluent: Hexane:EtOAc = 1:3. Yield 14.0 mg, 57%, 77:23 er. HPLC: Chiralpak IA-3 column (4.6 × 150 mm), heptane/i-PrOH 90:10, 1.0 ml/min; tr(major) = 12.3 min, tr (minor) = 9.7 min. HRMS (ESI): Exact mass calculated for $C_{14}H_{19}N_2O_2$ $[M+H]^+$ = 247.1447, found 247.1442. ^{1}H NMR (400 MHz, DMSO-d_6) δ = 7.97 – 7.86 (m, 1H), 7.68 (s, 1H), 7.58 (d, J = 7.0 Hz, 1H), 7.43 – 7.36 (m, 1H), 7.28 (t, J = 7.5 Hz, 1H), 7.18 (d, J = 7.5 Hz, 1H), 5.53 – 5.43 (m, 1H), 3.12 (dd, J = 16.1, 5.2 Hz, 1H), 3.05 (dd, J = 16.1, 6.0 Hz, 1H), 1.05 (s, 9H). ^{13}C NMR (101 MHz, DMSO-d_6) δ = 177.89, 164.27, 135.82, 131.64, 127.96, 127.65, 126.93, 126.44, 56.81, 37.91, 32.65, 26.86.

[e] All other used N-vinyl substituted amides underwent the same reaction, albeit much slower
[f] *p(R)*-**3** was used as the catalyst

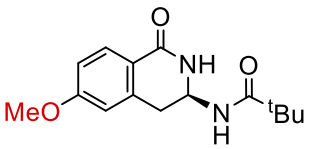

8g

(S)-N-(6-methoxy-1-oxo-1,2,3,4-tetrahydroisoquinolin-3-yl)pivalamide (*S*)-**8g.** White powder. Eluent: Hexane:EtOAc = 1:2. After chromatography the product contained a small admixture of p-methoxybenzamide (see ^{13}C NMR spectrum). Yield 15.2 mg, ~55%, 82:18 er. HPLC: Chiralpak IA-3 column (4.6 × 150 mm), heptane/i-PrOH 90:10, 1.0 ml/min; tr(major) = 16.7 min, tr (minor) = 18.6 min. HRMS (ESI): Exact mass calculated for $C_{15}H_{21}N_2O_3$ $[M+H]^+$ = 277.1552, found 277.1553. ^{1}H NMR (400 MHz, DMSO-d_6) δ = 8.07 – 7.91 (m, 2H), 7.89 – 7.63 (m, 1H), 7.00 – 6.80 (m, 2H), 5.40 (s, 1H), 3.79 (s, 3H), 3.30 – 2.87 (m, 2H), 1.06 (s, 9H). ^{13}C NMR (101 MHz, DMSO-d_6) δ = 177.34, 164.06, 162.02, 138.70, 129.10, 121.32, 112.76, 112.64, 56.86, 55.35, 38.02, 33.32, 27.18.

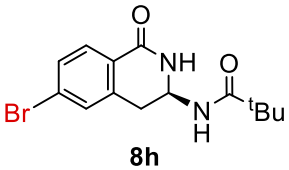

8h

(S)-N-(6-bromo-1-oxo-1,2,3,4-tetrahydroisoquinolin-3-yl)pivalamide (*S*)-**8h.** Grey powder. Eluent: Hexane:EtOAc = 1:3. Yield 13.6 mg, 42%, 87:13 er. HPLC: Chiralpak IA-3 column (4.6 × 150 mm), heptane/i-PrOH 90:10, 1.0 ml/min; tr(major) = 11.5 min, tr (minor) = 14.6 min. HRMS (ESI): Exact mass calculated for $C_{14}H_{17}N_2O_2BrNa$ $[M+Na]^+$ = 347.0371, found 347.0372. ^{1}H NMR (400 MHz, DMSO-d_6) δ = 8.28 (s, 1H), 8.03 (d, J = 7.4 Hz, 1H), 7.77 (d, J = 8.1 Hz, 1H), 7.60 – 7.48 (m, 2H), 5.48 – 5.36 (m, 1H), 3.14 (dd, J = 16.4, 5.2 Hz, 1H), 3.02 (dd, J = 16.4, 5.8 Hz, 1H), 1.05 (s, 9H). ^{13}C NMR (101 MHz, DMSO-d_6) δ = 177.28, 163.29, 139.02, 130.79, 129.81, 129.15, 127.84, 125.51, 56.50, 38.01, 32.56, 27.15.

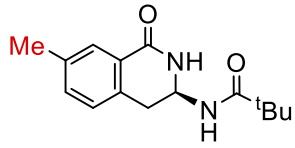

8i

(S)-N-(7-methyl-1-oxo-1,2,3,4-tetrahydroisoquinolin-3-yl)pivalamide (*S*)-**8i.** White powder. Eluent: Hexane:EtOAc = 1:2. Yield 19.9 mg, 77%, 70:30 er. HPLC: Chiralpak IA-3 column (4.6 × 150 mm), heptane/i-PrOH 90:10, 1.0 ml/min; tr(major) = 11.5 min, tr (minor) = 8.3 min. HRMS (ESI): Exact mass calculated for $C_{15}H_{20}N_2O_2Na$ $[M+Na]^+$ = 283.1422, found 283.1420. ^{1}H NMR (400 MHz, DMSO-d_6) δ = 8.10 (s, 1H), 7.96 (d, J = 7.4 Hz, 1H), 7.68 (s, 1H), 7.28 (dd, J = 7.8, 2.0 Hz, 1H), 7.17 (d, J = 7.7 Hz, 1H), 5.46 – 5.32 (m, 1H), 3.04 (dd, J = 16.0, 5.2 Hz, 1H), 2.97 (dd, J = 16.0, 6.3 Hz, 1H), 2.33 (s, 9H).^{13}C NMR (101 MHz, DMSO-d_6) δ = 177.29, 164.21, 135.85, 133.47, 132.54, 128.36, 128.02, 127.36, 56.83, 38.01, 32.64, 27.17, 20.70.

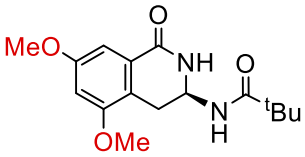

8j

(S)-N-(5,7-dimethoxy-1-oxo-1,2,3,4-tetrahydroisoquinolin-3-yl)pivalamide (*S*)-**8j.** White solid. Eluent: Hexane:EtOAc = 2:3. Yield 27.2 mg, 89%, 69:32 er. HPLC: Chiralpak IA-3 column (4.6 × 150 mm), heptane/i-PrOH 90:10, 1.0 ml/min; tr(major) = 15.2 min, tr (minor) = 12.5 min. HRMS (ESI): Exact mass calculated for $C_{16}H_{23}N_2O_4$ $[M+H]^+$ = 307.1658, found 307.1657. ^{1}H NMR (400 MHz, DMSO-d_6) δ = 8.14 (d, J = 2.8 Hz, 1H), 8.00 (d, J = 7.4 Hz, 1H), 7.02 (d, J = 2.4 Hz, 1H), 6.72 (d, J = 2.5 Hz, 1H), 5.47 – 5.31 (m, 1H), 3.79 (s, 3H), 3.79 (s, 3H), 2.87 (dd, appears as d, J = 6.1 Hz, 2H), 1.06 (s, 9H).^{13}C NMR (101 MHz, DMSO-d_6) δ = 177.30, 163.98, 158.76, 157.13, 129.90, 117.23, 102.12, 102.10, 56.55, 55.81, 55.27, 38.01, 27.17, 26.37.

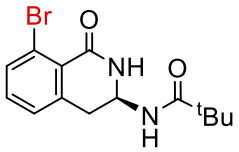

8k

(S)-N-(8-bromo-1-oxo-1,2,3,4-tetrahydroisoquinolin-3-yl)pivalamide (*S*)-**8k.** Grey powder. Eluent: Hexane:EtOAc = 1:3. Yield 3.9 mg, 12%. HRMS (ESI): Exact mass calculated for $C_{14}H_{18}N_2O_2Br$ $[M+H]^+$ = 325.0557, found 325.0550. ^{1}H NMR (300 MHz, $CDCl_3$) δ = 7.67 (d, J = 7.9 Hz, 1H), 7.40 – 7.09 (m, 2H), 6.68 (s, 1H), 6.06 (d, J = 7.5 Hz, 1H), 5.63 – 5.51 (m, 1H), 3.42 (dd, J = 15.9, 5.0 Hz, 1H), 3.01 (dd, J = 15.9, 3.8 Hz, 1H), 1.11 (s, 9H). ^{13}C NMR (101 MHz, $CDCl_3$) δ = 138.13, 135.31, 132.84, 128.02, 56.38, 34.99, 27.44. The signals of 5 quaternary carbon atoms of **8k** were not observed due to the low concentration of the sample.

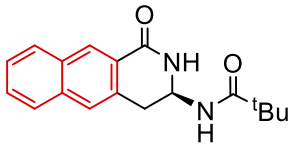

8l

(S)-N-(1-oxo-1,2,3,4-tetrahydrobenzo[g]isoquinolin-3-yl)pivalamide (*S*)-**8l.** Grey powder. Eluent: EtOAc:MeOH = 95:5. Yield 15.4 mg, 52%, 87:13 er. HPLC: Chiralpak IA-3 column (4.6 × 150 mm), heptane/i-PrOH 90:10, 1.0 ml/min; tr(major) = 21.0 min, tr (minor) = 18.6 min. HRMS (ESI): Exact mass calculated for $C_{18}H_{21}N_2O_2$ $[M+H]^+$ = 297.1603, found 297.1603. ^{1}H NMR (400 MHz, DMSO-d_6) δ = 8.50 (s, 1H), 8.36 (s, 1H), 8.07 (d, J = 8.1 Hz, 1H), 8.00 (d, J = 7.2 Hz, 1H), 7.90 (d, J = 8.2 Hz, 1H), 7.79 (s, 1H), 7.65 – 7.47 (m, 2H), 5.56 – 5.29 (m, 1H), 3.27 (dd, J = 15.9, 4.8 Hz, 1H), 3.18 (dd, J = 15.8, 5.8 Hz, 1H), 1.04 (s, 9H). ^{13}C NMR (101 MHz, DMSO-d_6) δ = 177.34, 164.03, 134.62, 132.66, 131.59, 129.11, 127.95, 127.90, 127.05, 126.26, 125.99, 56.88, 38.03, 33.39, 27.17.

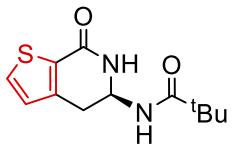

8m

(R)-N-(7-oxo-4,5,6,7-tetrahydrothieno[2,3-c]pyridin-5-yl)pivalamide (*R*)-**8m.** Grey powder. Eluent: Hexane:EtOAc = 2:1. Yield 11.6 mg, 46%, 85:15 er. HPLC: Chiralpak IA-3 column (4.6 × 150 mm), heptane/i-PrOH 90:10, 1.0 ml/min; tr(major) = 14.1 min, tr (minor) = 11.2 min. HRMS (ESI): Exact mass calculated for $C_{12}H_{17}N_2O_2S$ $[M+H]^+$ = 253.1011, found 253.1007. ^{1}H NMR (400 MHz, DMSO-d_6) δ = 8.11 (s, 1H), 7.94 (s, 1H), 7.79 (s, 1H), 7.06 (s, 1H), 5.49 (s, 1H), 3.05 (dd, J = 16.7, 5.7 Hz, 1H), 2.98 – 2.91 (m, 1H), 1.07 (s, 9H). ^{13}C NMR (101 MHz, DMSO-d_6) δ = 177.27, 161.15, 142.45, 131.32, 130.39, 127.80, 58.07, 38.01, 29.95, 27.17.

X-ray diffraction studies

X-ray diffraction data for **3** and **6a** were collected with a Bruker Quest D8 CMOS diffractometer; those of **8h-Me**, with a Bruker APEXII Quazar CCD diffractometer, both using graphite monochromated Mo-Kα radiation (λ = 0.71073 Å, ω-scans). Structures were solved using Intrinsic Phasing with the ShelXT[13] structure solution program in Olex2[14] and then refined with the XL refinement package[15] using Least-Squares minimization against F^2 in the anisotropic approximation for non-hydrogen atoms. Hydrogen atoms of NH groups in **8h-Me** were located from difference Fourier synthesis, positions of other hydrogen atoms were calculated, and they all were refined in the isotropic approximation within the riding model. Crystal data and structure refinement parameters are given in Table S2. CCDC 2324051 (**3**), 2324049 (**6a**) and 2324050 (**8h-Me**) contain the supplementary crystallographic data for this paper.

Table S2. Crystal data and structure refinement parameters for **3**, **6a** and **8hMe**.

	3	**6a**	**8h-Me**
Empirical formula	$C_{28}H_{40}Cl_4Ru_2$	$C_{35}H_{41}Cl_4OPRu$	$C_{15}H_{19}BrN_2O_2$
Formula weight	720.54	751.52	339.23
T, K	100	100	220
Crystal system	Monoclinic	Monoclinic	Monoclinic
Space group	*P2₁/c*	*P2₁*	*P2₁/c*
Z	4	2	4
a, Å	12.2863(4)	10.0658(2)	7.049(3)
b, Å	18.7694(5)	15.2520(4)	11.480(5)
c, Å	12.3374(3)	11.7038(3)	19.450(8)
α, °	90	90	90
β, °	93.047(2)	110.3460(10)	98.623(4)
γ, °	90	90	90
V, Å^3	2841.06(14)	1684.71(7)	1556.1(11)
D_{calc} (g cm^{-1})	1.685	1.481	1.448
Linear absorption, μ (cm^{-1})	14.56	8.57	26.45
F(000)	1456	772	696
$2\theta_{max}$, °	54	58	54
Reflections measured	30298	22525	24861
Independent reflections	6200	8409	6497
Observed reflections [$I > 2\sigma(I)$]	4856	7187	3457
Parameters	341	379	394
R1	0.0766	0.0431	0.0679
wR2	0.1690	0.0764	0.1504
GOF	1.183	1.019	1.059
$\Delta\rho_{max}$/ $\Delta\rho_{min}$ (e Å^{-3})	1.165/-0.942	0.466/-0.471	0.538/-0.655
Flack parameter	-	0.02(3)	0.049(12)

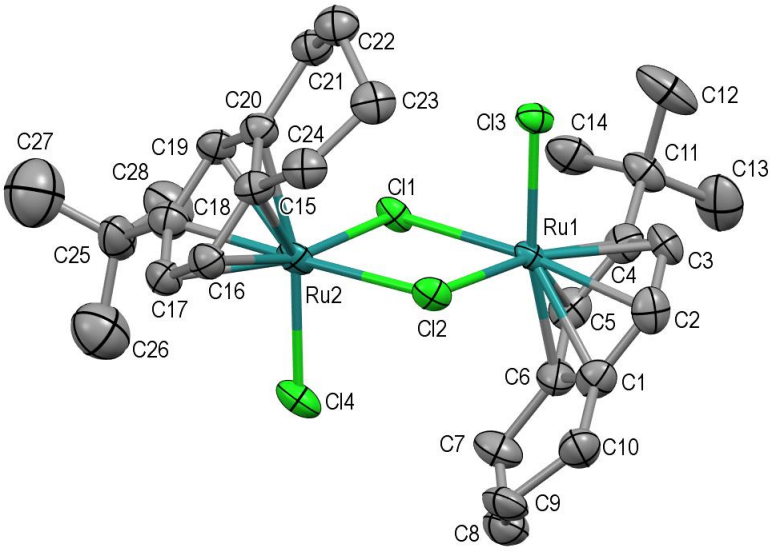

Figure S3. General view of **3** at 100K; the minor component of the disorder is not shown. Hydrogen atoms are omitted for clarity; other atoms are drawn as thermal ellipsoids at 50% probability level.

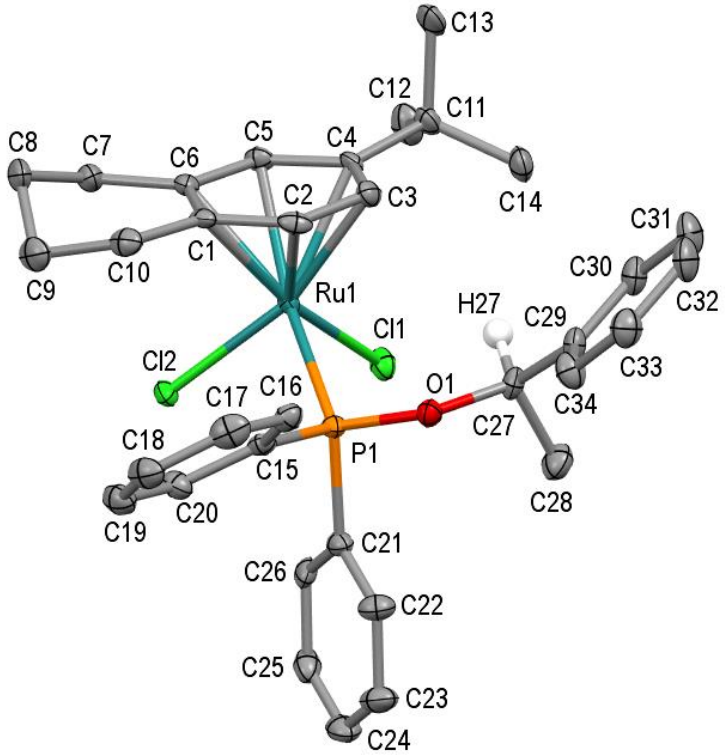

Figure S4. General view of **6a** at 100K; the minor component of the disorder and solvate CH_2Cl_2 molecule are not shown. Hydrogen atoms, except stereogenic CH, are omitted for clarity; other atoms are drawn as thermal ellipsoids at 50% probability level.

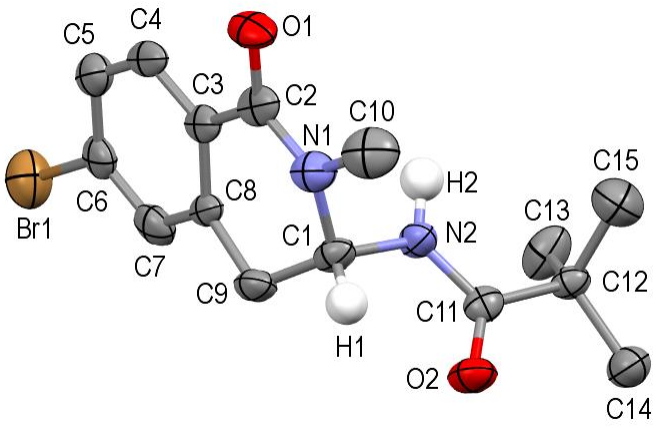

Figure S5. General view of **8h-Me** at 220K; second symmetry-independent molecule is not shown. Hydrogen atoms, except NH and stereogenic CH, are omitted for clarity; other atoms are drawn as thermal ellipsoids at 50% probability level.

DFT calculations

All calculations were carried out using Orca 5.0.3 software.[16] Composite B97-3c method was used for geometry optimization.[17] Solvation was taken into account using CPCM model (hexafluoro-2-propanol solvent parameters: dielectric constant 16.7, refractive index 1.275). Transition states were optimized via initial relaxed surface scans. The optimized geometries were verified to have no negative frequencies for all intermediates and only one negative frequency for transition states. Visualization was carried out using ChemCraft 1.8 software (http://www.chemcraftprog.com/). Cartesian coordinates and energies of the optimized structures are available in ESI as combined xyz file.

Although the results of the calculations correlate with the experimental findings they should be considered as estimates and treated with caution. The main source of potential errors is the specific solvation of molecules by hexafluoro-2-propanol via hydrogen bonding, which cannot be taken into account correctly by usual computational methods. Hopefully, the specific solvation is similar for isomeric structures, so the errors in relative energies are not so pronounced. It should be also noted, that accurate estimation of enantioselectivity requires extensive calculations with consideration of various conformations of transition states,[18] which are far beyond this work.

The reactions of the metallacycle intermediate with different alkenes were analyzed using the simplified models with C_6H_6 representing arene ligand **1**, N-vinyl-acetamide representing N-vinyl-pivaloylamide, and propene representing 1-hexene (Figure S6).

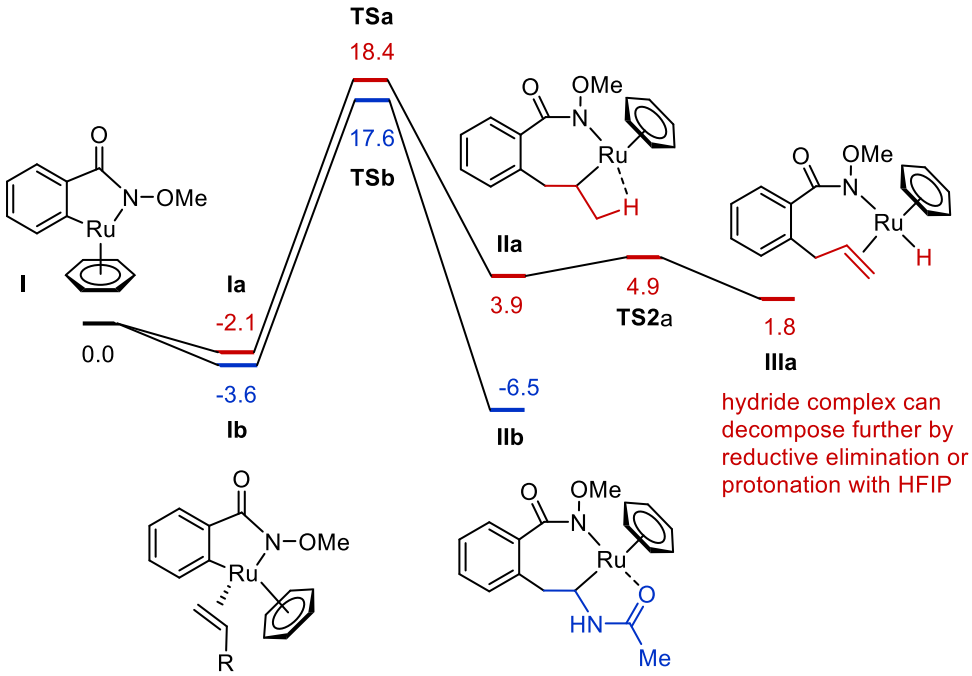

Figure S6. Energy profile for interaction of the model metallacycle intermediate with propene and N-vinyl-acetamide. Free energies are given in kcal mol^{-1} at 298 K relative to the starting reagents.

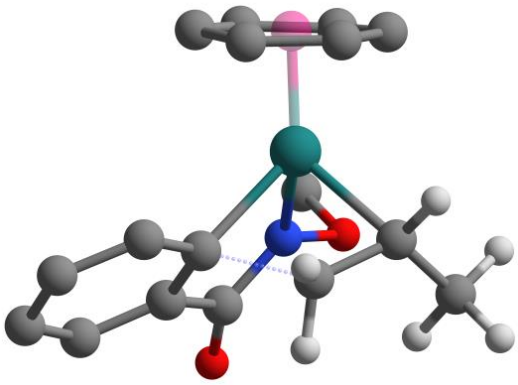

TSa

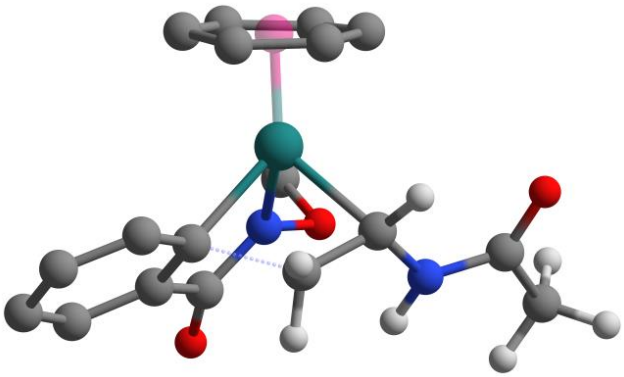

TSb

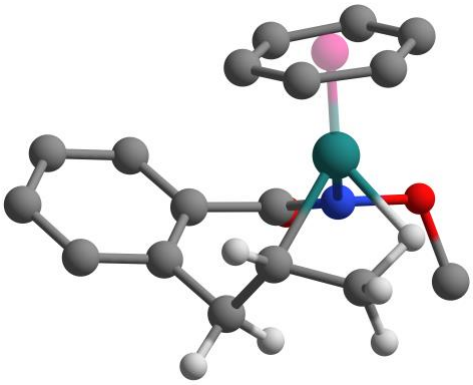

IIa

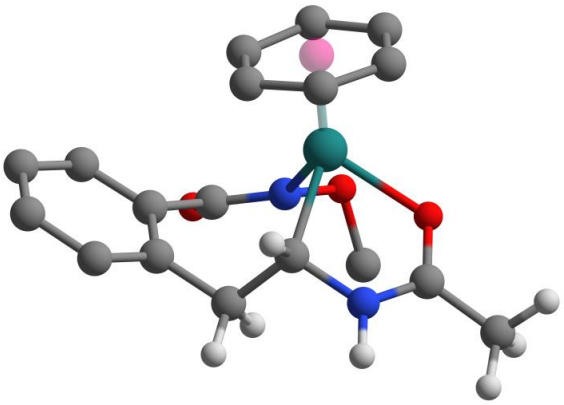

IIb

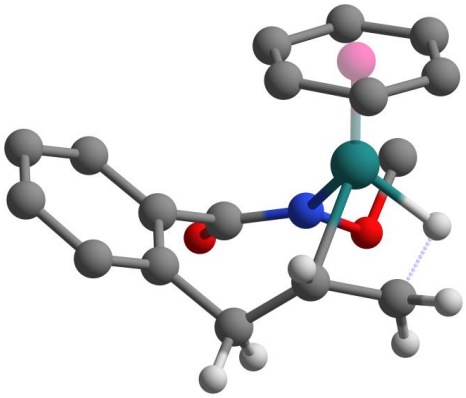

TS2a

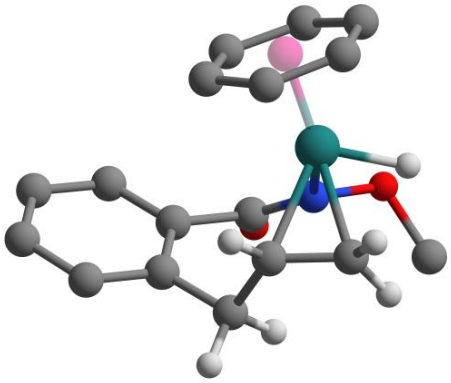

IIIa

Figure S7. Optimized structures of the key intermediates and transition states. Hydrogen atoms of the C_6H_6 ring and N-methoxy-benzamide are omitted for clarity. Dummy atom is inserted in the center of the coordinated arene ring for illustration.

The stereochemistry of interaction of the metallacycle intermediate **B** with N-vinyl-pivaloylamide was analyzed by calculating the energies of two conformers **B1** and **B2** and four possible transition states, that can originate from these conformers (Figure S8).

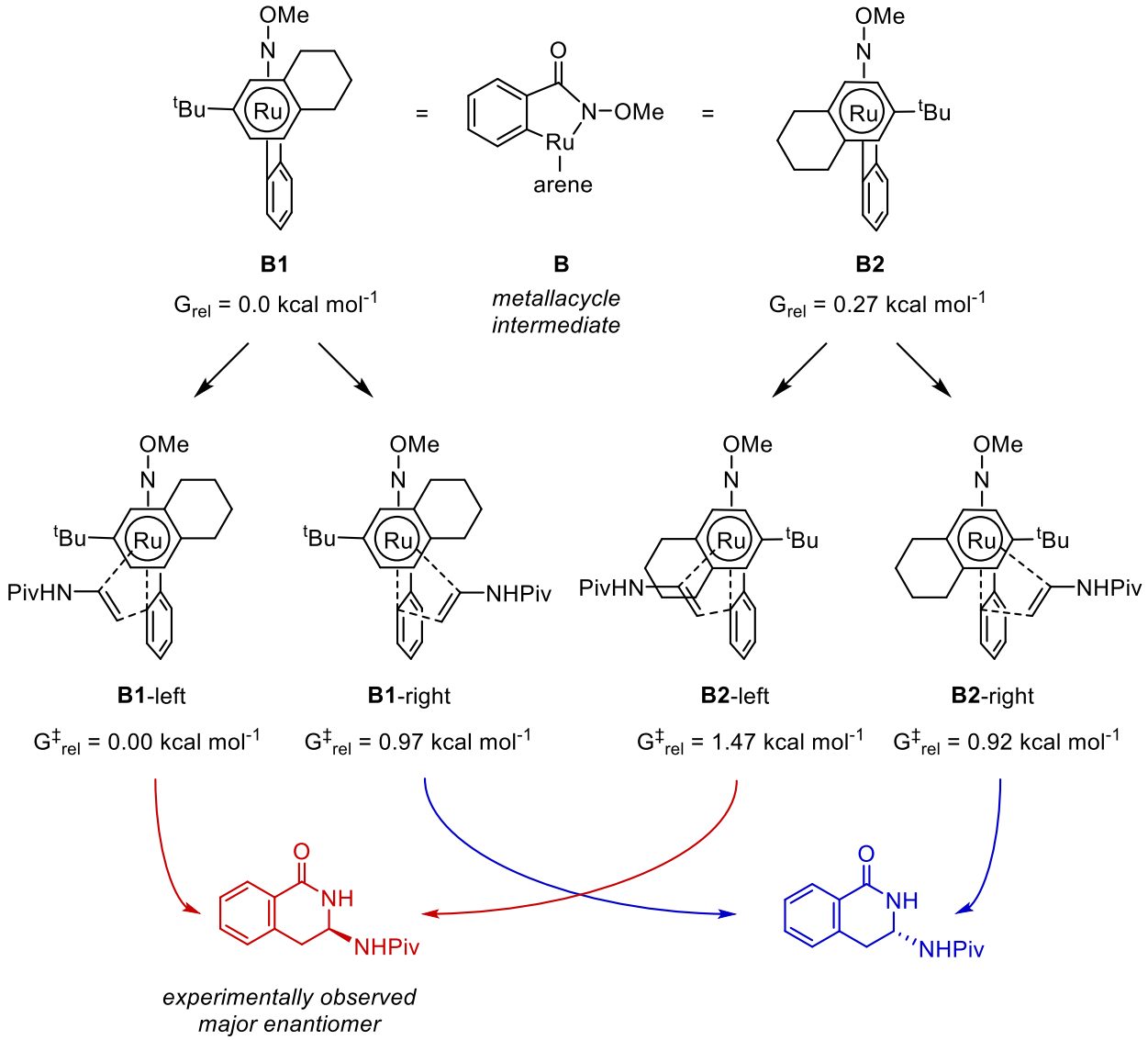

Figure S8. Comparison of energies of possible transition states for the stereo-determining step of the catalytic reaction. Free energies are given in kcal mol^{-1} at 298 K relative to the most stable conformer.

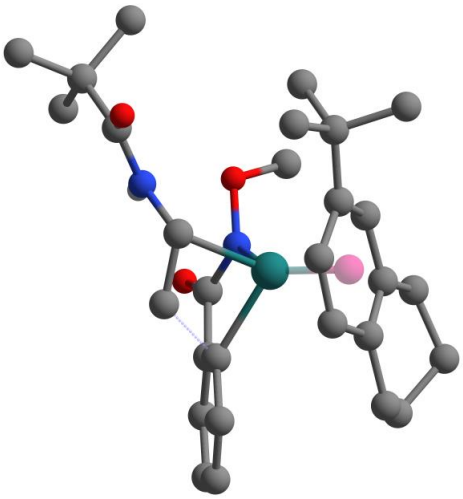

B1-left

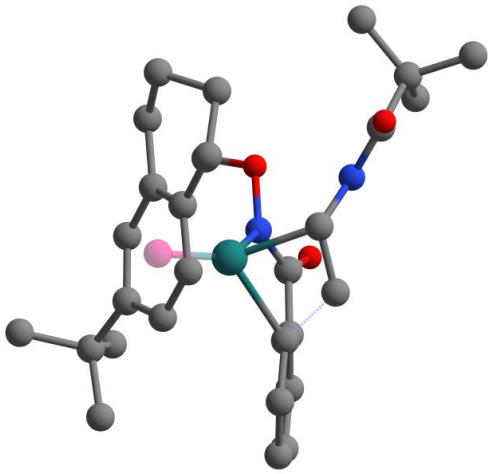

B1-right

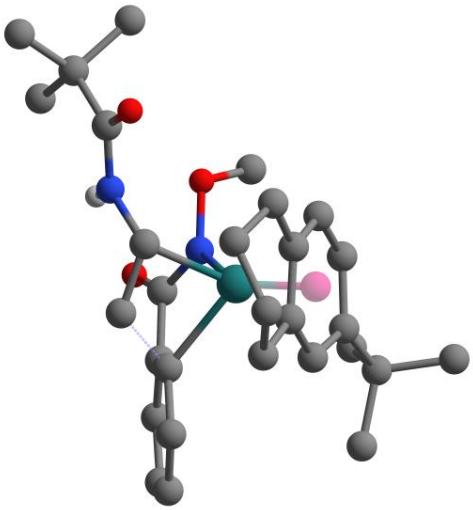

B2-left

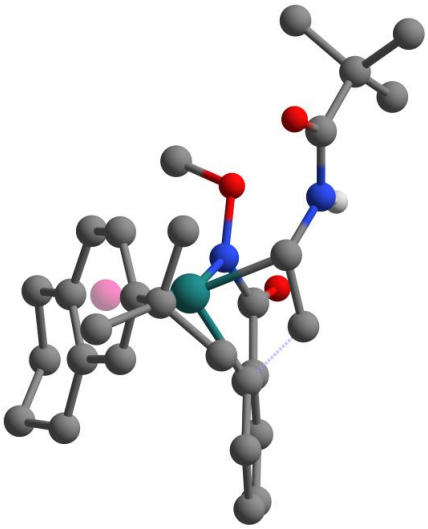

B2-right

Figure S9. Optimized structures of the transition states. All hydrogen atoms, except NH are omitted for clarity. Dummy atom is inserted in the center of the coordinated arene ring for illustration.

References

1 C.-Q. Wang, L. Ye, C. Feng and T.-P. Loh, *J. Am. Chem. Soc.*, 2017, **139**, 1762–1765.

2 E. J. Corey, R. K. Bakshi and S. Shibata, *J. Am. Chem. Soc.*, 1987, **109**, 5551–5553.

3 Y. Zhang, S. Torker, M. Sigrist, N. Bregović and P. Dydio, *J. Am. Chem. Soc.*, 2020, **142**, 18251–18265.

4 S. Tu and C. Zhang, *Org. Process Res. Dev.*, 2015, **19**, 2045–2049.

5 M. Makarova, O. I. Afanasyev, F. Kliuev, Y. V. Nelyubina, M. Godovikova and D. Chusov, *J. Organomet. Chem.*, 2021, **941**, 121806.

6 A. Pan, M. Chojnacka, R. Crowley, L. Göttemann, B. E. Haines and K. G. M. Kou, *Chem. Sci.*, 2022, **13**, 3539–3548.

7 O. N. Gorunova, I. M. Novitskiy, M. V. Livantsov, Y. K. Grishin, K. A. Kochetkov and V. V. Dunina, *J. Organomet. Chem.*, 2015, **783**, 96–104.

8 K. Masutani, T. Minowa, Y. Hagiwara and T. Mukaiyama, *Bull. Chem. Soc. Jpn.*, 2006, **79**, 1106–1117.

9 P. Pertici, S. Bertozzi, R. Lazzaroni, G. Vitulli and M. A. Bennett, *J. Organomet. Chem.*, 1988, **354**, 117–121.

10 D. Laws, C. D. Poff, E. M. Heyboer and S. B. Blakey, *Chem. Soc. Rev.*, 2023, **52**, 6003–6030.

11 H. Zhai, M. Liu, C. Wang, S. Qiu, J. Wei, H. Yang and Y. Wu, *J. Org. Chem.*, 2021, **86**, 14915–14927.

12 C. K. Giri, S. Dana and M. Baidya, *Chem. Commun.*, 2021, **57**, 10536–10539.

13 G. M. Sheldrick, *Acta Crystallogr. A*, 2015, **71**, 3–8.

14 O. V. Dolomanov, L. J. Bourhis, R. J. Gildea, J. A. K. Howard and H. Puschmann, *J. Appl. Crystallogr.*, 2009, **42**, 339–341.

15 G. M. Sheldrick, *Acta Crystallogr. Sect. A*, 2008, **64**, 112–122.

16 F. Neese, *WIREs Comput. Mol. Sci.*, 2022, **12**, e1606.

17 J. G. Brandenburg, C. Bannwarth, A. Hansen and S. Grimme, *J. Chem. Phys.*, 2018, **148**, 64104.

18 R. Laplaza, J.-G. Sobez, M. D. Wodrich, M. Reiher and C. Corminboeuf, *Chem. Sci.*, 2022, **13**, 6858–6864.

Chiral HPLC data

8a racemate

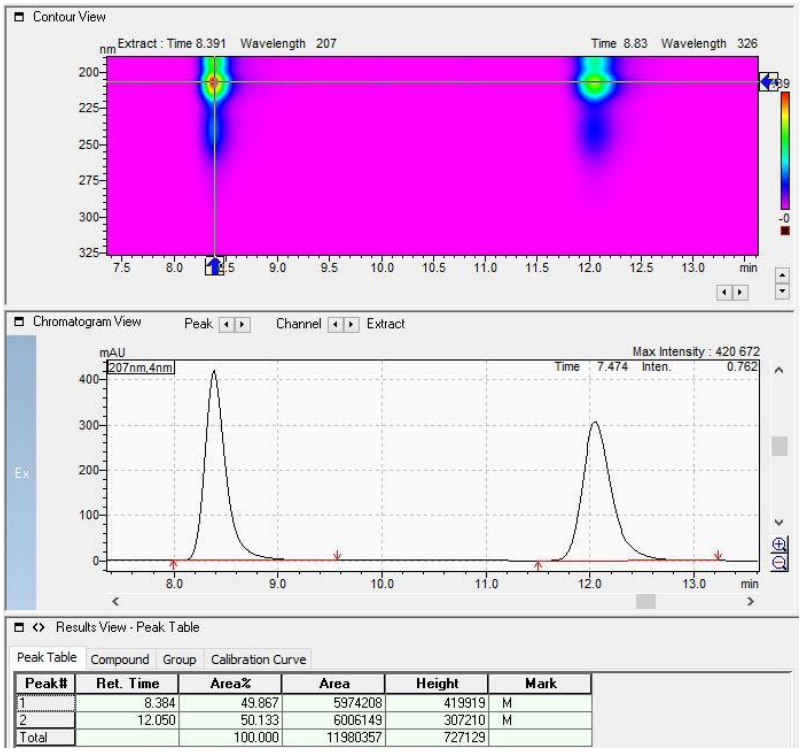

Peak#	Ret. Time	Area%	Area	Height	Mark
1	8.384	49.867	5974208	419919	M
2	12.050	50.133	6006149	307210	M
Total		100.000	11980357	727129	

(*S*)-**8a** chiral compound

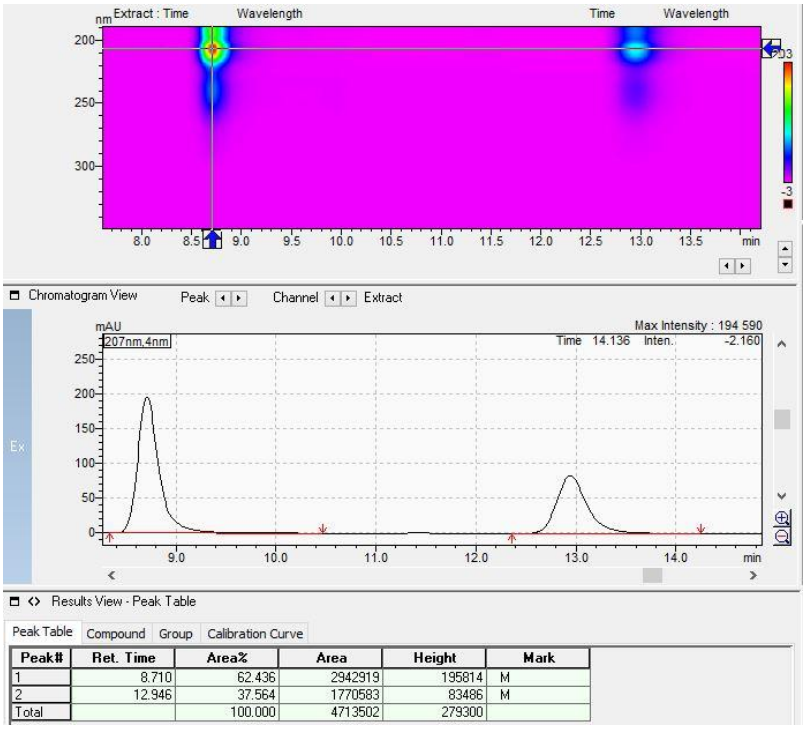

Peak#	Ret. Time	Area%	Area	Height	Mark
1	8.710	62.436	2942919	195814	M
2	12.946	37.564	1770583	83486	M
Total		100.000	4713502	279300	

8b racemate

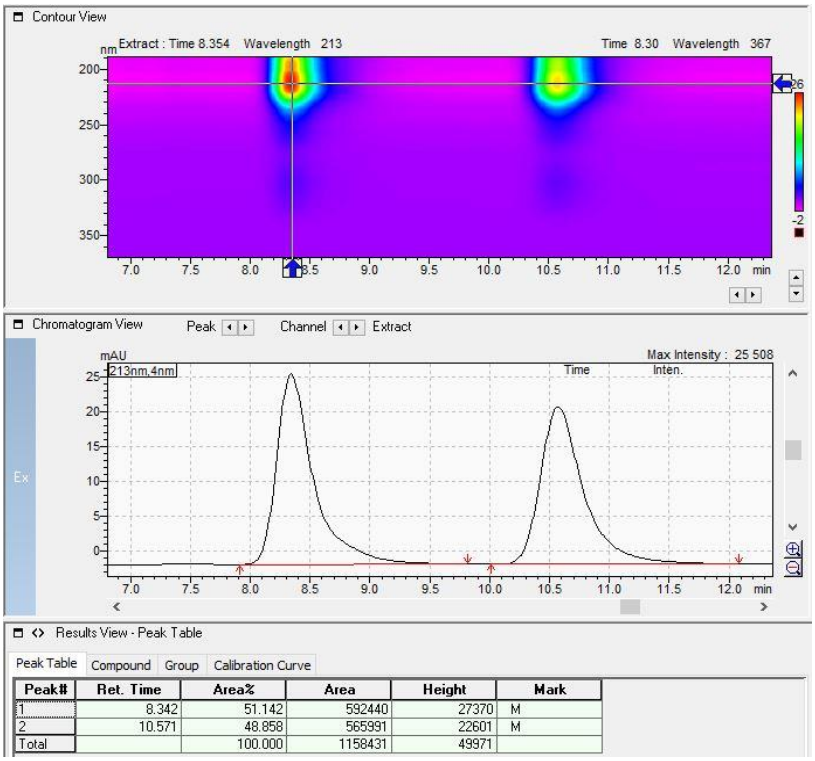

Peak#	Ret. Time	Area%	Area	Height	Mark
1	8.342	51.142	592440	27370	M
2	10.571	48.858	565991	22601	M
Total		100.000	1158431	49971	

(*S*)-**8b** chiral compound

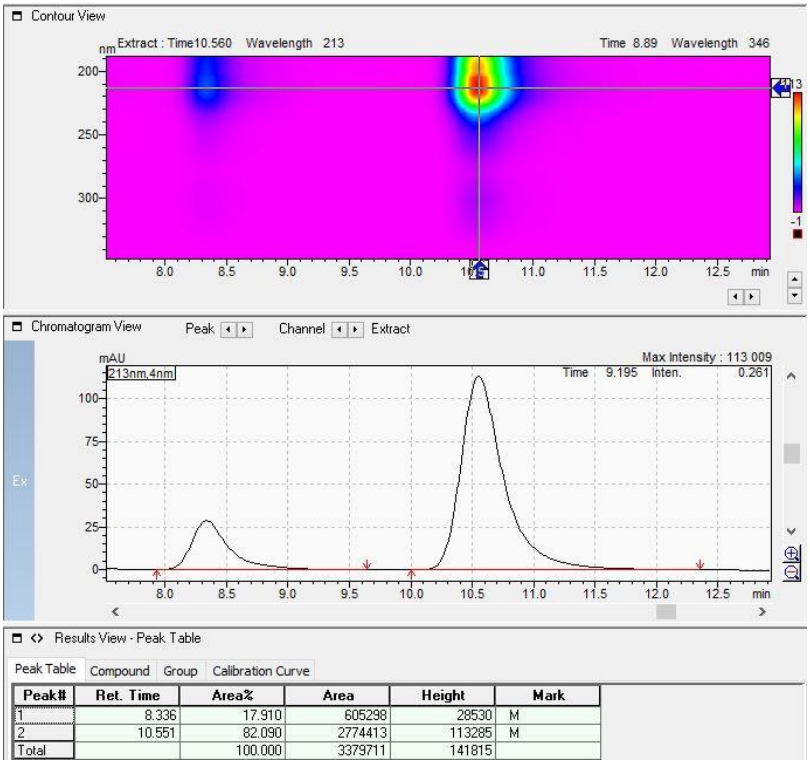

Peak#	Ret. Time	Area%	Area	Height	Mark
1	8.336	17.910	605298	28530	M
2	10.551	82.090	2774413	113285	M
Total		100.000	3379711	141815	

8c racemate

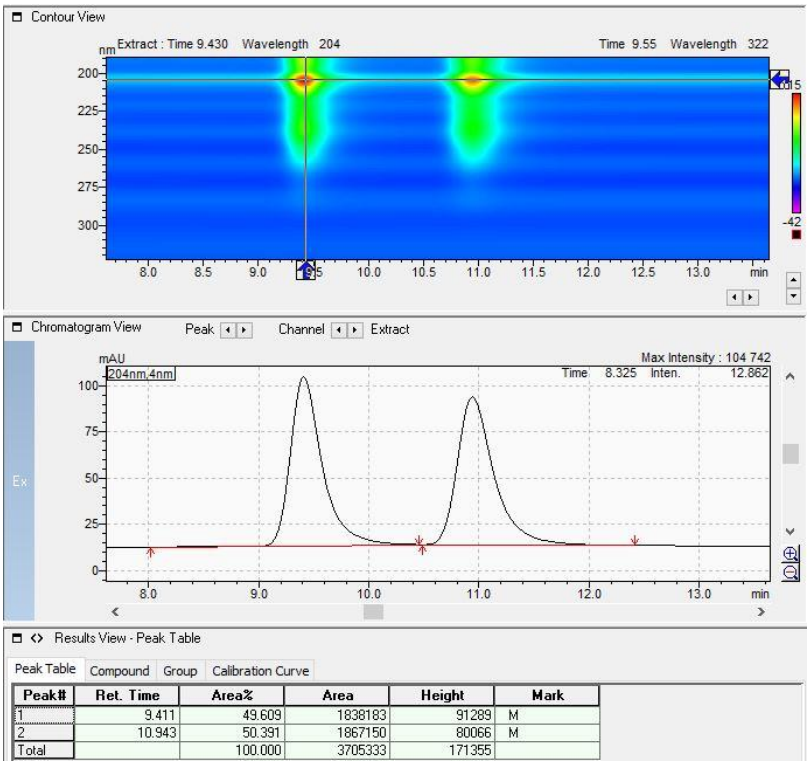

Peak#	Ret. Time	Area%	Area	Height	Mark
1	9.411	49.609	1838183	91289	M
2	10.943	50.391	1867150	80066	M
Total		100.000	3705333	171355	

(*S*)-**8c** chiral compound

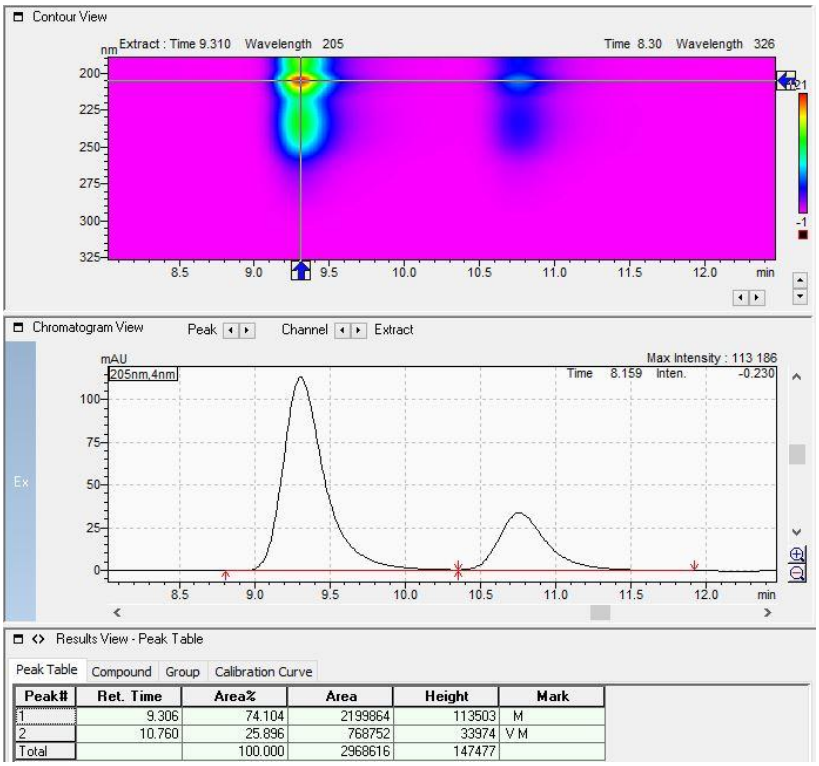

Peak#	Ret. Time	Area%	Area	Height	Mark
1	9.306	74.104	2199864	113503	M
2	10.760	25.896	768752	33974	V M
Total		100.000	2968616	147477	

8d racemate

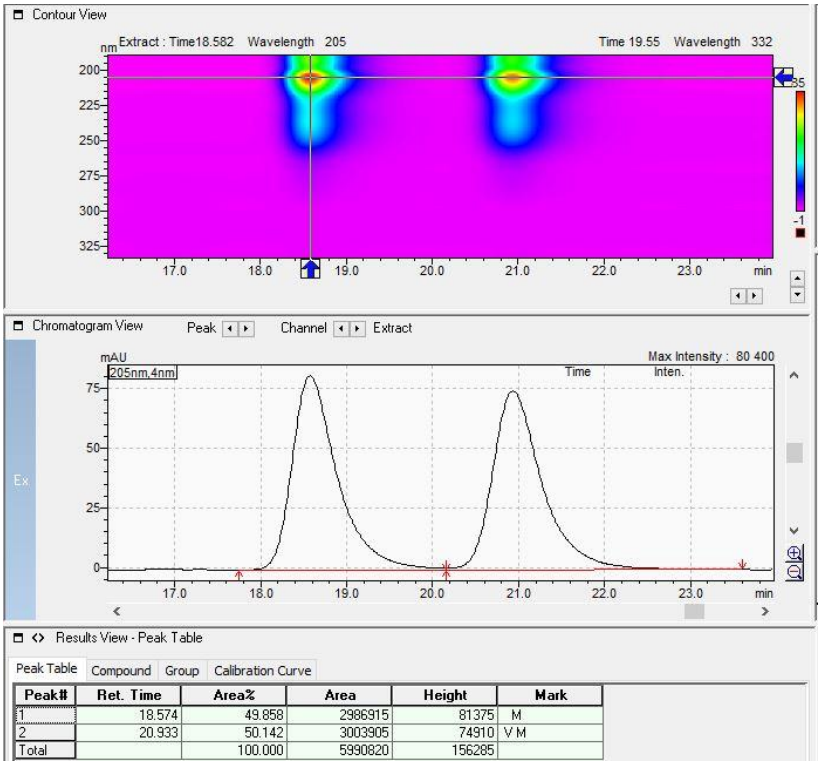

Peak#	Ret. Time	Area%	Area	Height	Mark
1	18.574	49.858	2986915	81375	M
2	20.933	50.142	3003905	74910	V M
Total		100.000	5990820	156285	

(*S*)-**8d** chiral compound

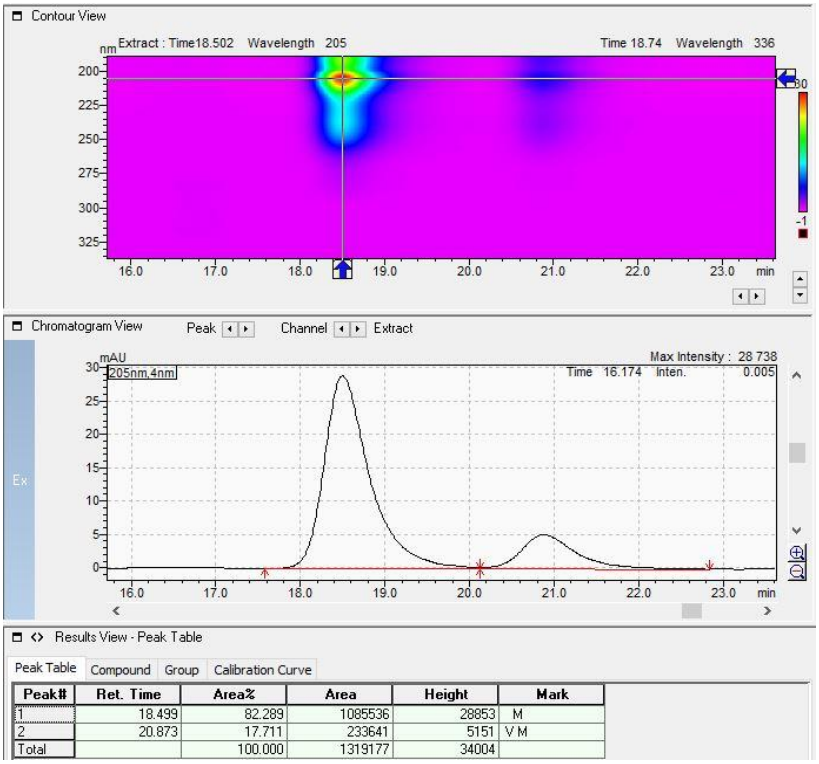

Peak#	Ret. Time	Area%	Area	Height	Mark
1	18.499	82.289	1085536	28853	M
2	20.873	17.711	233641	5151	V M
Total		100.000	1319177	34004	

8e racemate

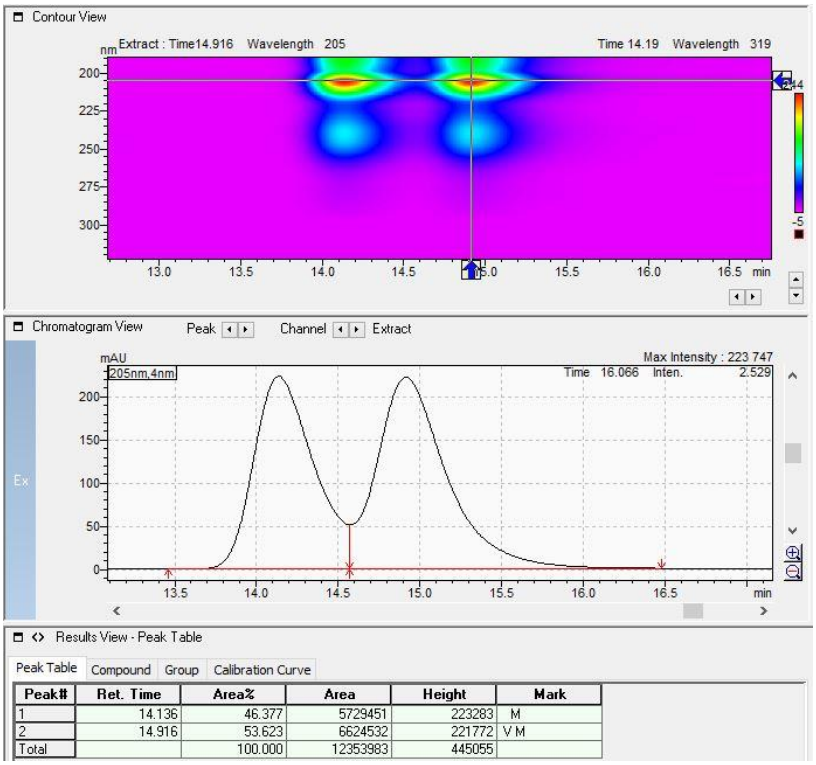

Peak#	Ret. Time	Area%	Area	Height	Mark
1	14.136	46.377	5729451	223283	M
2	14.916	53.623	6624532	221772	V M
Total		100.000	12353983	445055	

(*R*)-**8e** chiral compound

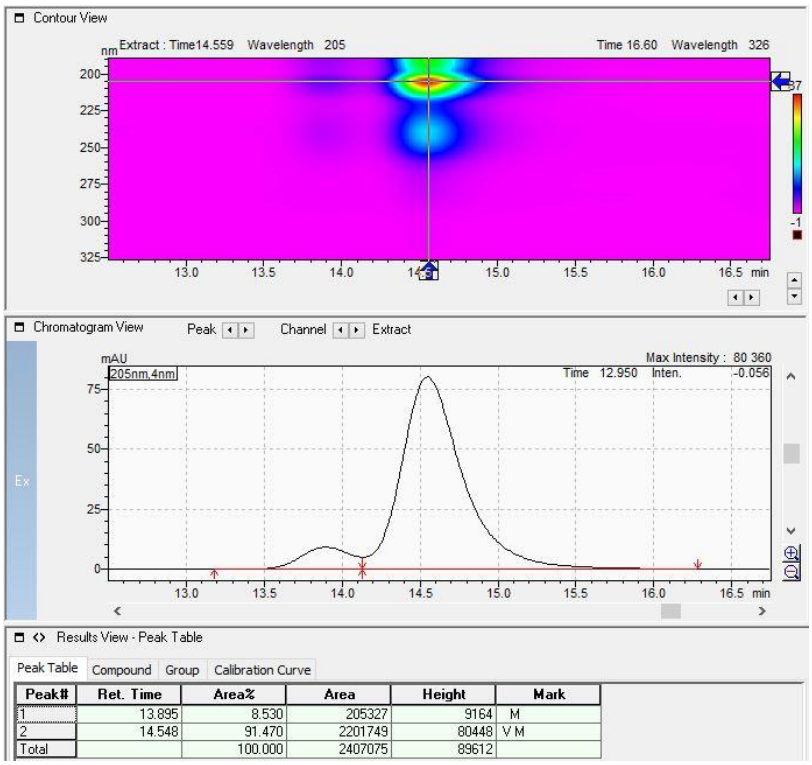

Peak#	Ret. Time	Area%	Area	Height	Mark
1	13.895	8.530	205327	9164	M
2	14.548	91.470	2201749	80448	V M
Total		100.000	2407075	89612	

8f racemate

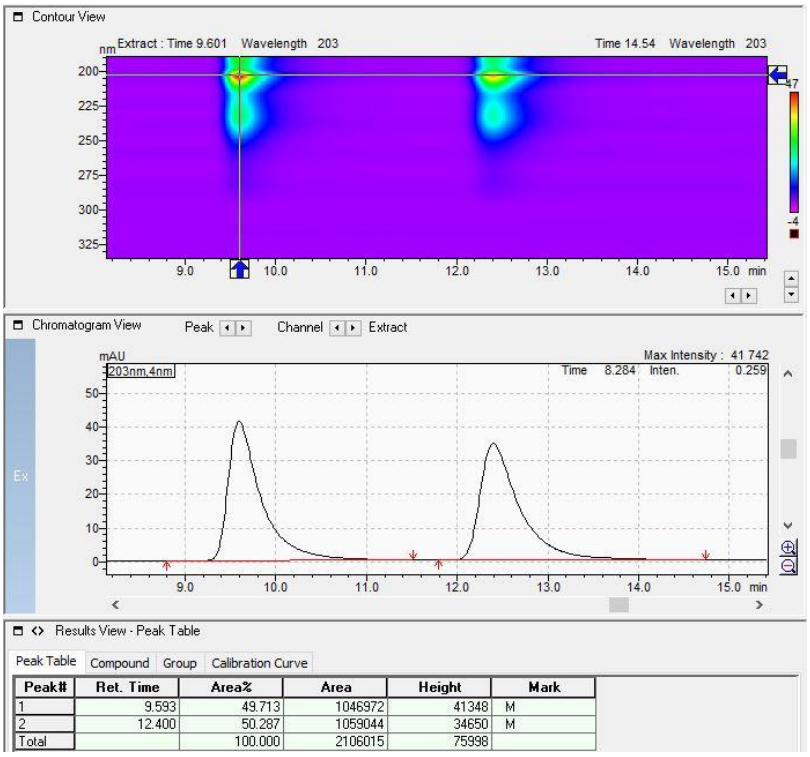

Peak#	Ret. Time	Area%	Area	Height	Mark
1	9.593	49.713	1046972	41348	M
2	12.400	50.287	1059044	34650	M
Total		100.000	2106015	75998	

(*S*)-**8f** chiral compound

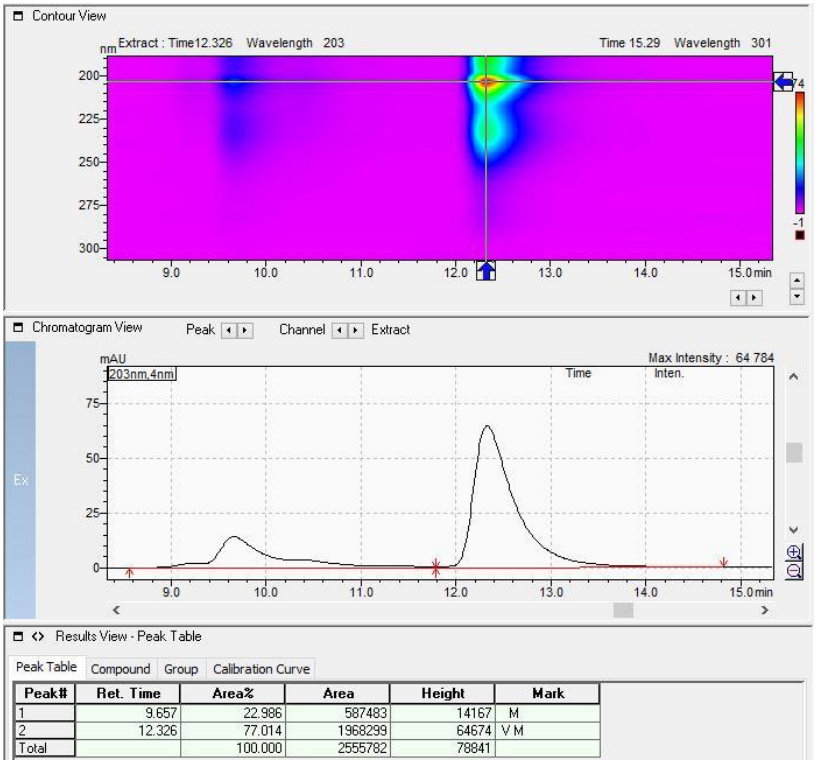

Peak#	Ret. Time	Area%	Area	Height	Mark
1	9.657	22.986	587483	14167	M
2	12.326	77.014	1968299	64674	V M
Total		100.000	2555782	78841	

8g racemate

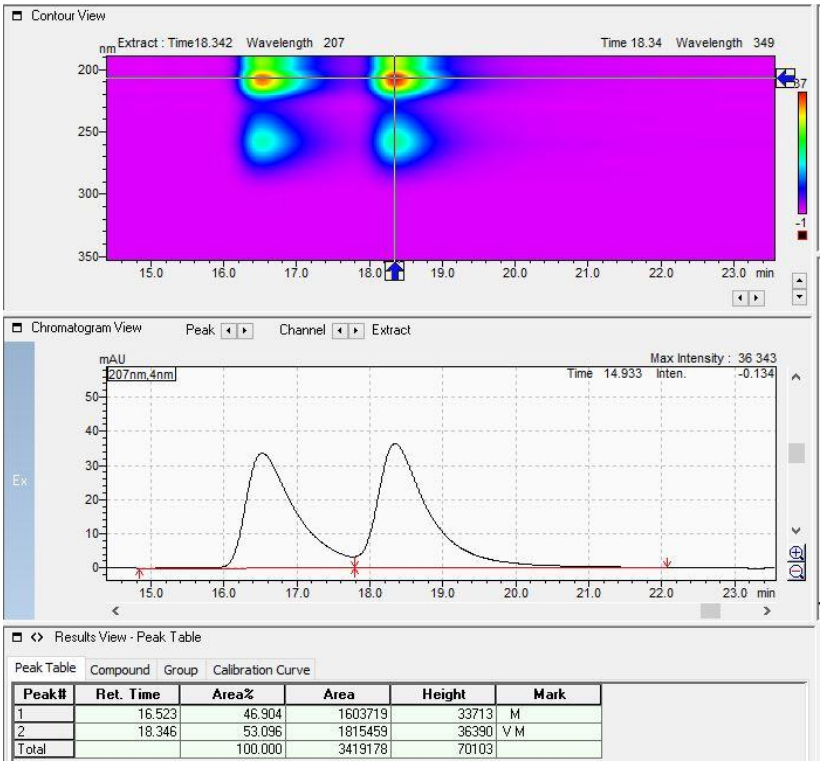

Peak#	Ret. Time	Area%	Area	Height	Mark
1	16.523	46.904	1603719	33713	M
2	18.346	53.096	1815459	36390	V M
Total		100.000	3419178	70103	

(*S*)-**8g** chiral compound

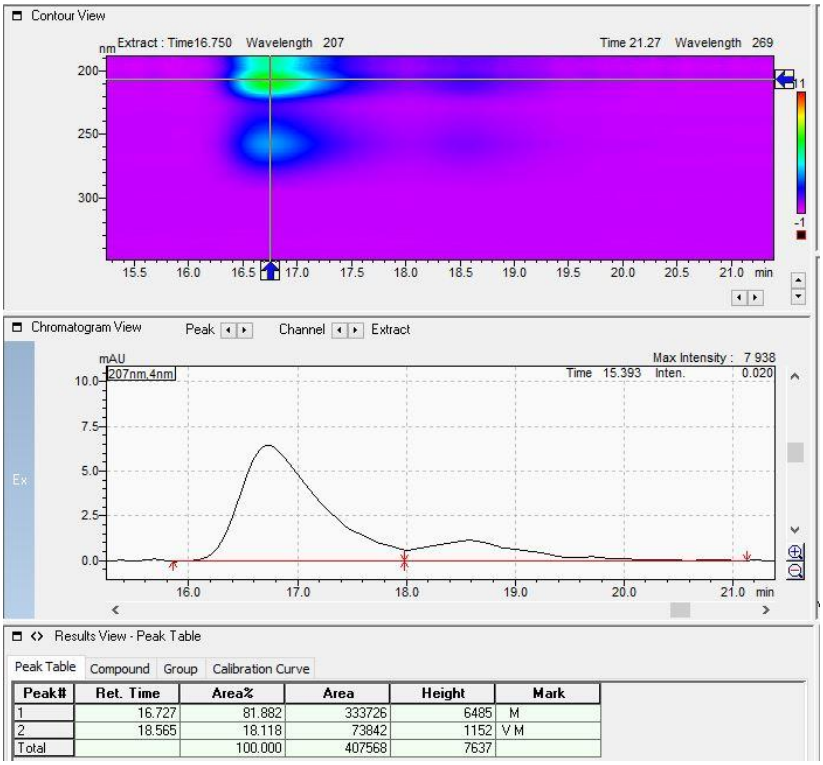

Peak#	Ret. Time	Area%	Area	Height	Mark
1	16.727	81.882	333726	6485	M
2	18.565	18.118	73842	1152	V M
Total		100.000	407568	7637	

8h racemate

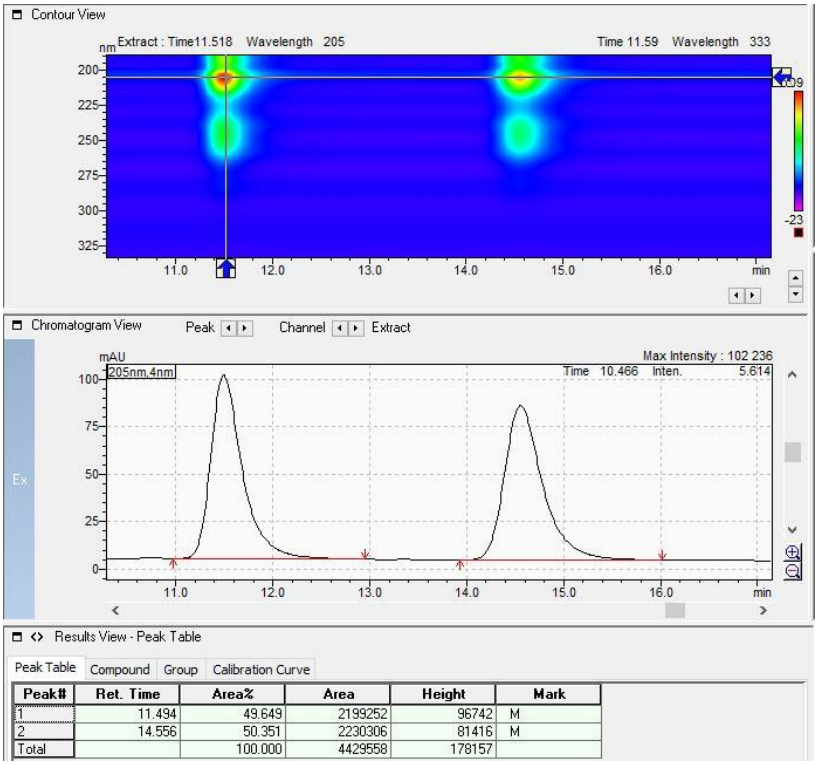

Peak#	Ret. Time	Area%	Area	Height	Mark
1	11.494	49.649	2199252	96742	M
2	14.556	50.351	2230306	81416	M
Total		100.000	4429558	178157	

(*S*)-**8h** chiral compound

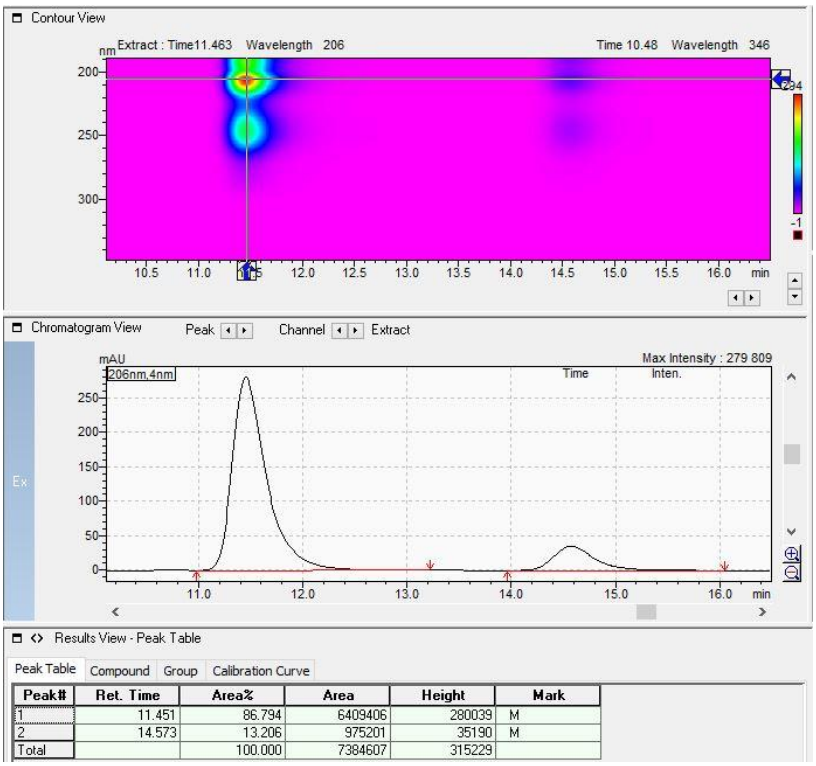

Peak#	Ret. Time	Area%	Area	Height	Mark
1	11.451	86.794	6409406	280039	M
2	14.573	13.206	975201	35190	M
Total		100.000	7384607	315229	

8i racemate

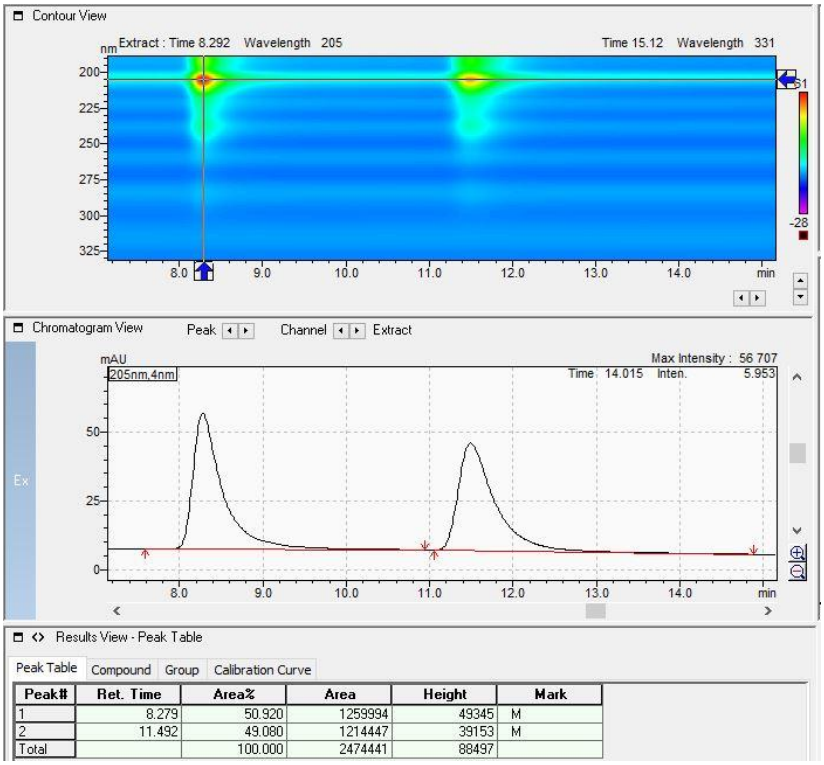

Peak#	Ret. Time	Area%	Area	Height	Mark
1	8.279	50.920	1259994	49345	M
2	11.492	49.080	1214447	39153	M
Total		100.000	2474441	88497	

(*S*)-**8i** chiral compound

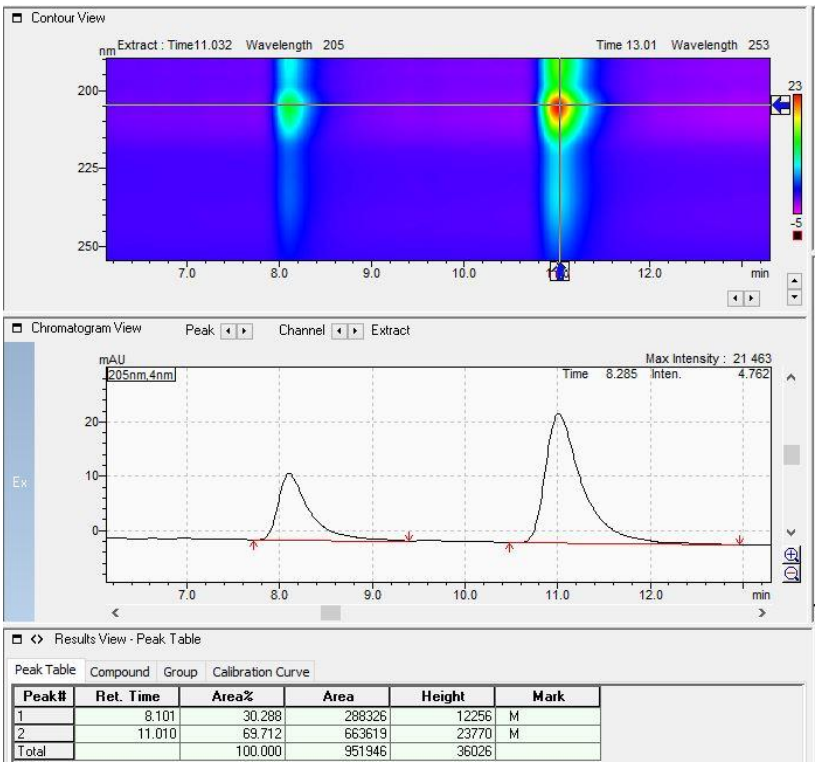

Peak#	Ret. Time	Area%	Area	Height	Mark
1	8.101	30.288	288326	12256	M
2	11.010	69.712	663619	23770	M
Total		100.000	951946	36026	

8j racemate

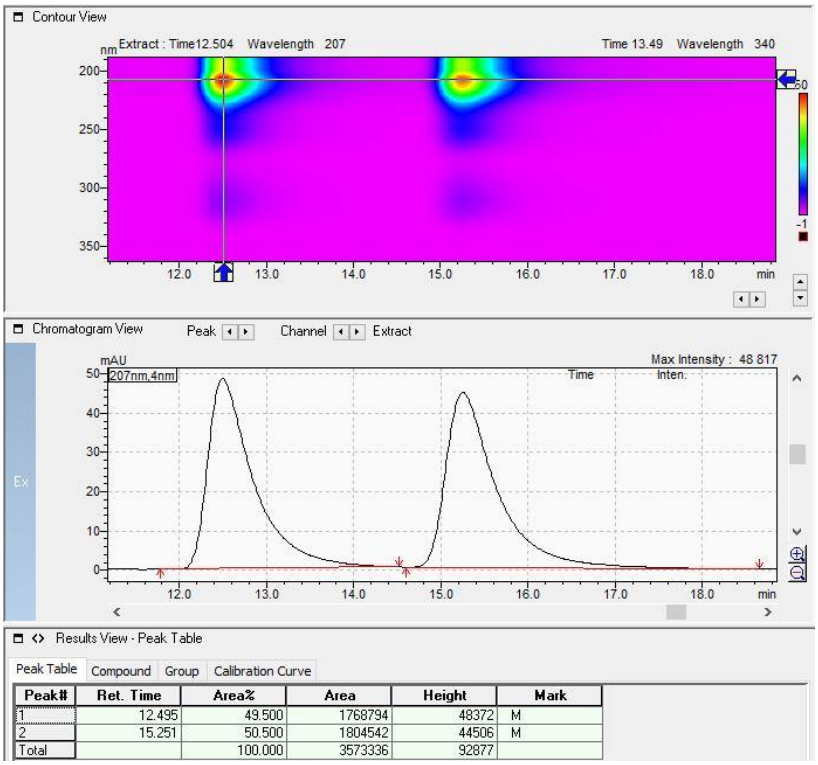

Peak#	Ret. Time	Area%	Area	Height	Mark
1	12.495	49.500	1768794	48372	M
2	15.251	50.500	1804542	44506	M
Total		100.000	3573336	92877	

(*S*)-**8j** chiral compound

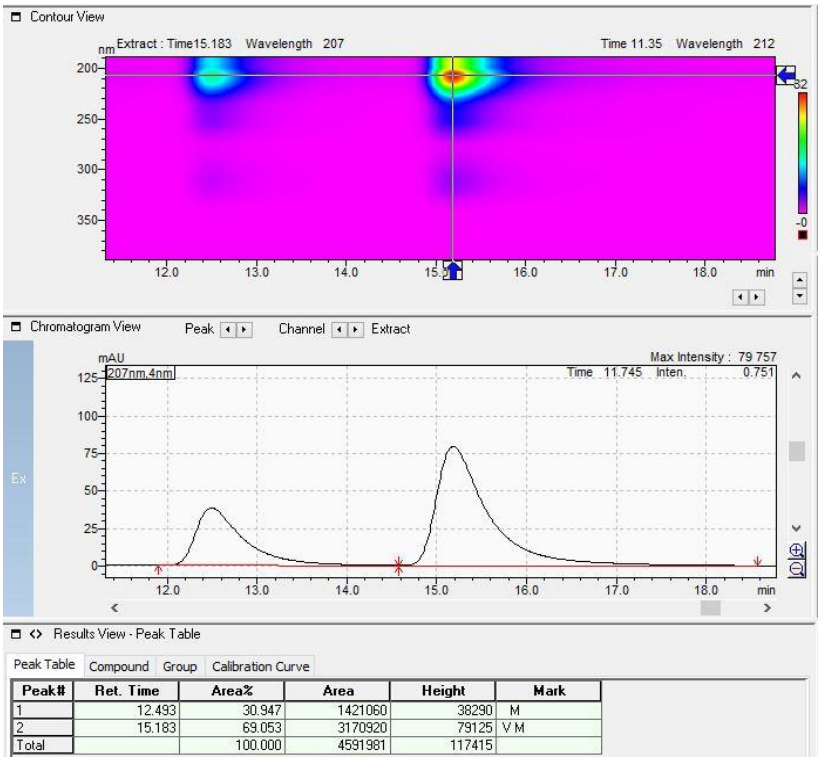

Peak#	Ret. Time	Area%	Area	Height	Mark
1	12.493	30.947	1421060	38290	M
2	15.183	69.053	3170920	79125	V M
Total		100.000	4591981	117415	

8l racemate

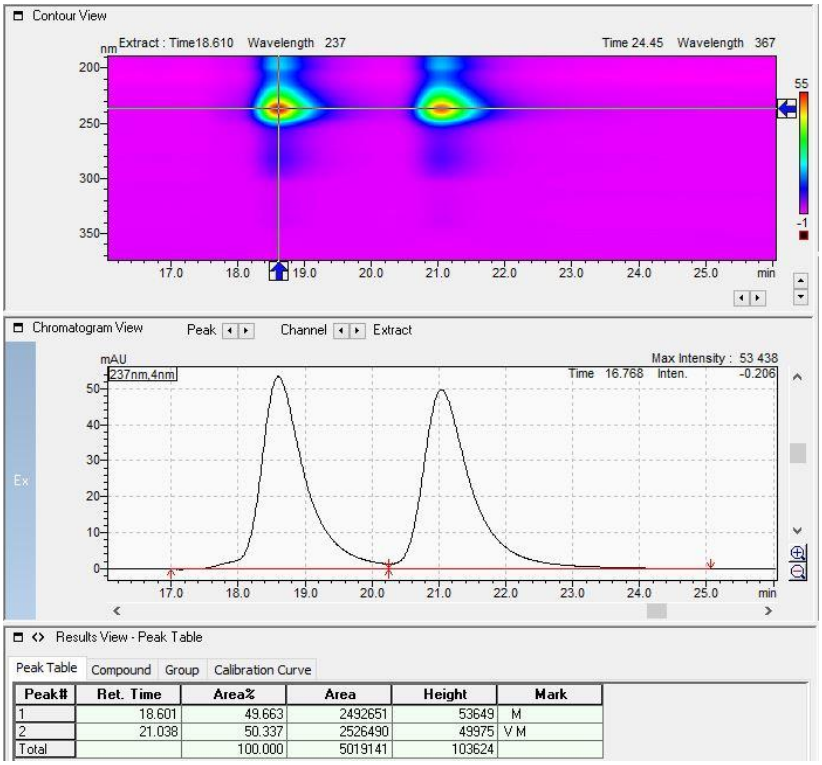

Peak#	Ret. Time	Area%	Area	Height	Mark
1	18.601	49.663	2492651	53649	M
2	21.038	50.337	2526490	49975	V M
Total		100.000	5019141	103624	

(*S*)-**8l** chiral compound

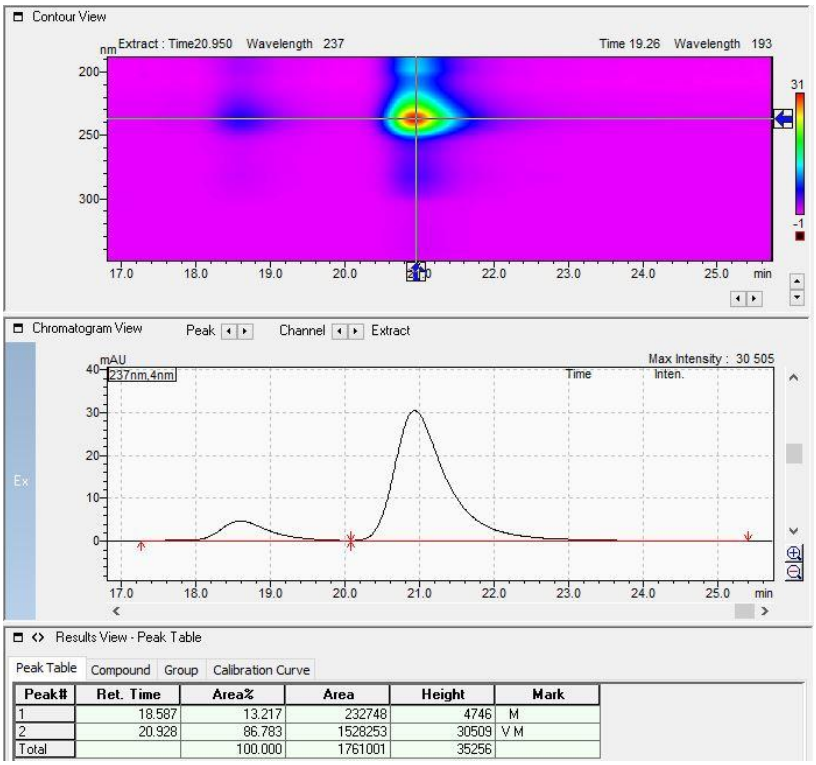

Peak#	Ret. Time	Area%	Area	Height	Mark
1	18.587	13.217	232748	4746	M
2	20.928	86.783	1528253	30509	V M
Total		100.000	1761001	35256	

(*S*)-**8l** after attempted racemization

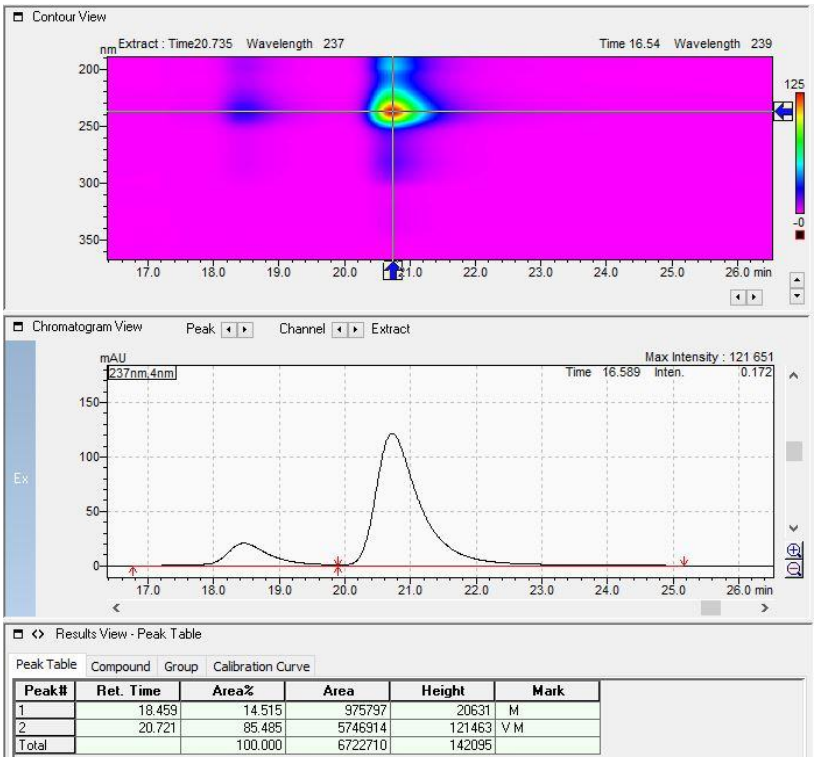

Peak#	Ret. Time	Area%	Area	Height	Mark
1	18.459	14.515	975797	20631	M
2	20.721	85.485	5746914	121463	V M
Total		100.000	6722710	142095	

8m racemate

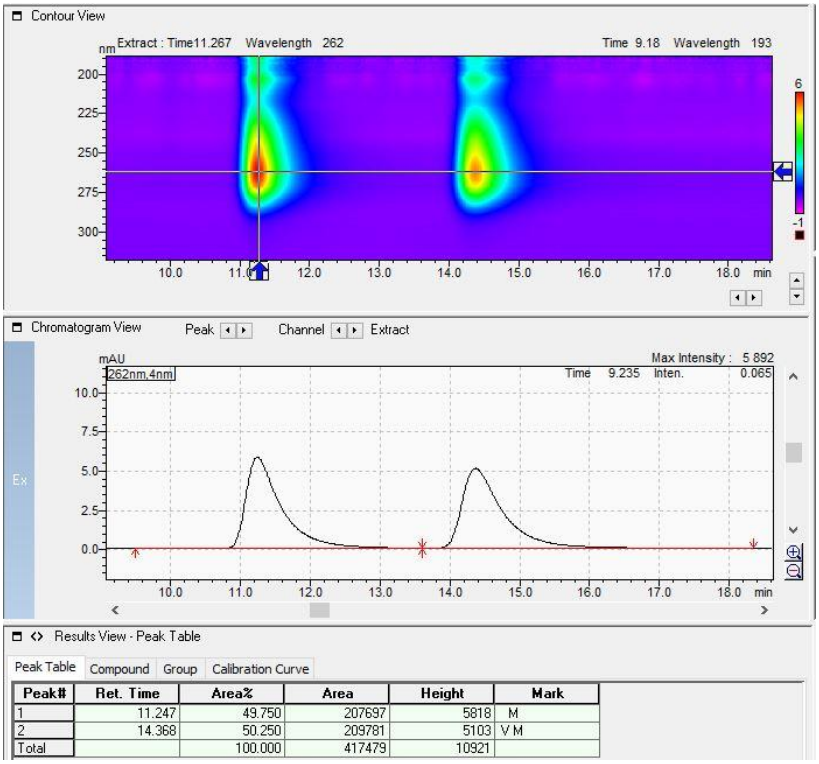

Peak#	Ret. Time	Area%	Area	Height	Mark
1	11.247	49.750	207697	5818	M
2	14.368	50.250	209781	5103	V M
Total		100.000	417479	10921	

(*R*)-**8m** chiral compound

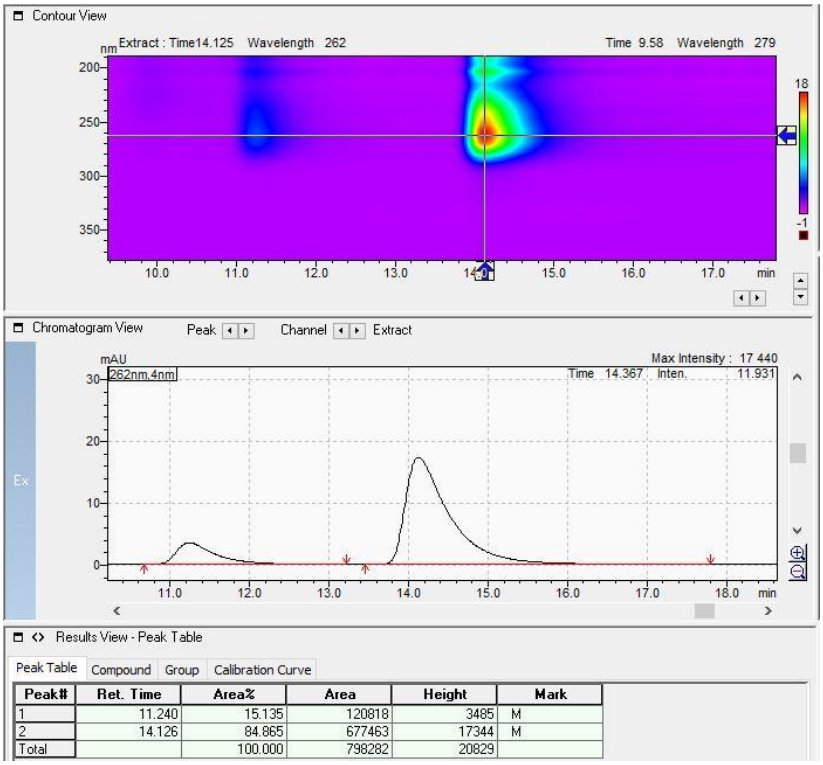

Results View - Peak Table

Peak Table | Compound | Group | Calibration Curve

Peak#	Ret. Time	Area%	Area	Height	Mark
1	11.240	15.135	120818	3485	M
2	14.126	84.865	677463	17344	M
Total		100.000	798282	20829	

Copies of NMR spectra

^{1}H NMR spectrum of 6-Tert-butyl-1,2,3,4-tetrahydronaphthalene (**1**) in $CDCl_3$

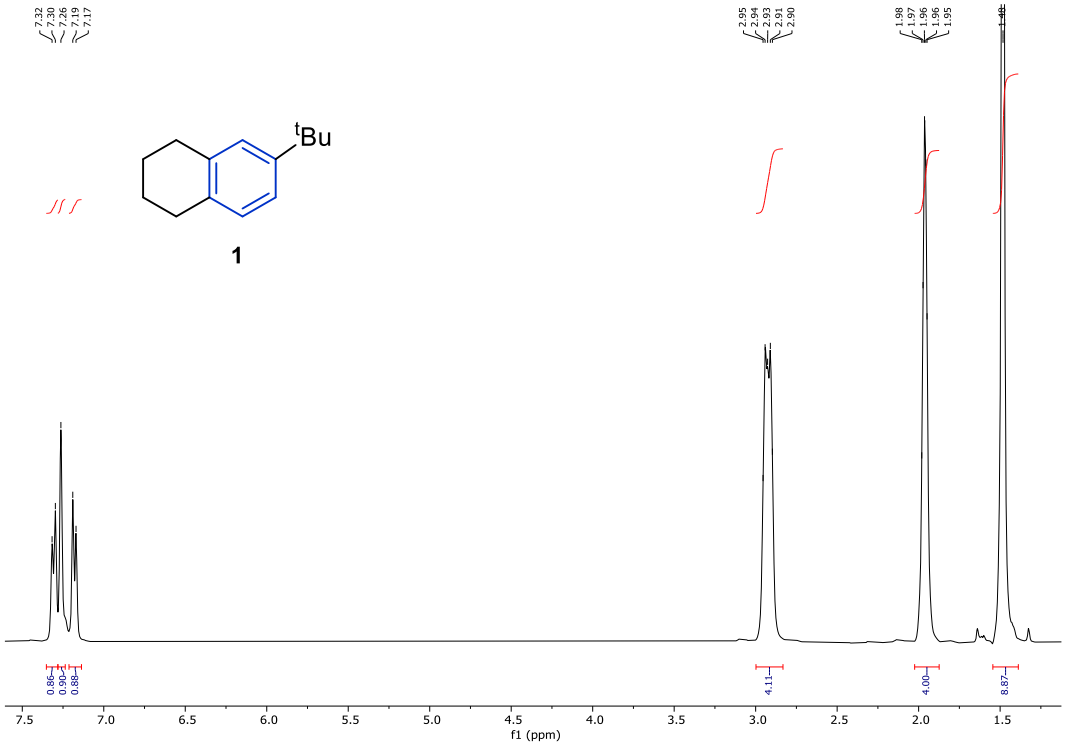

^{13}C NMR spectrum of 6-Tert-butyl-1,2,3,4-tetrahydronaphthalene (**1**) in $CDCl_3$

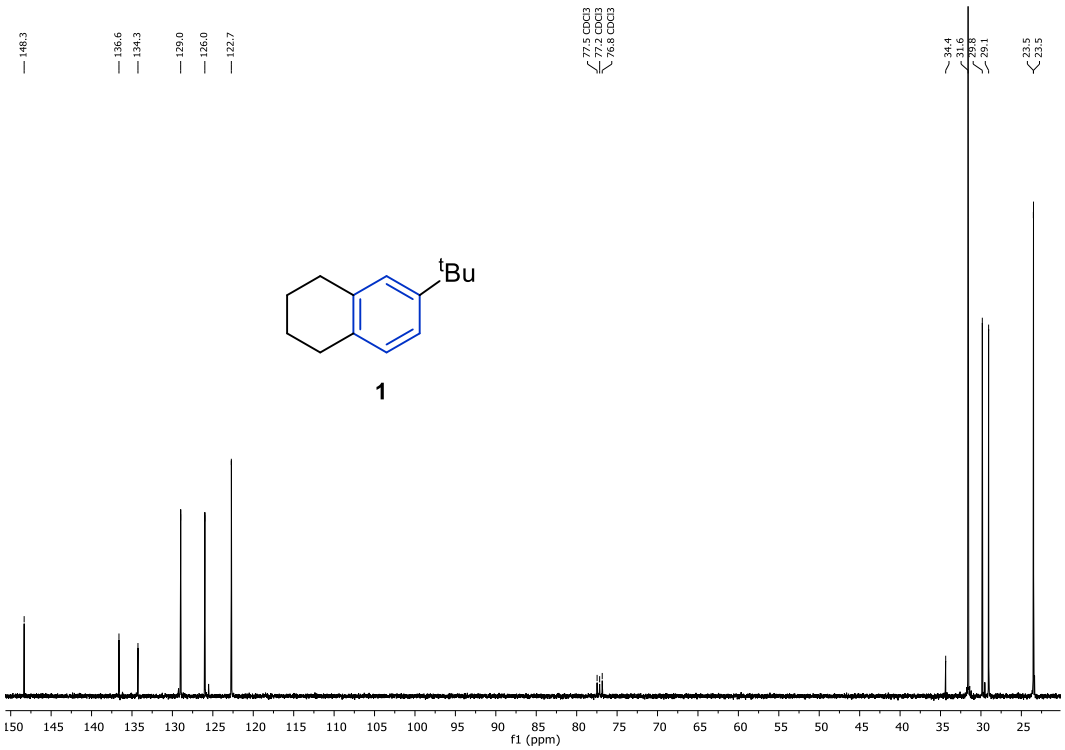

^{1}H NMR spectrum of (±)-**3** in $CDCl_3$

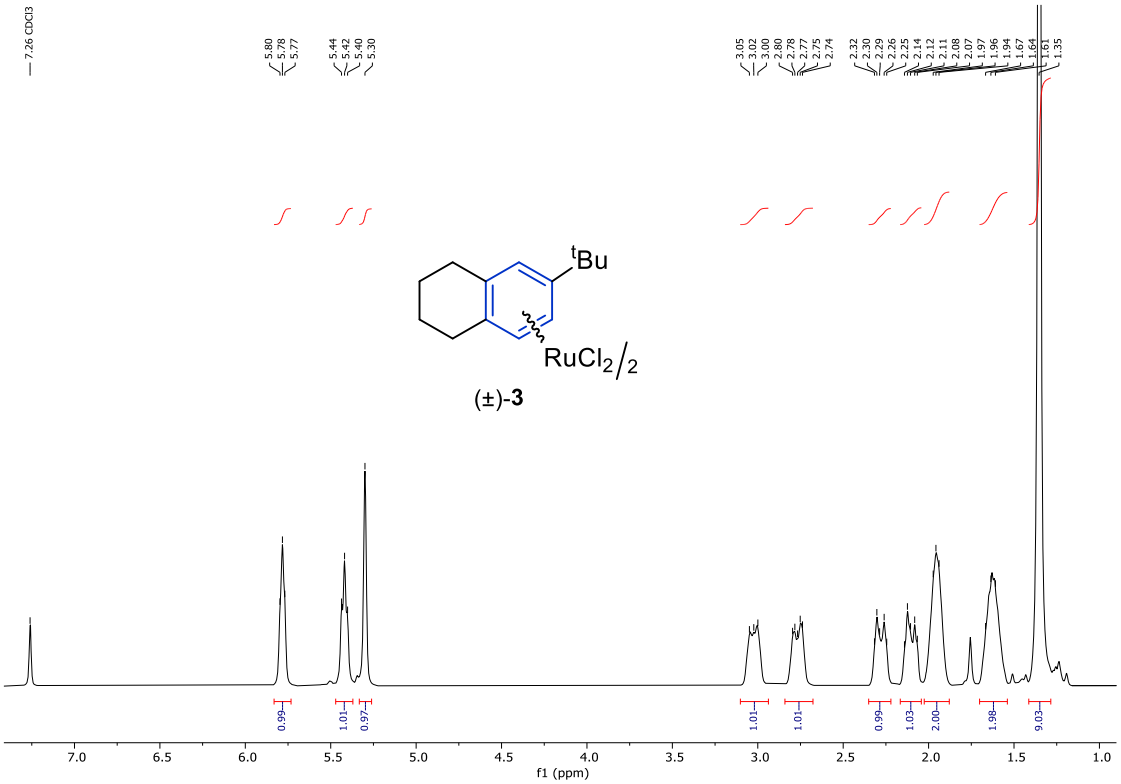

^{13}C NMR spectrum of (±)-**3** in $CDCl_3$

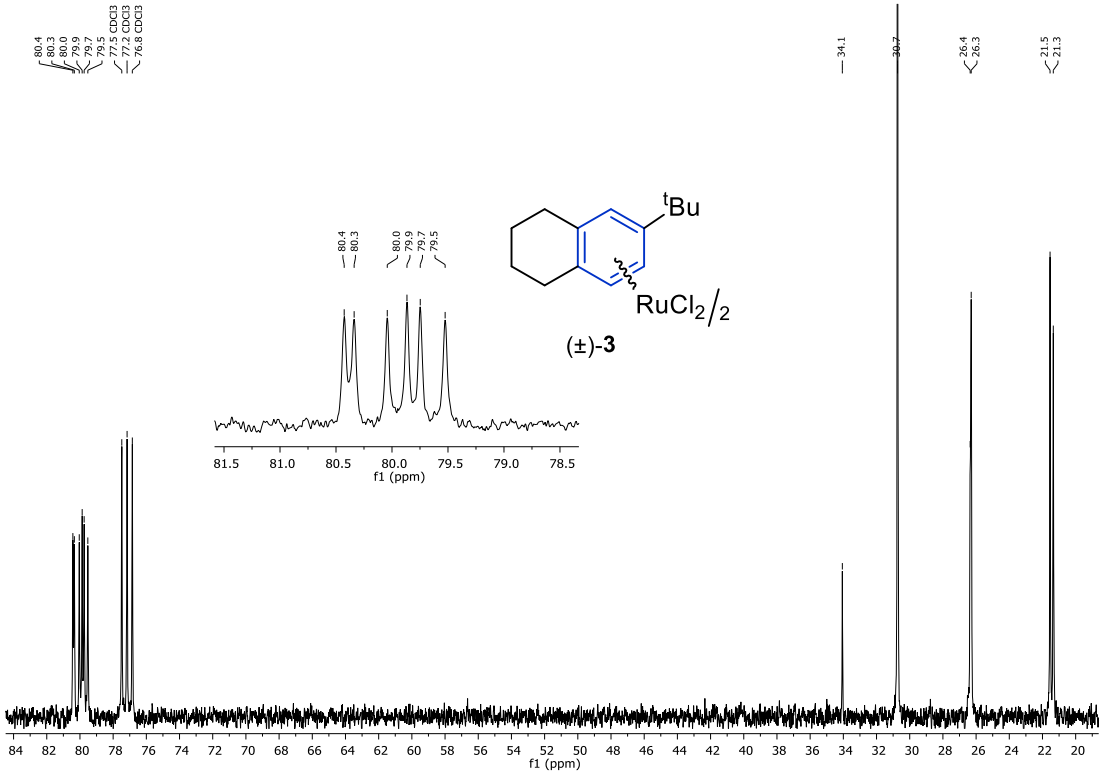

^{1}H NMR spectrum of **6a** in $CDCl_3$

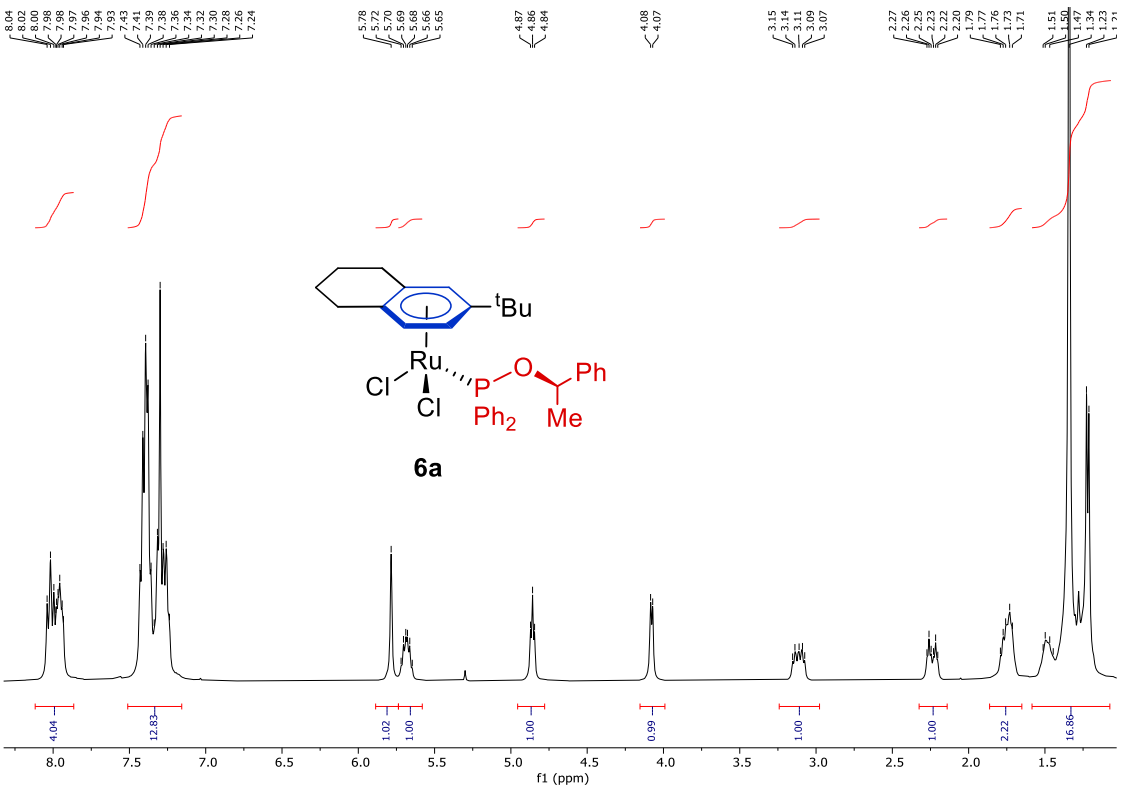

^{13}C NMR spectrum of **6a** in $CDCl_3$

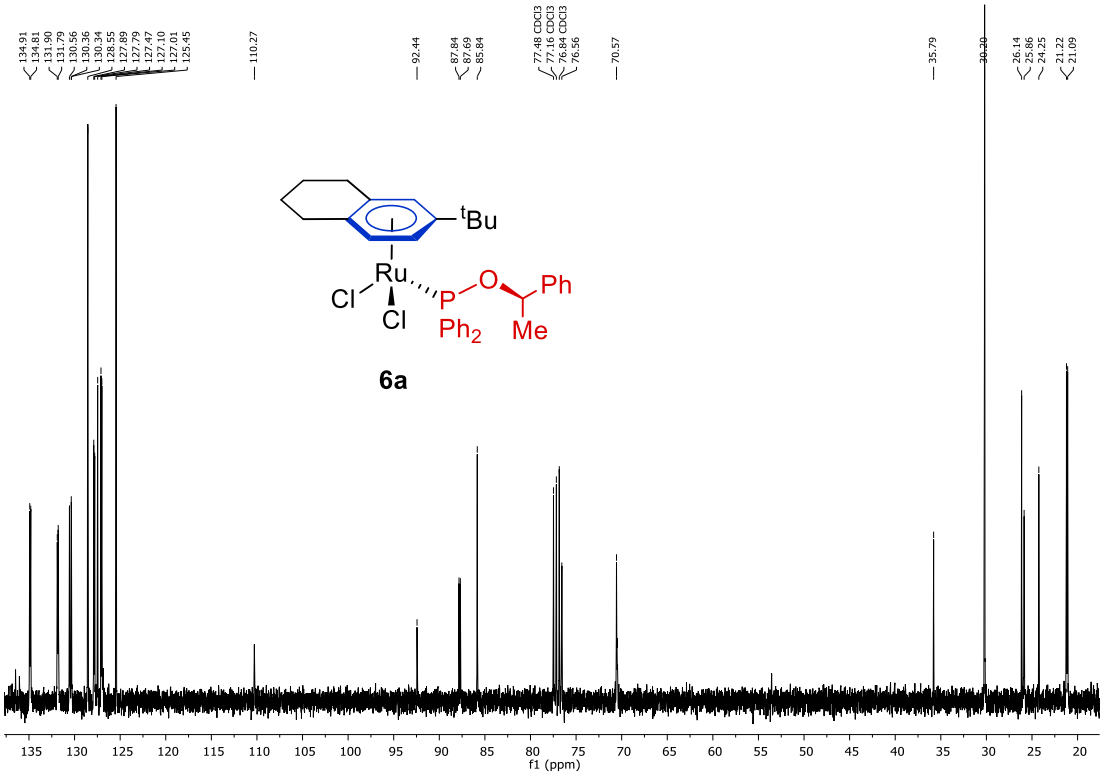

^{31}P NMR spectrum of **6a** in $CDCl_3$

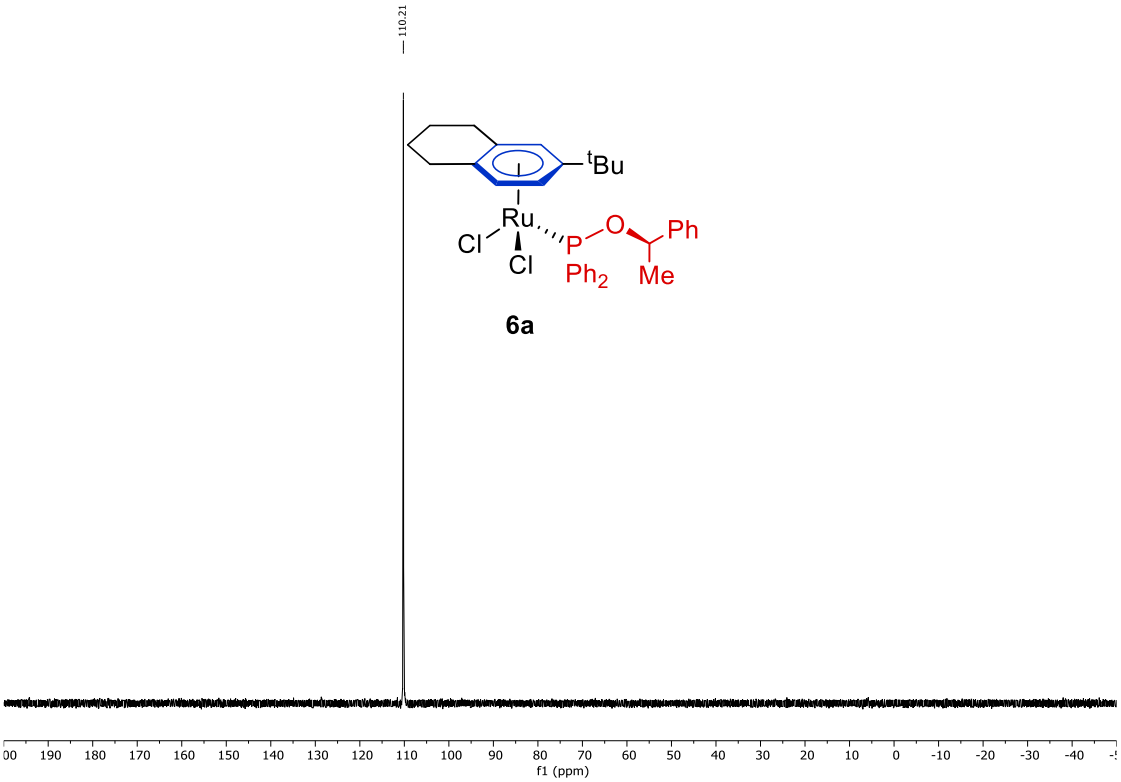

^{1}H NMR spectrum of **6b** in $CDCl_3$

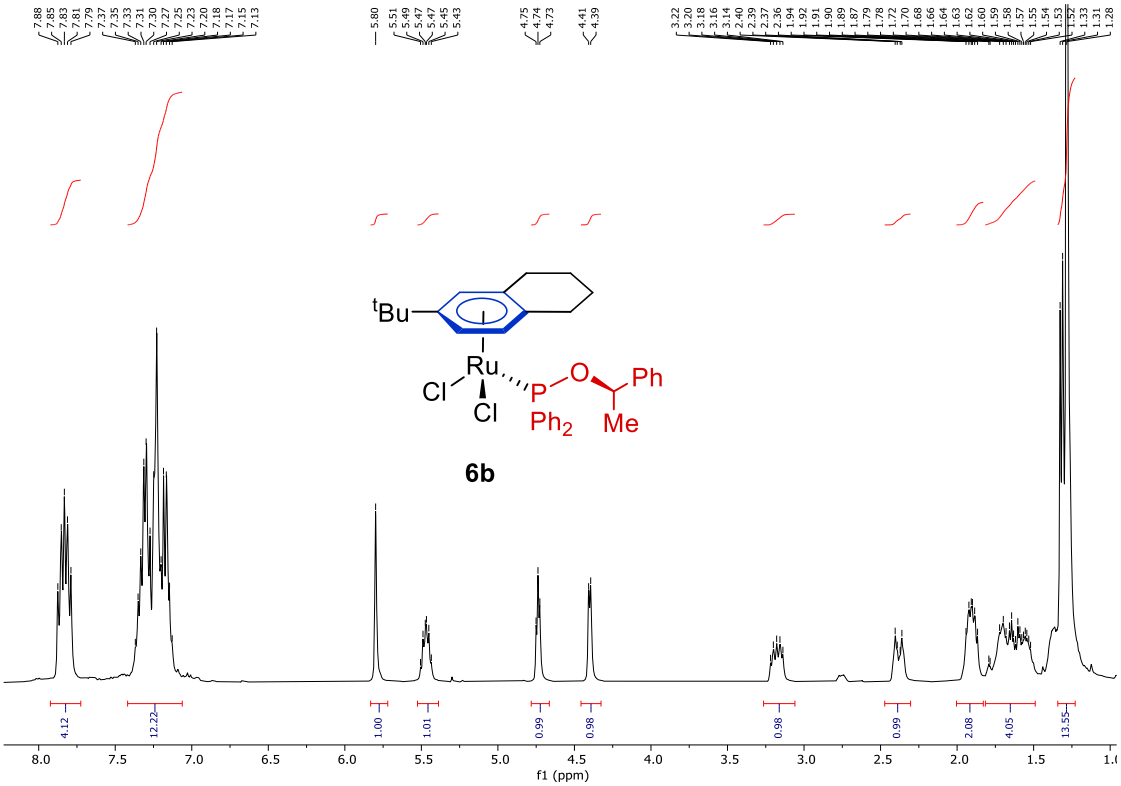

^{13}C NMR spectrum of **6b** in $CDCl_3$

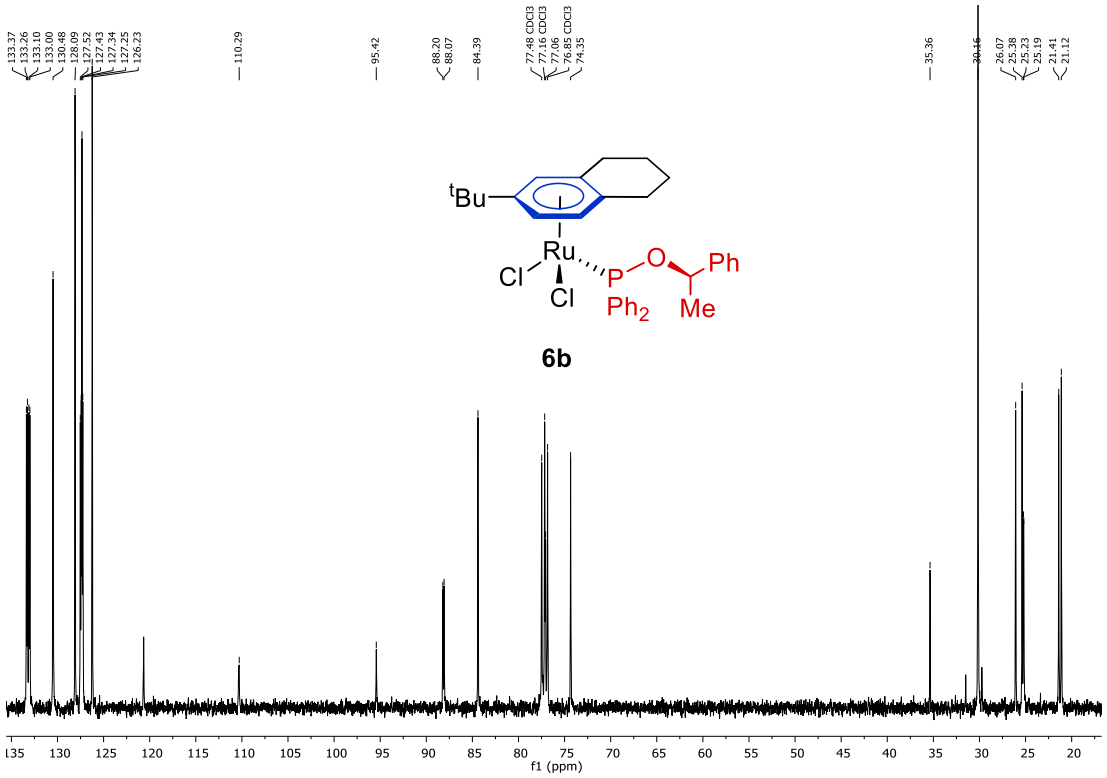

^{31}P NMR spectrum of **6b** in $CDCl_3$

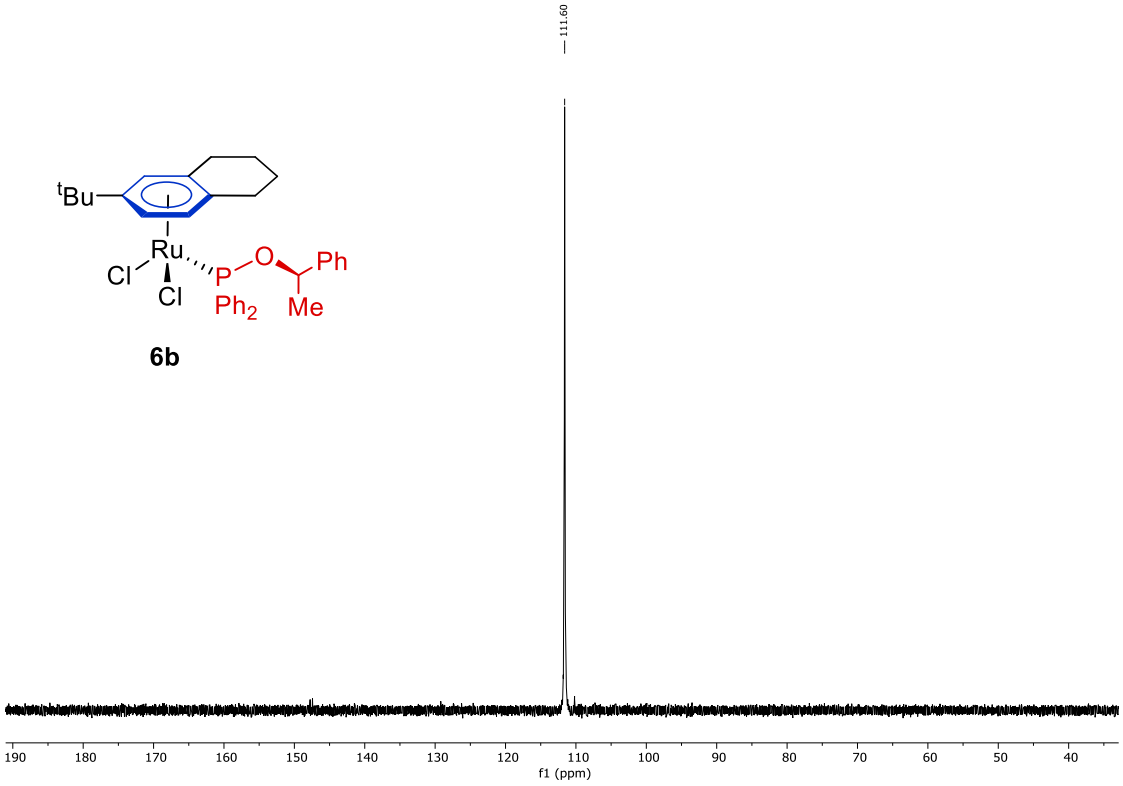

^{1}H NMR spectrum of **8c** in DMSO-d$_6$

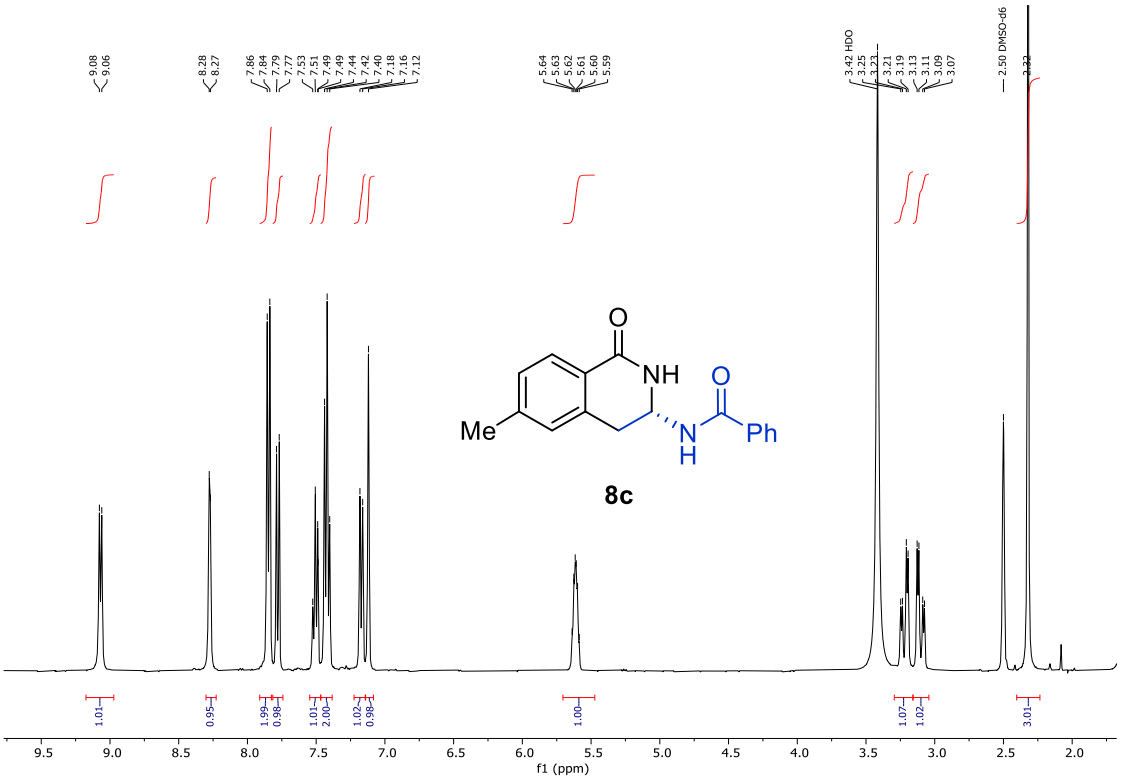

^{13}C NMR spectrum of **8c** in DMSO-d$_6$

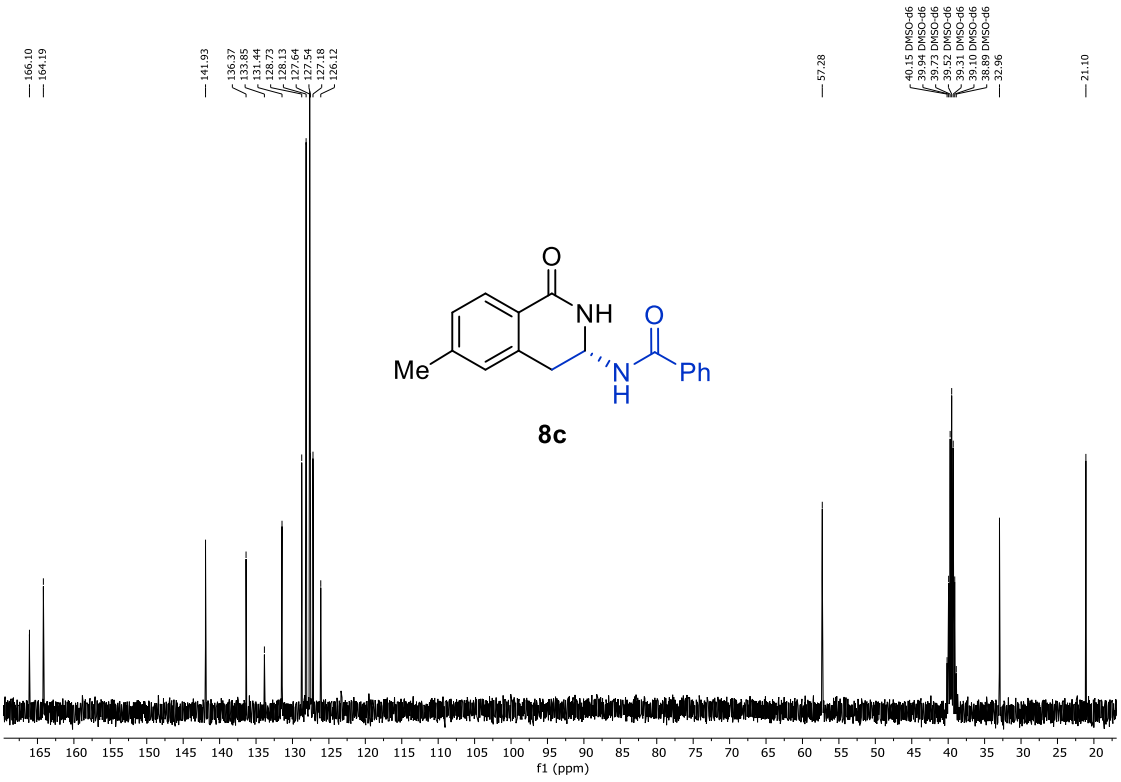

^{1}H NMR spectrum of **8d** in DMSO-d$_6$

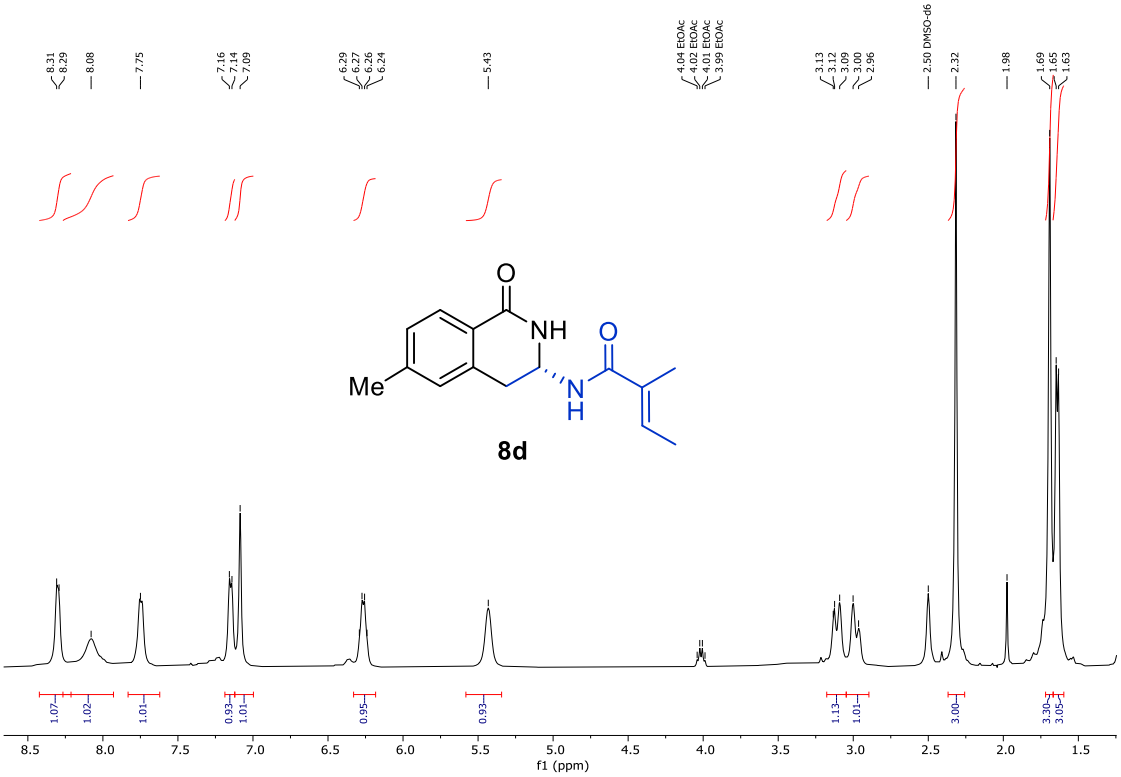

^{13}C NMR spectrum of **8d** in DMSO-d$_6$

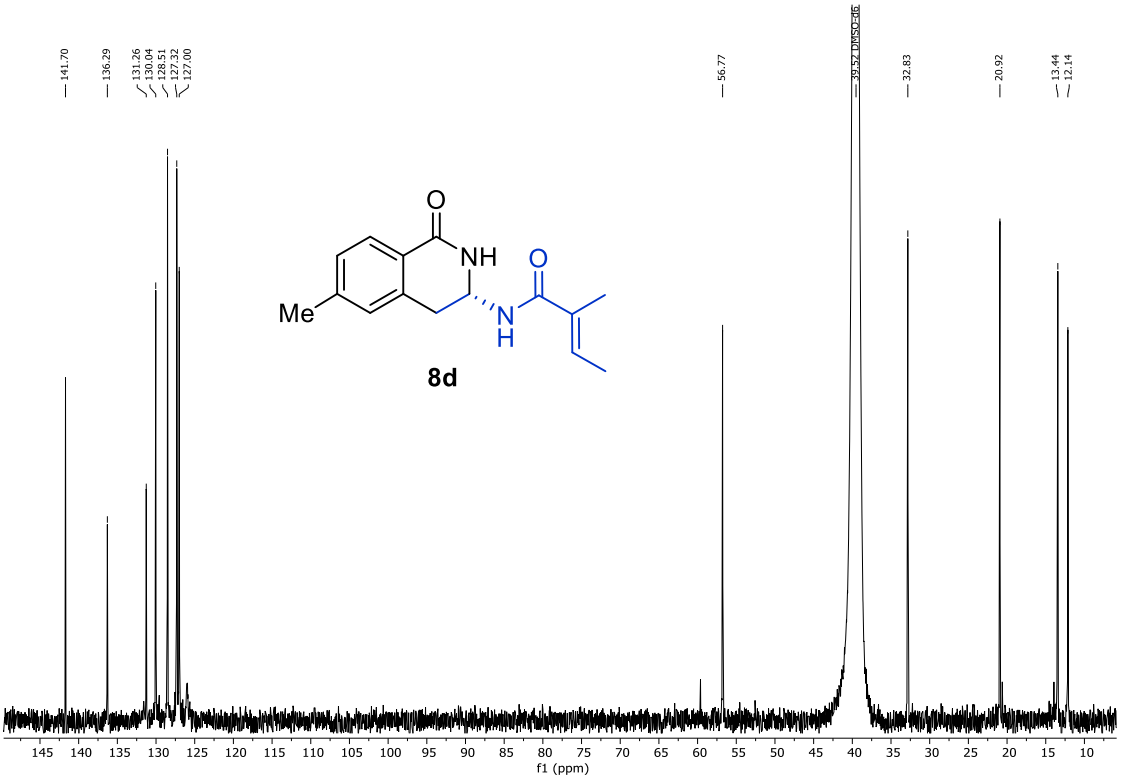

^{1}H NMR spectrum of **8e** in DMSO-d$_6$

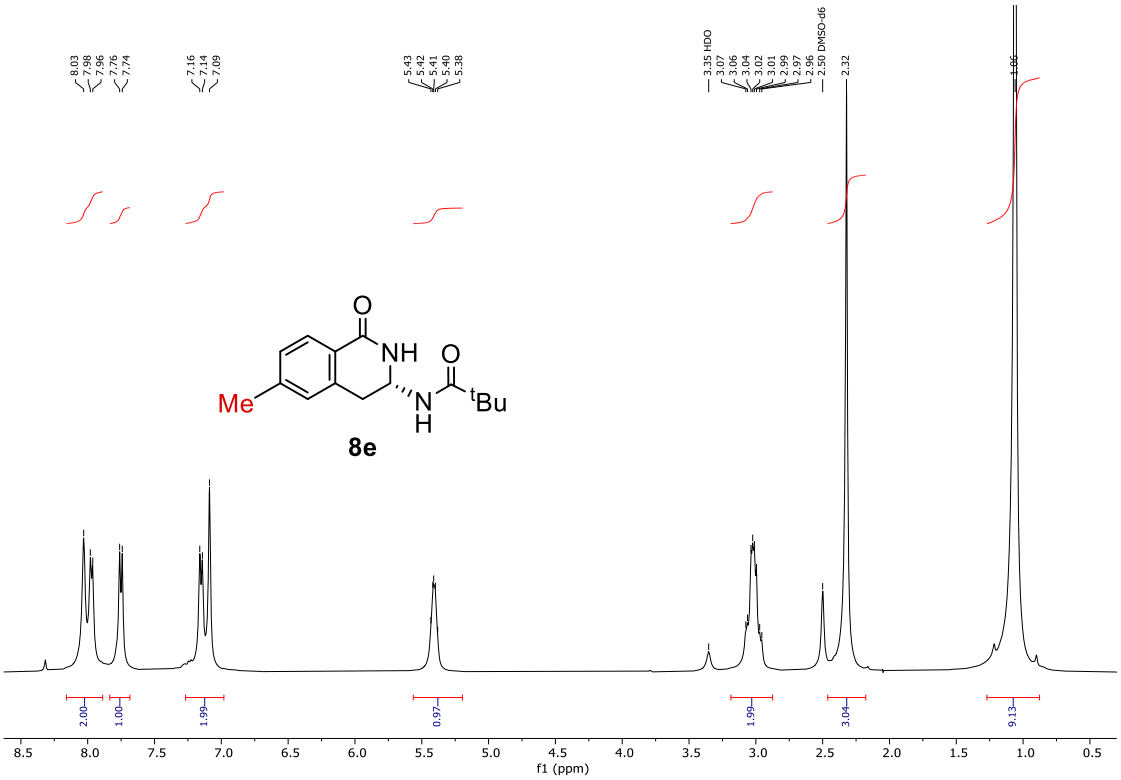

^{13}C NMR spectrum of **8e** in DMSO-d$_6$

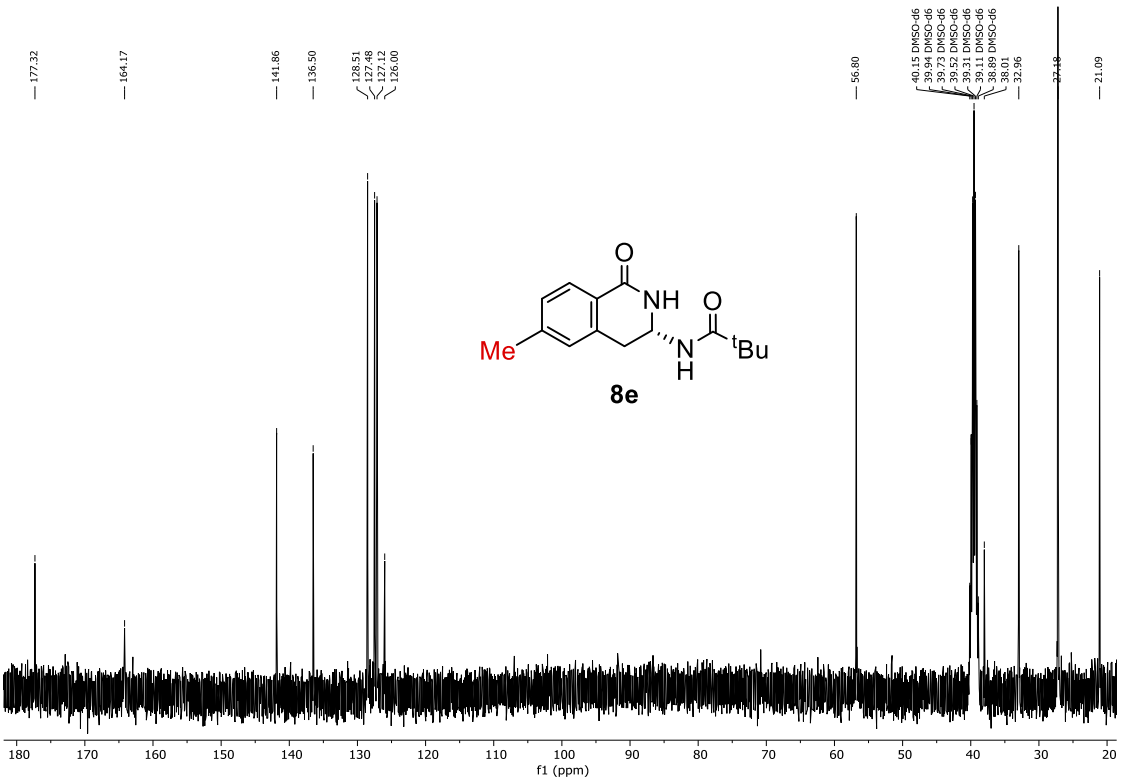

^{1}H NMR spectrum of **8f** in DMSO-d_6

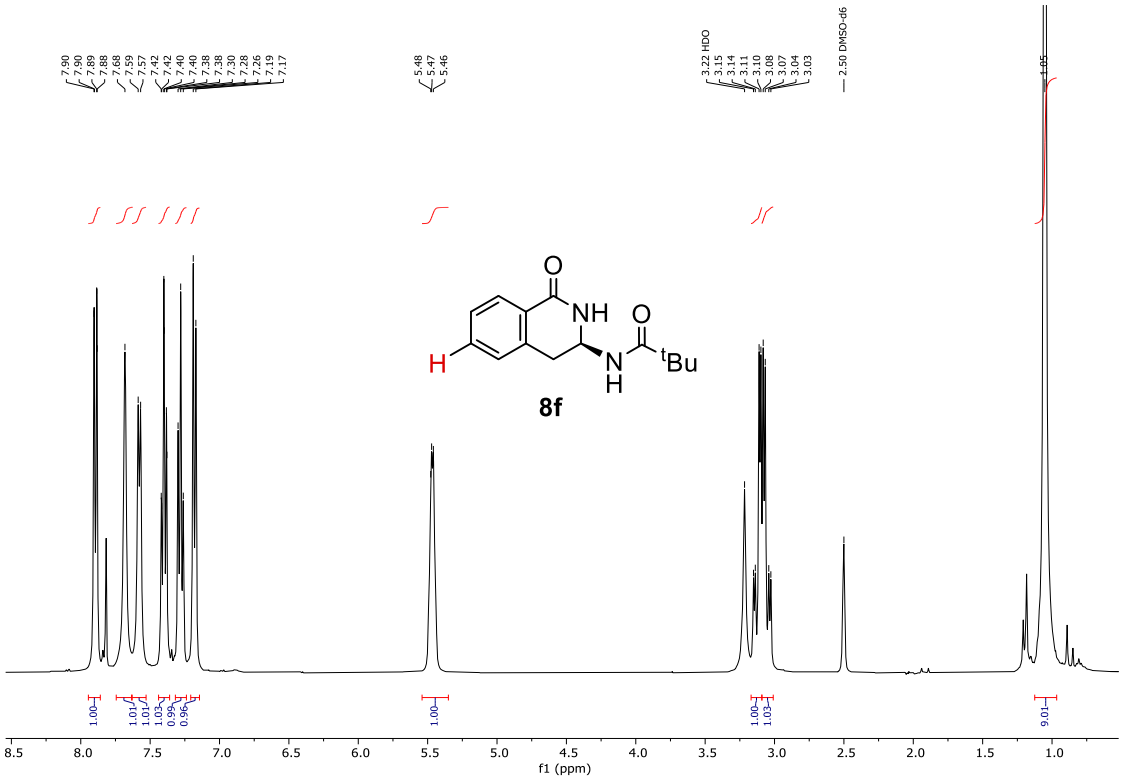

^{13}C NMR spectrum of **8f** in DMSO-d_6

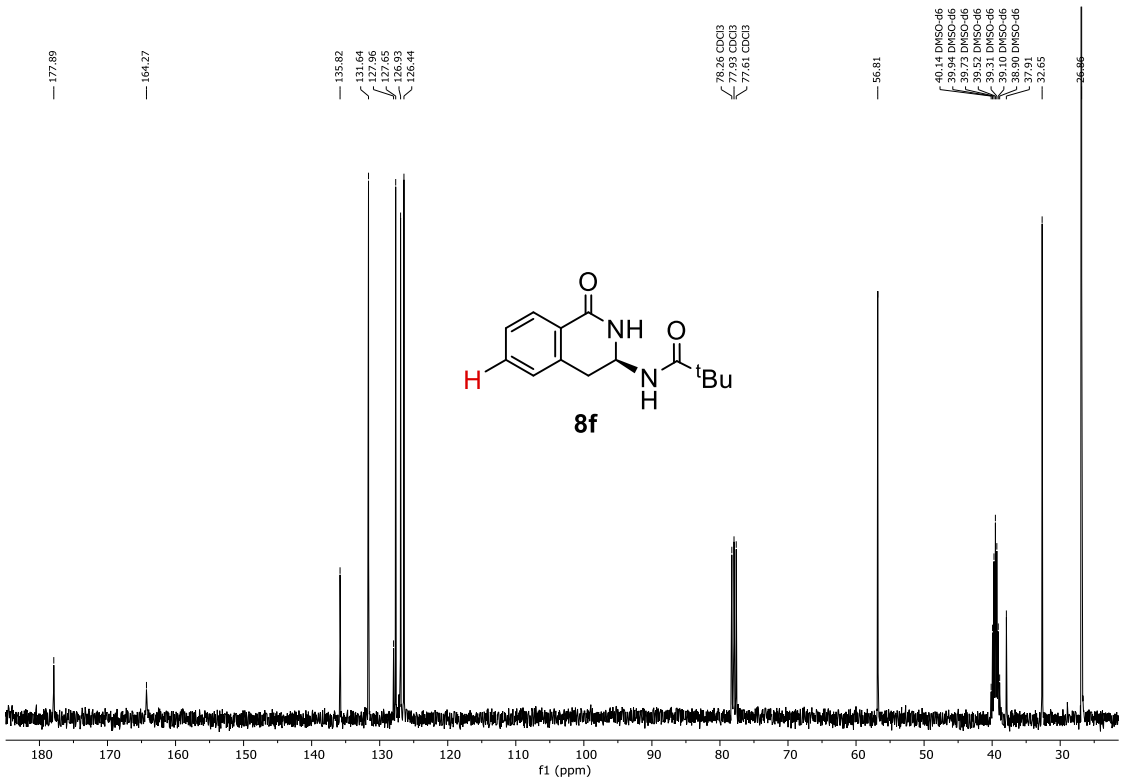

^{1}H NMR spectrum of **8g** in DMSO-d$_6$

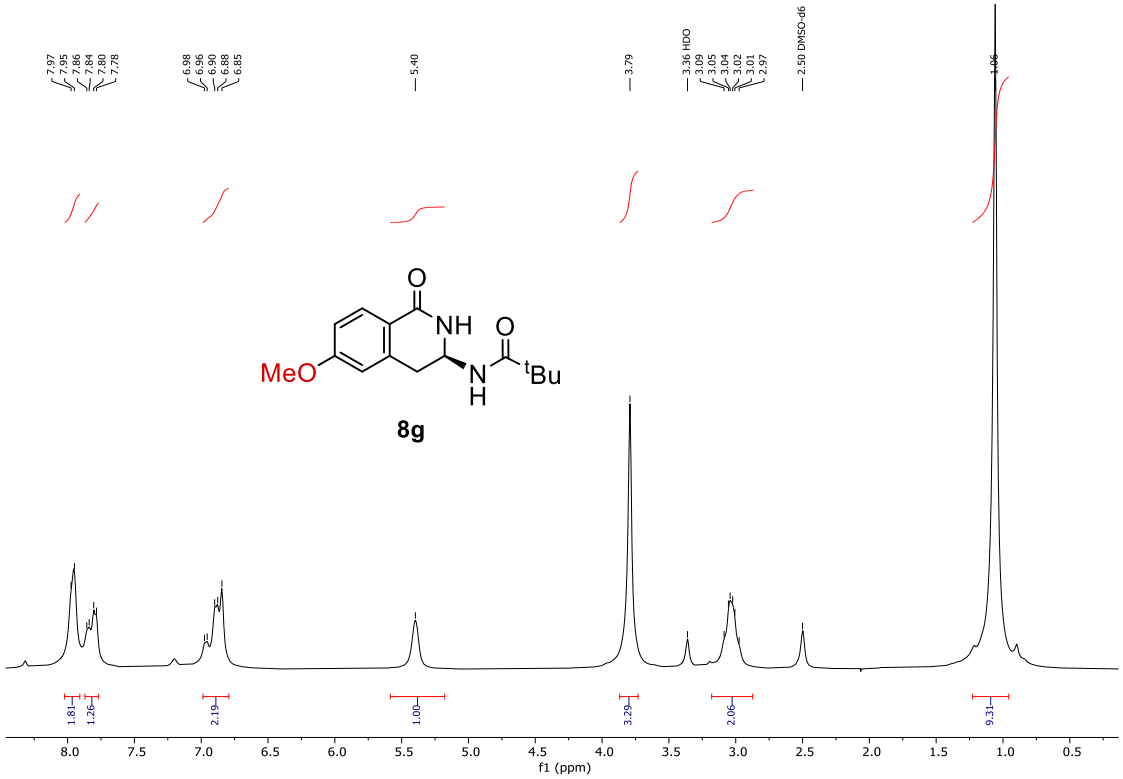

^{13}C NMR spectrum of **8g** in DMSO-d$_6$

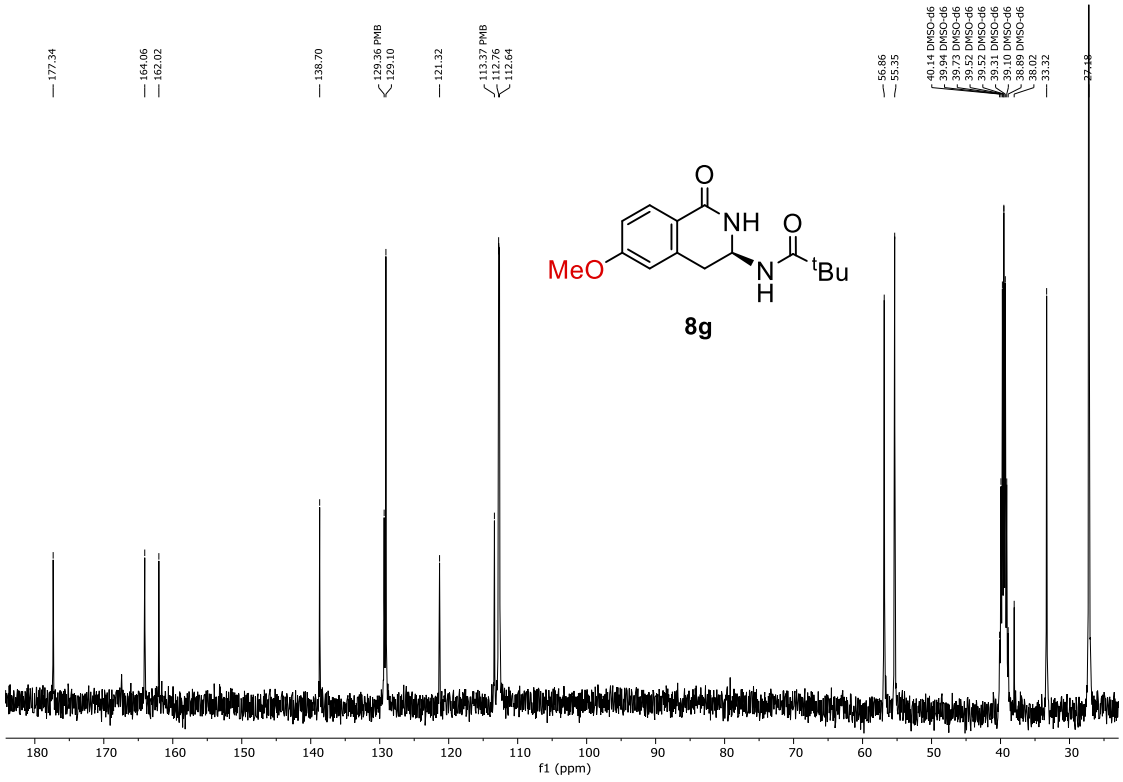

^{1}H NMR spectrum of **8h** in DMSO-d$_6$

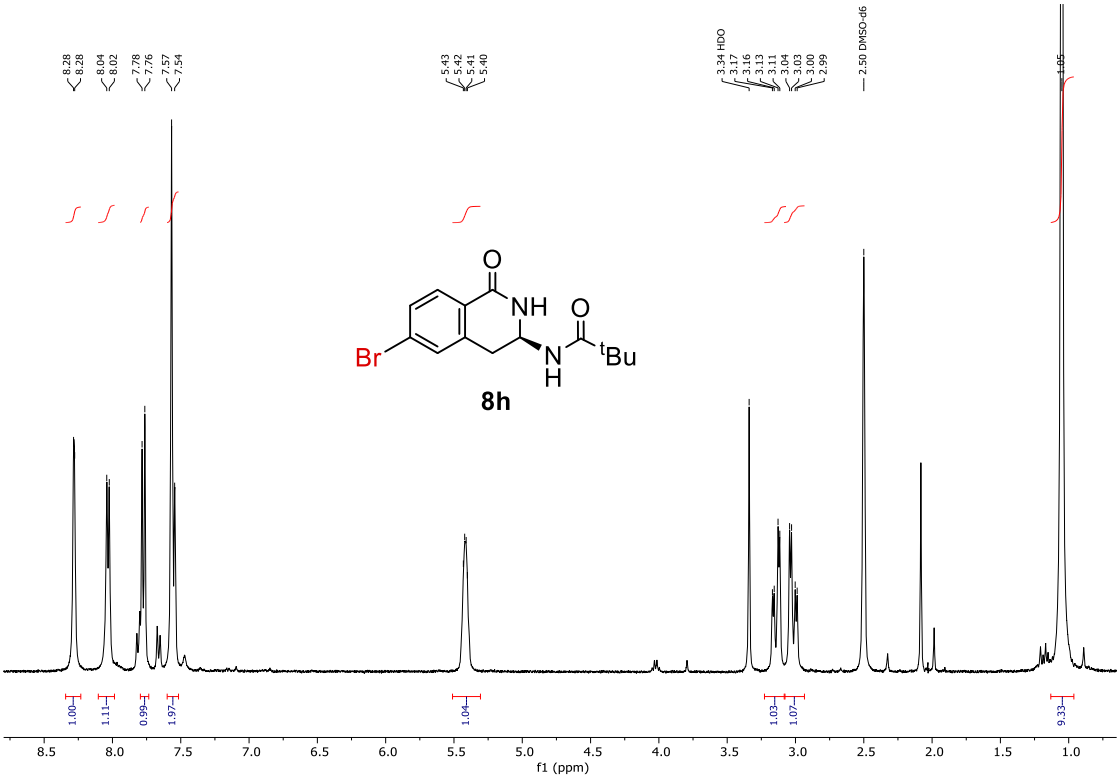

^{13}C NMR spectrum of **8h** in DMSO-d$_6$

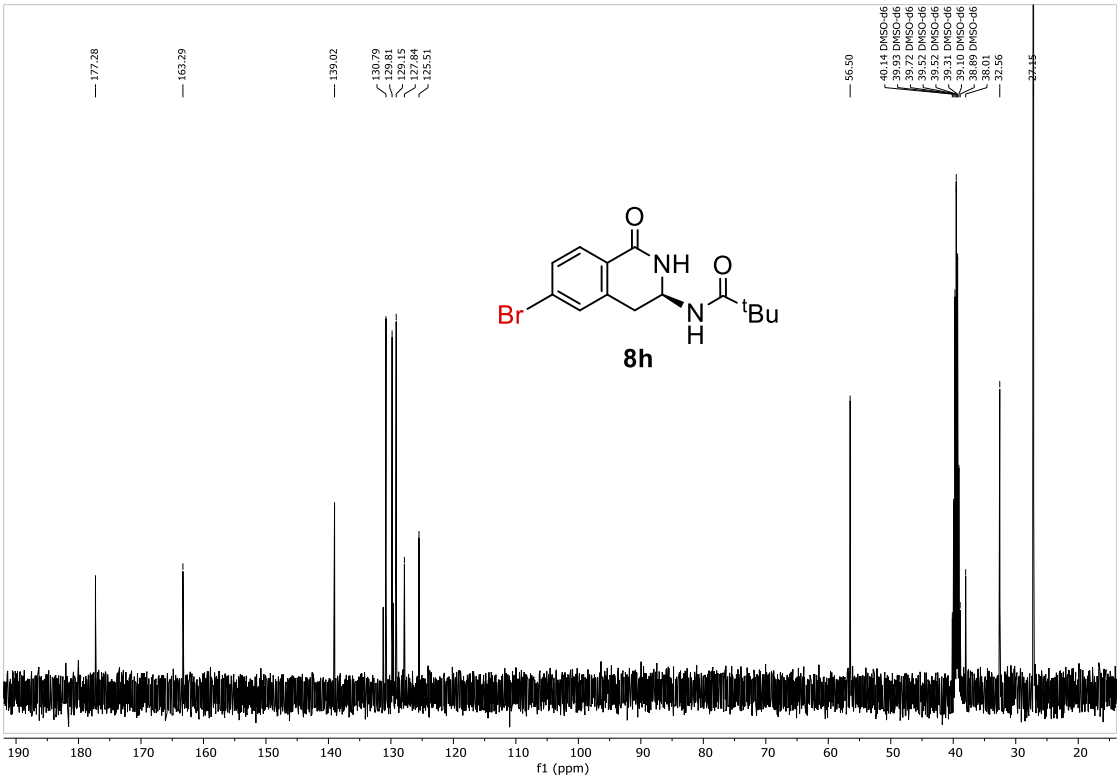

^{1}H NMR spectrum of **8i** in DMSO-d_6

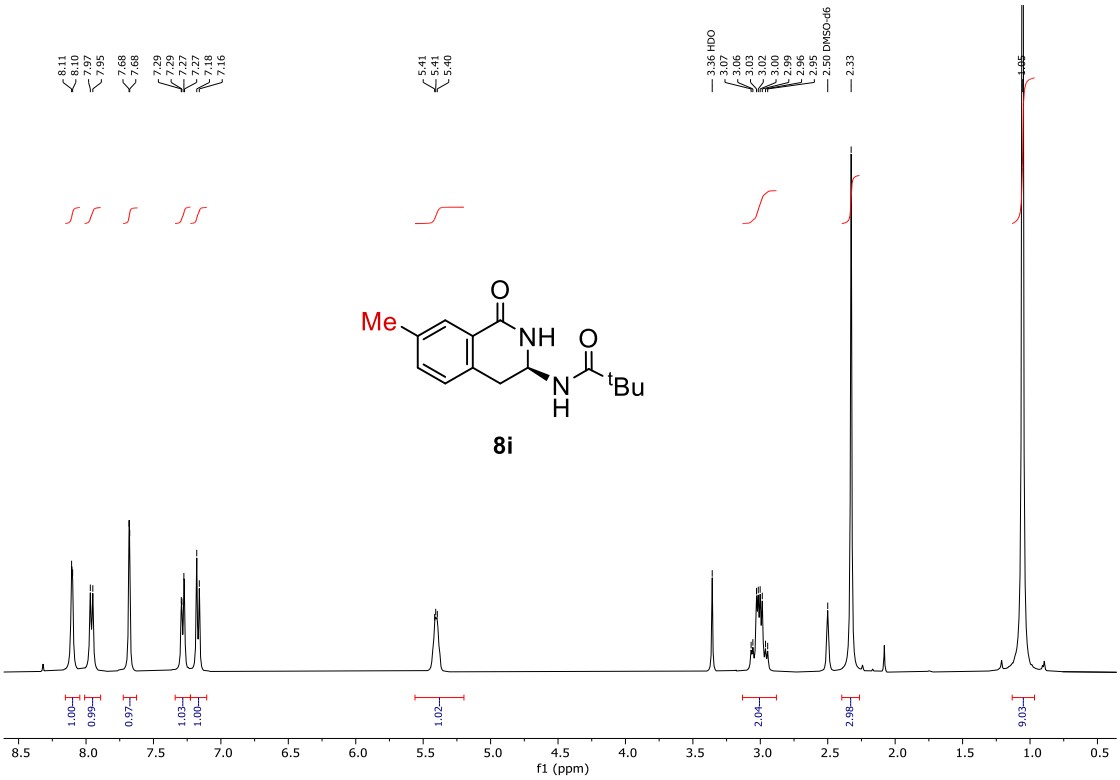

^{13}C NMR spectrum of **8i** in DMSO-d_6

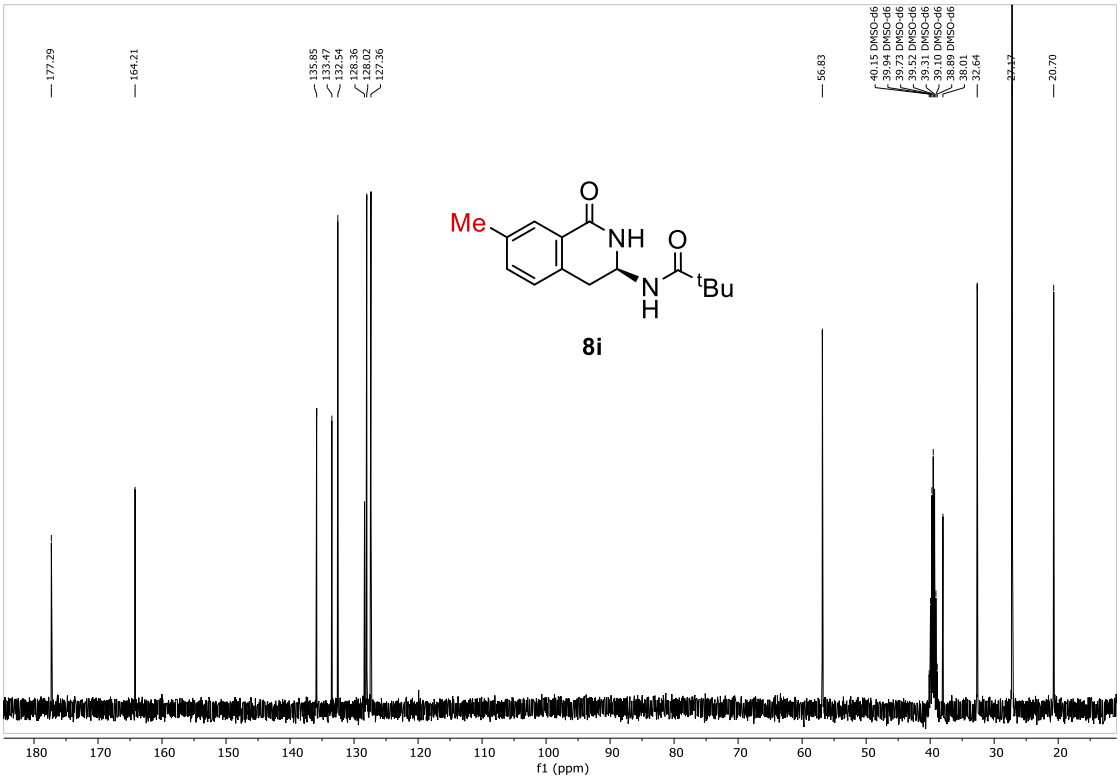

^{1}H NMR spectrum of **8j** in DMSO-d$_6$

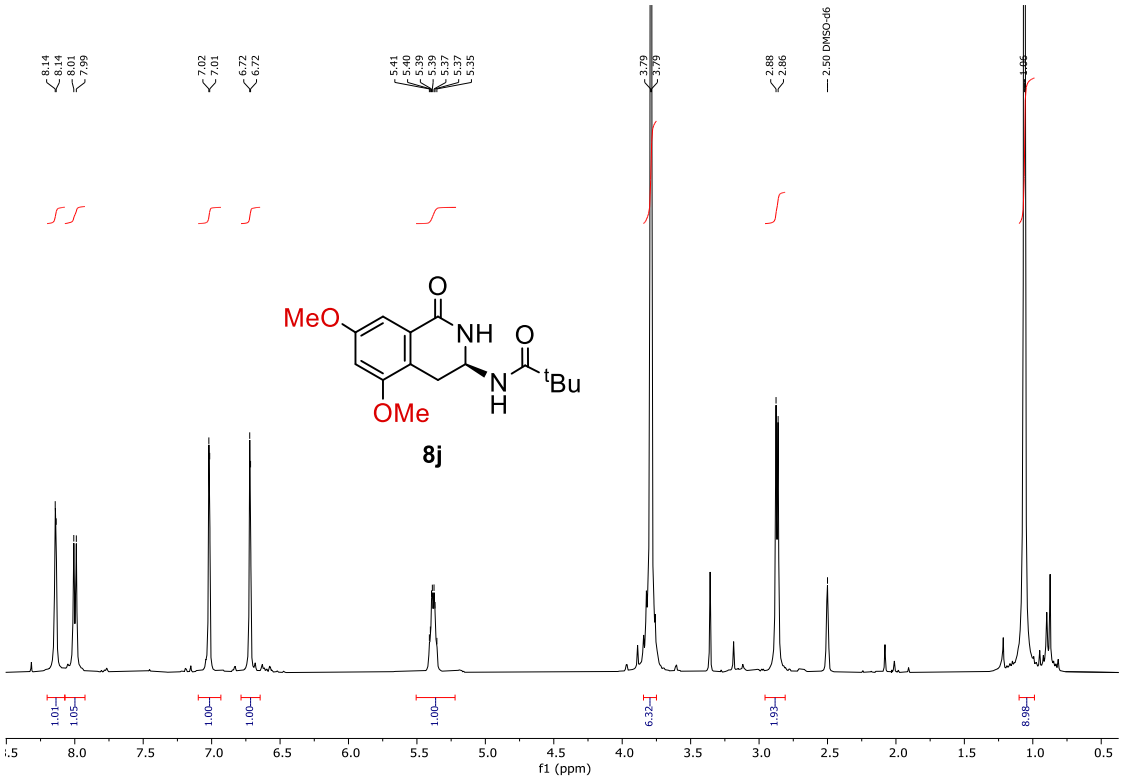

^{13}C NMR spectrum of **8j** in DMSO-d$_6$

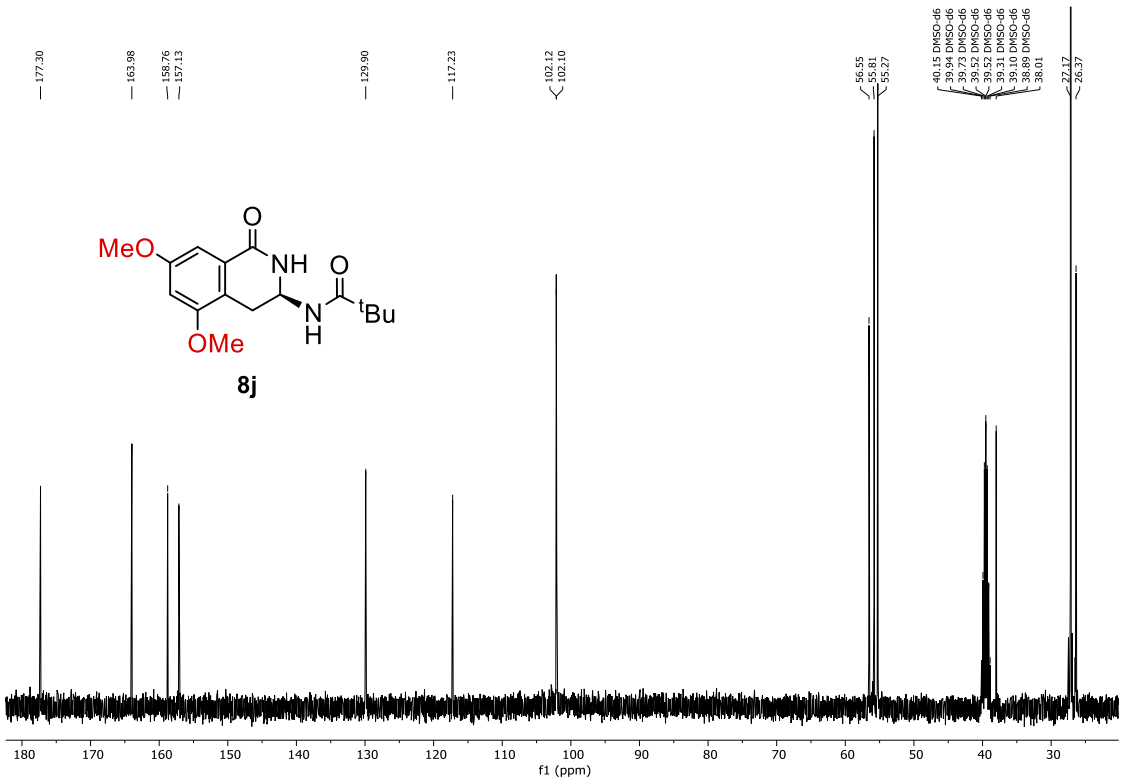

^{1}H NMR spectrum of **8k** in $CDCl_3$

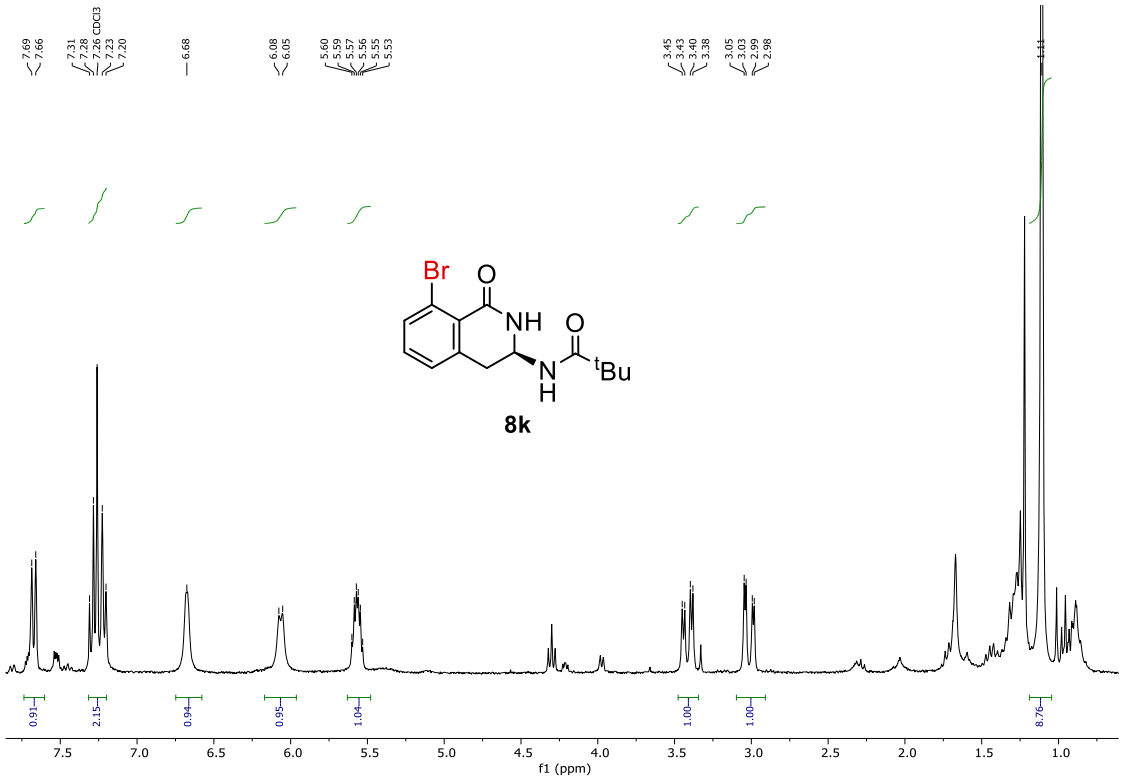

^{13}C NMR spectrum of **8k** in $CDCl_3$

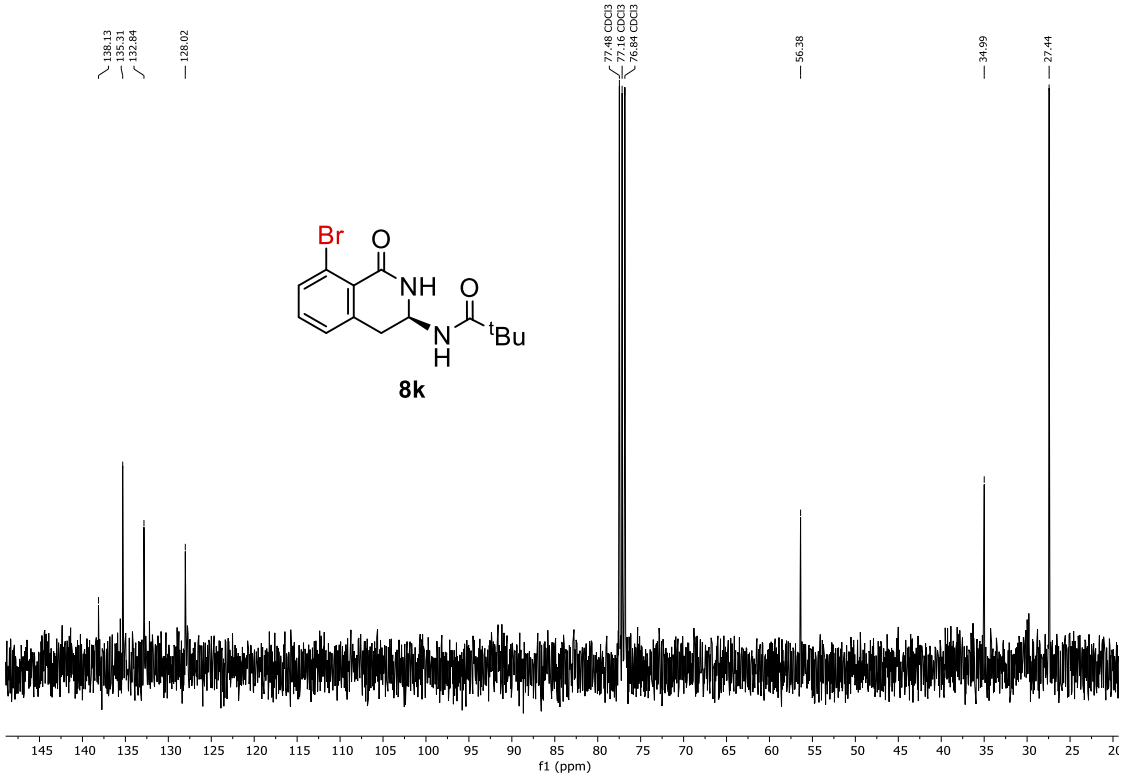

^{1}H NMR spectrum of **8l** in DMSO-d_6

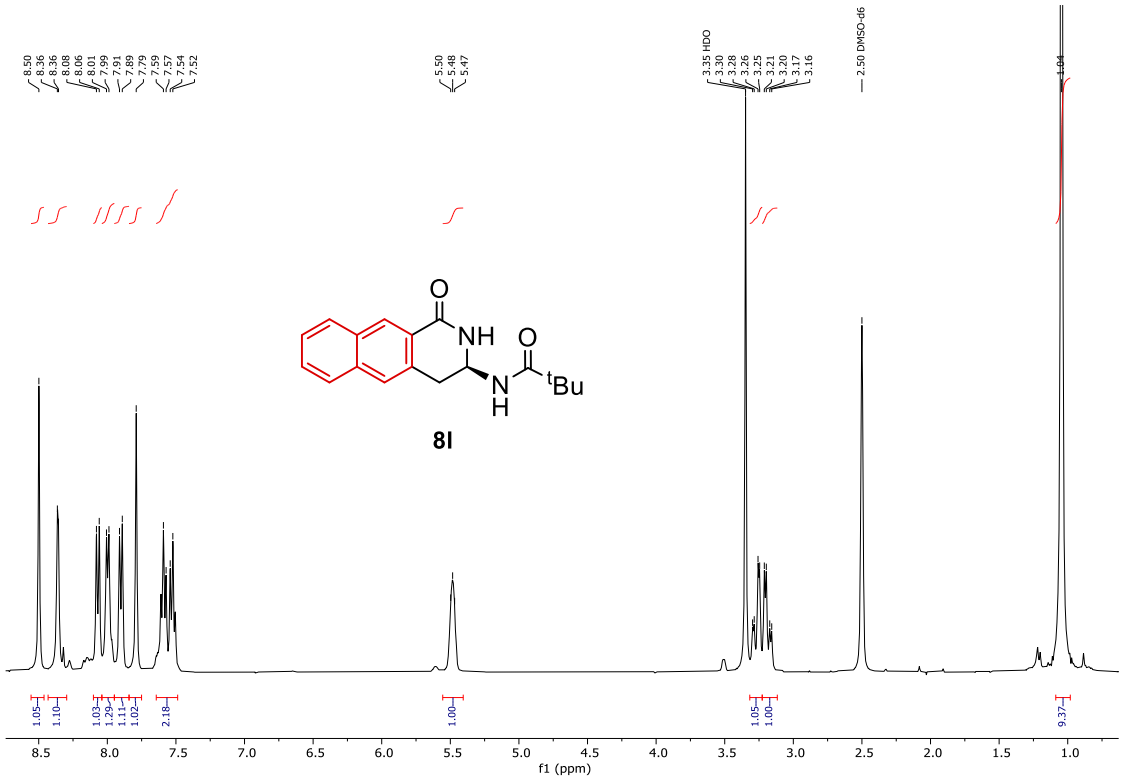

^{13}C NMR spectrum of **8l** in DMSO-d_6

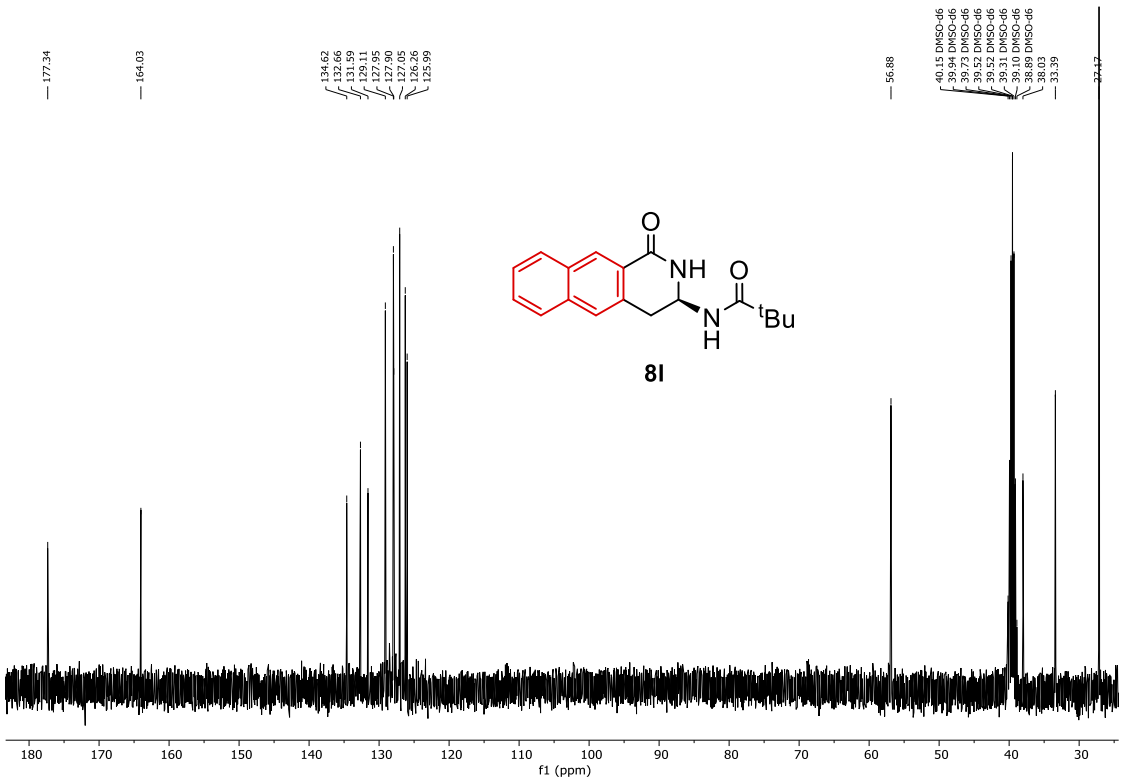

^{1}H NMR spectrum of **8m** in DMSO-d_6

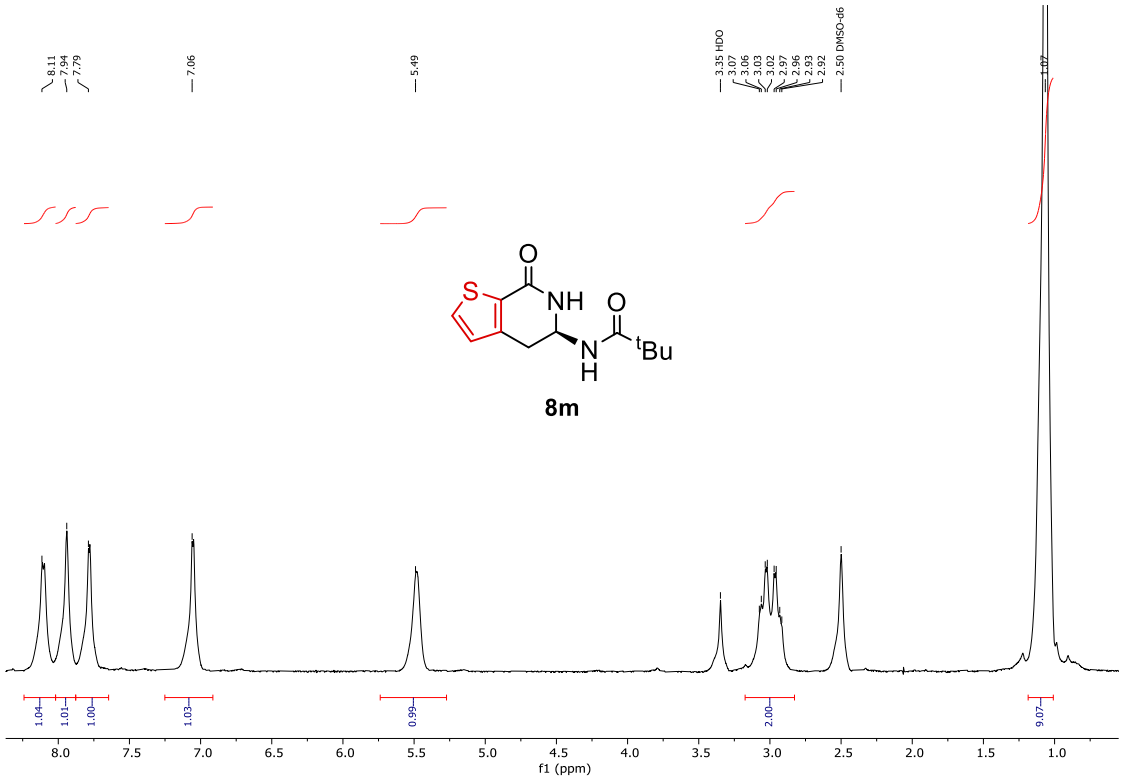

^{13}C NMR spectrum of **8m** in DMSO-d_6

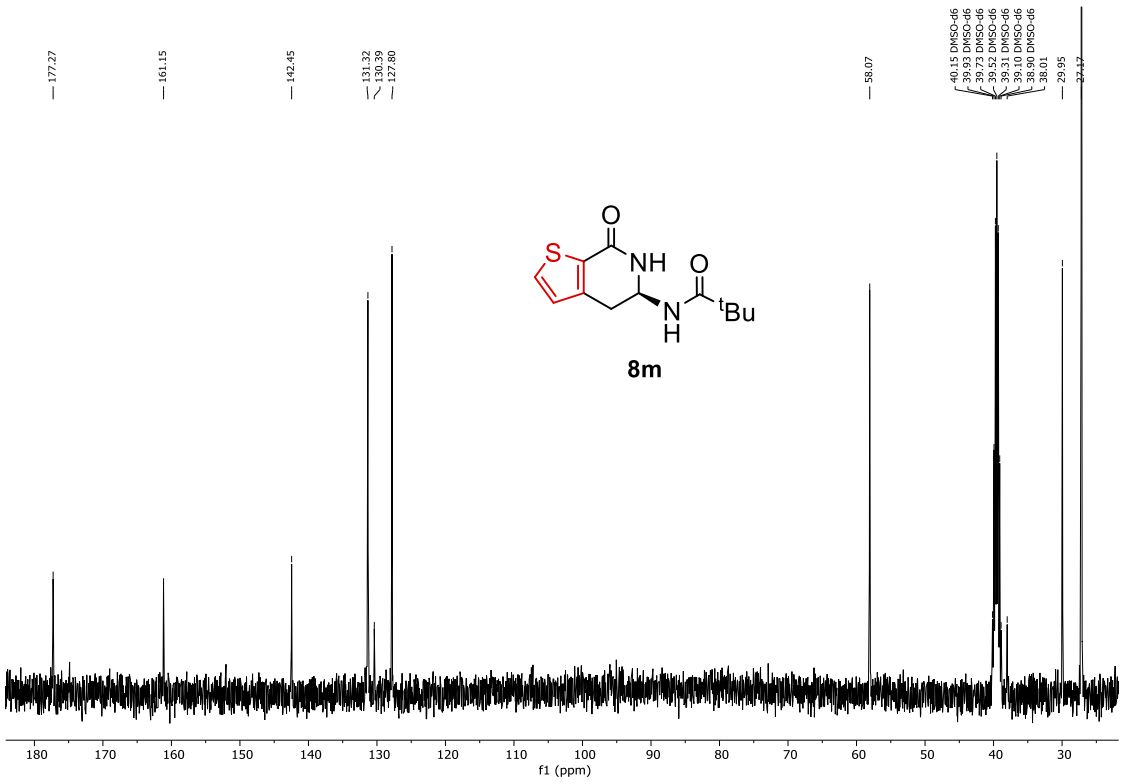

^{1}H NMR spectrum of **8h-Me** in $CDCl_3$

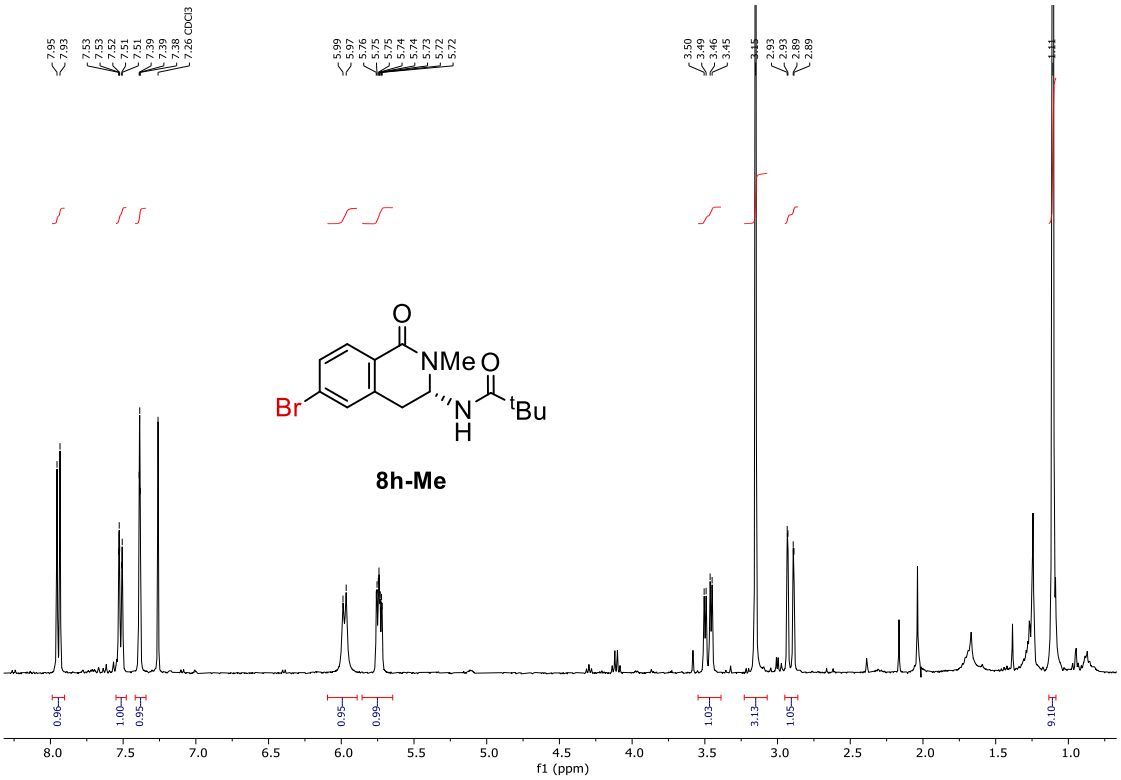

^{13}C NMR spectrum of **8h-Me** in $CDCl_3$

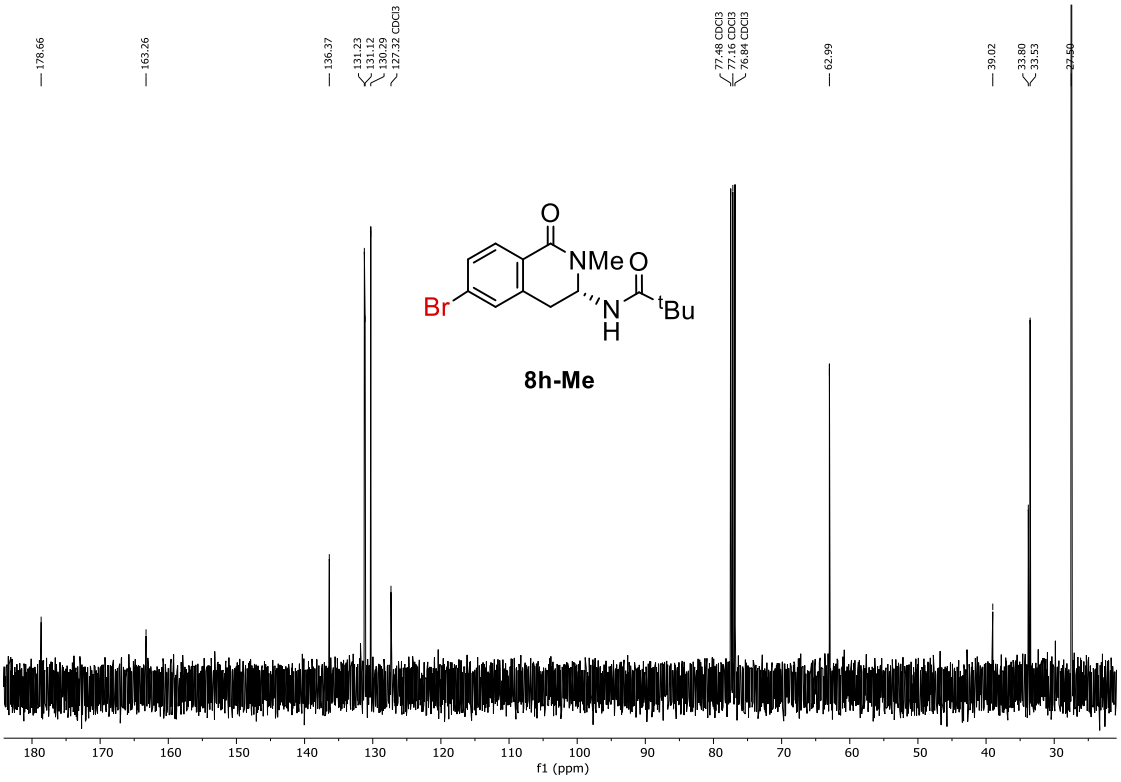

^{1}H NMR spectrum of **HFIP-NVP** in $CDCl_3$

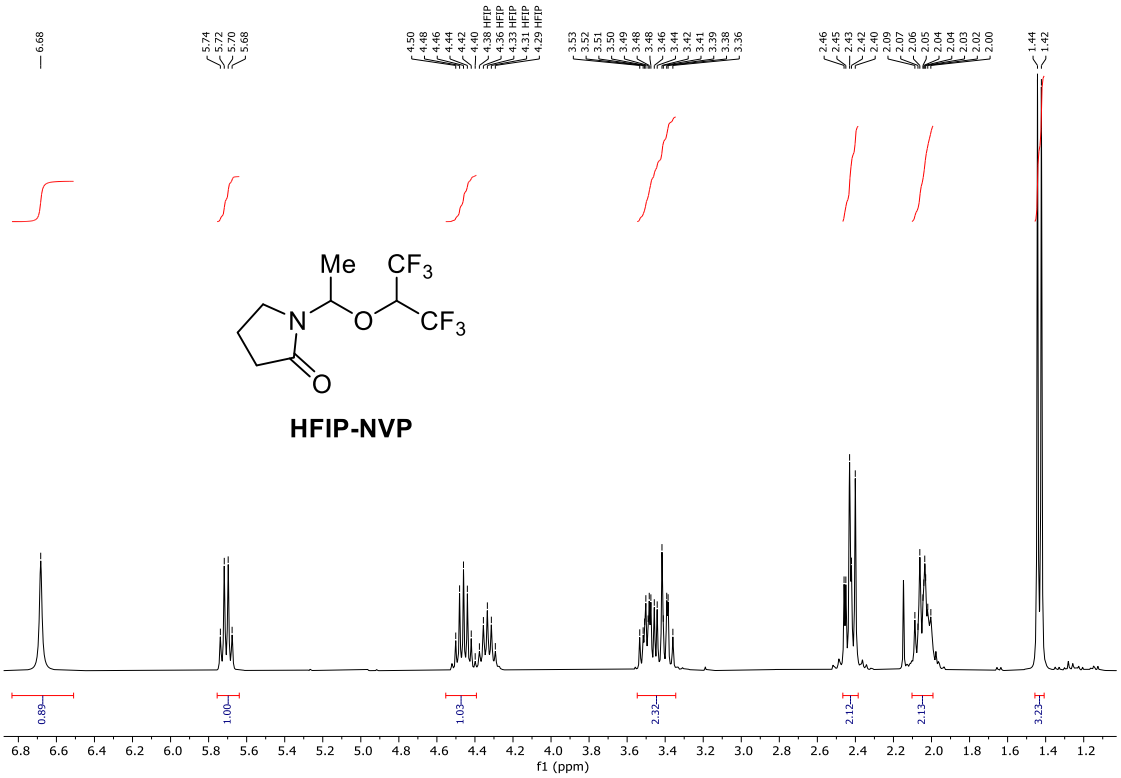

^{13}C NMR spectrum of **HFIP-NVP** in $CDCl_3$

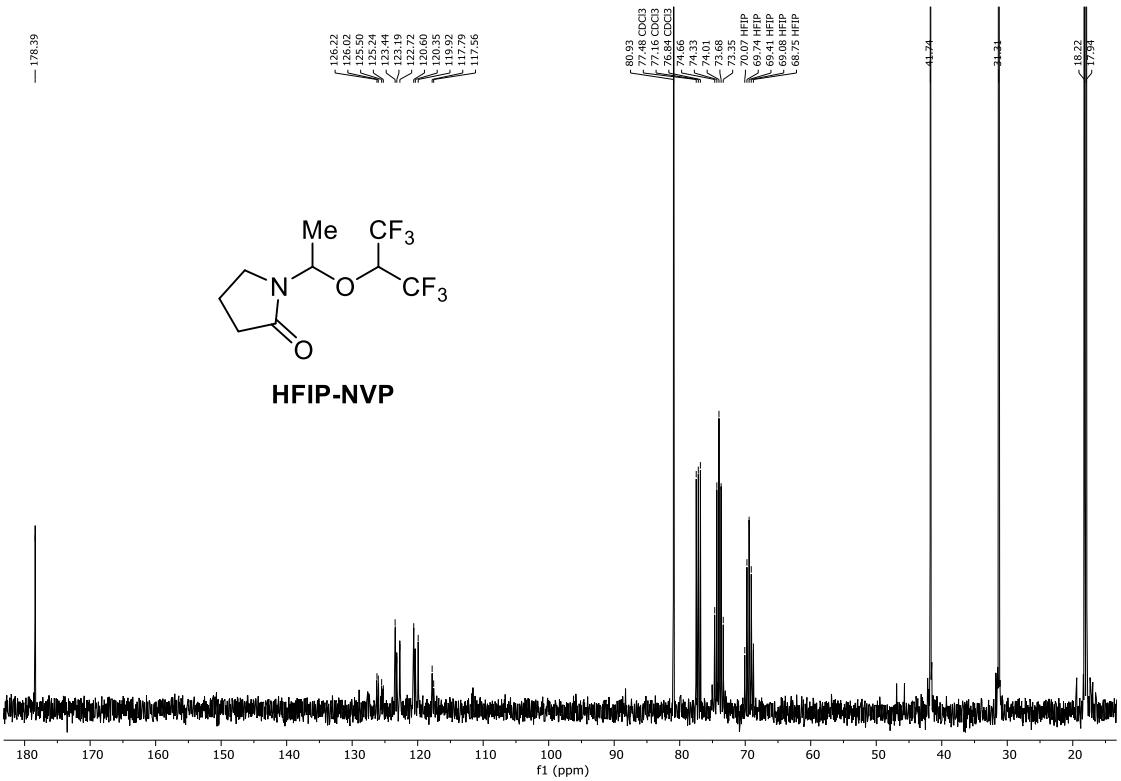

^{19}F NMR spectrum of **HFIP-NVP** in $CDCl_3$